

1995

Geochemistry and geohydrology of the Deccan volcanic rocks of Akole Taluka, Ahmednagar District, Maharashtra State, India.

Shashank. Agarwal
University of Windsor

Follow this and additional works at: <http://scholar.uwindsor.ca/etd>

Recommended Citation

Agarwal, Shashank., "Geochemistry and geohydrology of the Deccan volcanic rocks of Akole Taluka, Ahmednagar District, Maharashtra State, India." (1995). *Electronic Theses and Dissertations*. Paper 2219.

This online database contains the full-text of PhD dissertations and Masters' theses of University of Windsor students from 1954 forward. These documents are made available for personal study and research purposes only, in accordance with the Canadian Copyright Act and the Creative Commons license—CC BY-NC-ND (Attribution, Non-Commercial, No Derivative Works). Under this license, works must always be attributed to the copyright holder (original author), cannot be used for any commercial purposes, and may not be altered. Any other use would require the permission of the copyright holder. Students may inquire about withdrawing their dissertation and/or thesis from this database. For additional inquiries, please contact the repository administrator via email (scholarship@uwindsor.ca) or by telephone at 519-253-3000ext. 3208.



National Library
of Canada

Acquisitions and
Bibliographic Services Branch

395 Wellington Street
Ottawa, Ontario
K1A 0N4

Bibliothèque nationale
du Canada

Direction des acquisitions et
des services bibliographiques

395, rue Wellington
Ottawa (Ontario)
K1A 0N4

Your file *Votre référence*

Our file *Notre référence*

NOTICE

The quality of this microform is heavily dependent upon the quality of the original thesis submitted for microfilming. Every effort has been made to ensure the highest quality of reproduction possible.

If pages are missing, contact the university which granted the degree.

Some pages may have indistinct print especially if the original pages were typed with a poor typewriter ribbon or if the university sent us an inferior photocopy.

Reproduction in full or in part of this microform is governed by the Canadian Copyright Act, R.S.C. 1970, c. C-30, and subsequent amendments.

AVIS

La qualité de cette microforme dépend grandement de la qualité de la thèse soumise au microfilmage. Nous avons tout fait pour assurer une qualité supérieure de reproduction.

S'il manque des pages, veuillez communiquer avec l'université qui a conféré le grade.

La qualité d'impression de certaines pages peut laisser à désirer, surtout si les pages originales ont été dactylographiées à l'aide d'un ruban usé ou si l'université nous a fait parvenir une photocopie de qualité inférieure.

La reproduction, même partielle, de cette microforme est soumise à la Loi canadienne sur le droit d'auteur, SRC 1970, c. C-30, et ses amendements subséquents.

Canada

**Geochemistry and Geohydrology
of the Deccan Volcanic Rocks of
Akole Taluka, Ahmednagar District, Maharashtra State, India**

by

Shashank Agarwal

**A thesis submitted to the Faculty of
Graduate Studies and Research
through the Department of Geology
in partial fulfilment of the requirements
for the degree of Master of Science
at the University of Windsor
Windsor, Ontario, Canada**

1994



National Library
of Canada

Acquisitions and
Bibliographic Services Branch

395 Wellington Street
Ottawa, Ontario
K1A 0N4

Bibliothèque nationale
du Canada

Direction des acquisitions et
des services bibliographiques

395, rue Wellington
Ottawa (Ontario)
K1A 0N4

Your file *Voire référence*

Our file *Notre référence*

THE AUTHOR HAS GRANTED AN
IRREVOCABLE NON-EXCLUSIVE
LICENCE ALLOWING THE NATIONAL
LIBRARY OF CANADA TO
REPRODUCE, LOAN, DISTRIBUTE OR
SELL COPIES OF HIS/HER THESIS BY
ANY MEANS AND IN ANY FORM OR
FORMAT, MAKING THIS THESIS
AVAILABLE TO INTERESTED
PERSONS.

L'AUTEUR A ACCORDE UNE LICENCE
IRREVOCABLE ET NON EXCLUSIVE
PERMETTANT A LA BIBLIOTHEQUE
NATIONALE DU CANADA DE
REPRODUIRE, PRETER, DISTRIBUER
OU VENDRE DES COPIES DE SA
THESE DE QUELQUE MANIERE ET
SOUS QUELQUE FORME QUE CE SOIT
POUR METTRE DES EXEMPLAIRES DE
CETTE THESE A LA DISPOSITION DES
PERSONNE INTERESSEES.

THE AUTHOR RETAINS OWNERSHIP
OF THE COPYRIGHT IN HIS/HER
THESIS. NEITHER THE THESIS NOR
SUBSTANTIAL EXTRACTS FROM IT
MAY BE PRINTED OR OTHERWISE
REPRODUCED WITHOUT HIS/HER
PERMISSION.

L'AUTEUR CONSERVE LA PROPRIETE
DU DROIT D'AUTEUR QUI PROTEGE
SA THESE. NI LA THESE NI DES
EXTRAITS SUBSTANTIELS DE CELLE-
CI NE DOIVENT ETRE IMPRIMES OU
AUTREMENT REPRODUITS SANS SON
AUTORISATION.

ISBN 0-612-01430-4

Canada

© **Shashank Agarwal, 1994**

ALL RIGHTS RESERVED.

Abstract

The study area is bounded between longitudes $73^{\circ} 45' E$ and $73^{\circ} 55' E$ and latitudes $19^{\circ} 30' N$ and $19^{\circ} 40' N$. It comprises three tribal villages of Manhere, Ambevangan and Titvi in the N-E part of the Ahmednagar District in the Deccan Trap region of the Western Ghats, Maharashtra State, India. The bedrock is massive tholeiitic basalt of the Thakurvadi Formation. The petrography and geochemistry of the 47 samples collected mainly from hand-dug wells and blastholes were examined in order to determine their petrogenesis and to establish the geochemical stratigraphy of the Thakurvadi Formation.

Petrographically the rocks are porphyritic to microphyric and aphyric, fine- to medium-grained massive basalts. They are commonly amygdaloidal filled with zeolites. Two suites were defined on the basis of phenocryst content: Suite No 1 with olivine, plagioclase, clinopyroxene assemblages, and Suite No 2 with olivine, plagioclase, clinopyroxene, and magnetite assemblages. Chemically the rocks are altered and show variation in composition, with increases in K_2O content and relatively small increases in Na_2O content. The SiO_2 , FM ($FeO + MgO + MnO$) and CaO (except in four samples) content were relatively less altered. The two petrographic suites were not found to be useful in interpreting the petrogenetic history. However, MgO-FeO diagrams and vector plots using the high field strength elements suggest that fractional crystallization was the dominant influence in the petrogenetic history of these basalts.

An attempt has been made to establish a stratigraphic sequence for 40 rock samples within the middle Thakurvadi Formation. In order to achieve uniformity of approach with the previous investigations, the samples were arranged in the increasing order to their elevation, and were plotted against the trace element chemistry and petrographic features at the interval of 20-30 m.

The results of the present study indicate no physiographic breaks in the rock chemistry. Marker horizon(s) such as Giant Plagioclase Basalts (2-5 cm) are not present; hence no distinct boundary or intra-formational sub-divisions were recognised. This suggests that the study area probably belongs to flows that show petrographically two distinct suites, but shows an overlap in chemistry. Because lavas pinch out and dip, it is difficult to correlate the chemical types in the study area with that of the reference section.

A brief account of the geohydrologic significance of bedrock features, with considerations of lineaments in the Deccan Trap is also given. The maximum concentration of lineaments was found to be in range of $N 150^{\circ}$ - $N180^{\circ}$ and $N 120^{\circ}$ to 150° . These lineaments predominantly were found to be zones of structural weakness along which there was formation of fractures. Some of the lineaments that occur in the study area, are suggested as the possible sites of groundwater occurrence. It is suggested that groundwater in the study area may occur in association with 1) ground features with fractures trending NNW-SSE 2) valley fills with unconsolidated material coinciding with the lineaments and 3) vesicular and weathered portions of the basaltic flows.

Acknowledgements

I would first like to confer my sincere gratitude towards my supervisors Dr. T.E. Smith and Dr. Frank Simpson, for their indispensable patience and guidance, that has allowed me to make this thesis presentable. Their benign support has always been a part of my success and achievements. Secondly, I would also like to express my sincere regards to Doug Steele and Michael John Harris, for their all round support and active participation in the discussions during my stay in the Department. Michelle Macdonald is appraised for providing valuable information on zeolites occurring in the study area. The geological maps with the location of samples and lineaments in the study area are prepared by Doug Steele, for which, he is thanked once again. Antun Knitil and Ingrid Churchill are thanked for their participation in petrological and geochemical preparations.

Finally, I would also like to express my sincere regards to the Dean of Graduate Studies, Dr. Lois K. Smedick, for providing her support at the time when I was financially unstable. Once again, I am very much delighted to have worked with all of you, and I hope, the social maturity I have gained during my stay at Windsor, will open doors of success for me in the near future.

Table of Contents

Abstract	iv
Acknowledgements	vi
List of Contents	vii
List of Figures	ix
List of Tables	xi
List of Appendices	118

Chapter 1

1. Introduction

1.1. Area of Study	1
1.2. Distribution of Deccan Basalts	4
1.3. Objectives of Investigation	7

Chapter 2

2. Regional Setting

2.1. Composition of Deccan Lavas	9
2.2. Age of Deccan Traps	11
2.3. Sources of Eruptions	17
2.4. Structural Features	21
2.4.1. Fold Structure	23
2.5. Problems of Stratigraphic Correlation	28
2.6. Petrogenetic and Geochemical Aspects of Deccan Traps	30

Chapter 3

3. Petrography and Petrogenesis

3.1. General Petrography	31
3.2. General Petrographic Description of Thin Sections	31
3.2.1. Petrographic Descriptions from Suite No 1	32
3.2.2. Petrographic Descriptions from Suite No 2	37
3.3. Description of Zeolites in the Study Area	39
3.4. Sequence of Crystallization and Mineral Paragenesis	44
3.4.1. Mineral Paragenesis of Basalts in the Study Area	45

Chapter 4

4. Geochemistry

4.1. Geochemical Methods Used for Analysis	48
4.2. Alteration of the Rocks as Recognized by LMPR Diagrams	54
4.3. Geochemical Variations Observed within Suite	58
4.3.1. Major Elements Variation	63
4.3.2. Trace Elements Variation	66
4.4. Petrogenesis of Basalts in the Study Area	73
4.5. Fractional Crystallization and Partial Melting Model	74

Chapter 5

5. Geochemical Stratigraphy

5.1. General Stratigraphy of Deccan Traps	80
5.2. Flow Stratigraphy of Thakurvadi Formation	86
5.3. Results of Present Study	91
5.4. Discussion	98

Chapter 6

6. Bedrock Geohydrology

6.1. Lava Flows in Deccan Trap region	101
6.2. Interflow Beds and Soil Horizons in Deccan Trap region	106
6.3. Description of Lineaments over Deccan Traps	107

Conclusions	113
--------------------	-----

References Cited	114
-------------------------	-----

Appendices	118
-------------------	-----

Vita Auctoris	133
----------------------	-----

List of Figures

Figure 1.	Map of India showing Maharashtra State and location of the study area	2
Figure 2.	Location of the study area	3
Figure 3.	Map of India showing distribution of Deccan Traps	5
Figure 4a.	Distribution of dykes over Western Ghats in Deccan Traps	19
Figure 4b.	Distribution of dykes along Narmada-Tapti Zone	19
Figure 5.	Tectonic framework of the western part of Deccan volcanic province	22
Figure 6.	Evolution of E-W structure in the Traps	26
Figure 7.	Evolution of E-W and N-S section across the geological map	27
Figure 8.	Section across a subsiding volcanic pile erupted from a migrating edifice	27
Figure 9.	Mineral assemblage photomicrograph of basalts representative of Suite # 1	33
Figure 10.	Mineral assemblage photomicrograph of basalts representative of Suite # 2	33
Figure 11.	Photomicrograph showing groundmass with intergranular and intersertal texture of basalts in the study area	34
Figure 12.	Photomicrograph showing sub-ophitic and intersertal texture of basalts in the study area	34
Figure 13.	Photomicrograph showing occurrence of textural domains of basalts in the study area	35
Figure 14.	Photomicrograph of basalts in the study area showing olivine enclosed by clinopyroxene phenocryst	35

Figure 15A-E	Photomicrographs of various zeolites in the study area	40
Figure 16.	Mineral paragenesis showing sequence of crystallization of basalts in the study area.	45
Figure 17.	Log Molecular Proportion Plots with K_2O and Na_2O	56
Figure 18.	Major element variation diagrams vs. Zr	64
Figure 19.	Trace element variation diagrams vs. Zr	67
Figure 20.	MgO-FeO sail diagram of Hanson and Langmuir (1978)	75
Figure 21.	Zr/Y vs. Zr plot of Pearce and Norry (1979)	77
Figure 22.	Nb;Y and; TiO_2 vs. Zr plots of Pearce and Norry (1979)	78
Figure 23.	Stratigraphic cross-section along the Western Ghats showing formation boundaries in Deccan Traps	82
Figure 24.	Geological sketch map of different formations in the Western Ghats of the Deccan Traps	83
Figure 25.	Chemical types in the Thakurvadi Formation of the reference section and its comparison with the geochemical and petrological analysis of basalt samples from Akole Taluka	95
Figure 26.	Intraflow structure of basalts in Deccan Traps	103
Figure 27.	Features associated with lava flows in Deccan Traps	105
Figure 28.	Length histogram for the lineaments in Deccan Traps	109
Figure 29.	Distribution of lineaments over Deccan Traps	110
Figure 30.	Rose diagrams showing principal and secondary direction of the lineaments in study area	111

List of Tables

Table 1.	Whole rock K- Ar ages of Deccan Traps	13
Table 2.	Evolution of Deccan Traps: a proposed time scale	15
Table 3.	Precision values of trace elements	52
Table 4.	Accuracy values of trace elements	53
Table 5.	Major element chemistry of Deccan basalts in Akole Taluka	59
Table 6.	Trace element chemistry of Deccan basalts in Akole Taluka	61
Table 7.	Lithostratigraphic sub-division of Deccan basalts in Western Ghats	81
Table 8.	Chemical types of Khadri et al. (1988); their petrographic and chemical characteristics	88
Table 9.	Elevation vs. chemical and petrographic features of the samples from the study area	92

Chapter 1

1. Introduction

1.1. Area of Study

The project area is bounded between longitudes $73^{\circ} 45' E$ and $73^{\circ} 55' E$ and latitudes $19^{\circ} 30' N$ and $19^{\circ} 40' N$. It is a part of the Deccan Trap region of Maharashtra State, India, and is located in the northeastern part of the Western Ghats (Figs. 1 and 2). The work was carried out in the framework of research on water-resource management by the Department of Geology at the University of Windsor, Bharatiya Agro Industries Foundation and the tribal and rural people of Akole Taluka, under way in the villages of Manhere, Ambevangan and Titvi in Akole Taluka, the northwestern part of Ahmadnagar District.

The bedrock is massive basalt, commonly amygdaloidal, overlain by a shallow, though variable soil cover. Flows are nearly horizontal over wide areas and are separated by volcanic ash or red bole in places. The study area has rugged topography in the western and northern parts. The hills in the north of the area near Manhere and Ambevangan are about 1500 m above sea level. Kalsubai to the west is the highest peak (1646 m) of the Western Ghats mountain range. The drainage system consists of ephemeral streams that are tributaries of the Pravara River, which rises in the hills to the west of Lake Arthur Hill, site of the Bhandardara Dam.

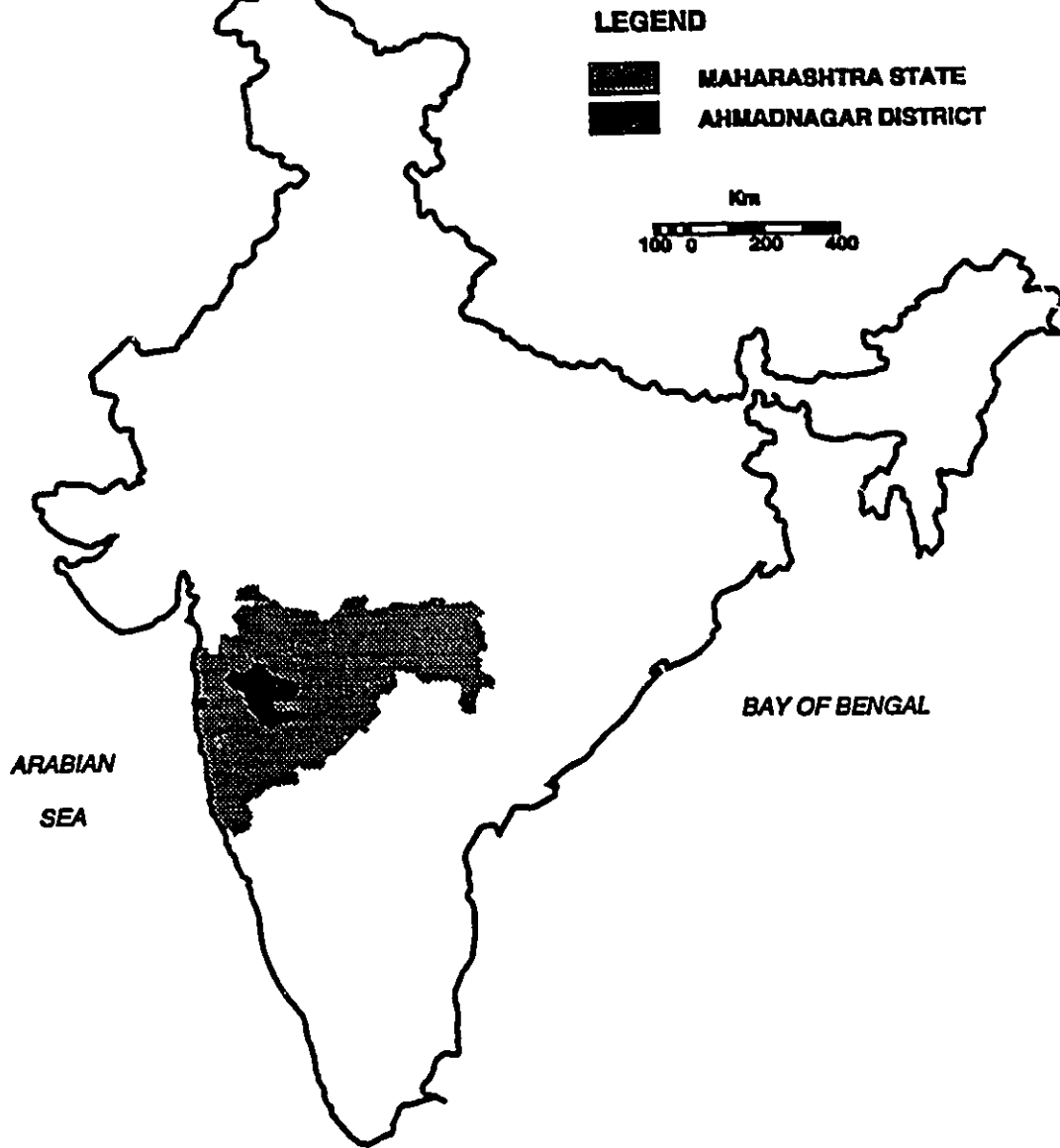


Figure 1- Map of India showing the State of Maharashtra and location of the study area.

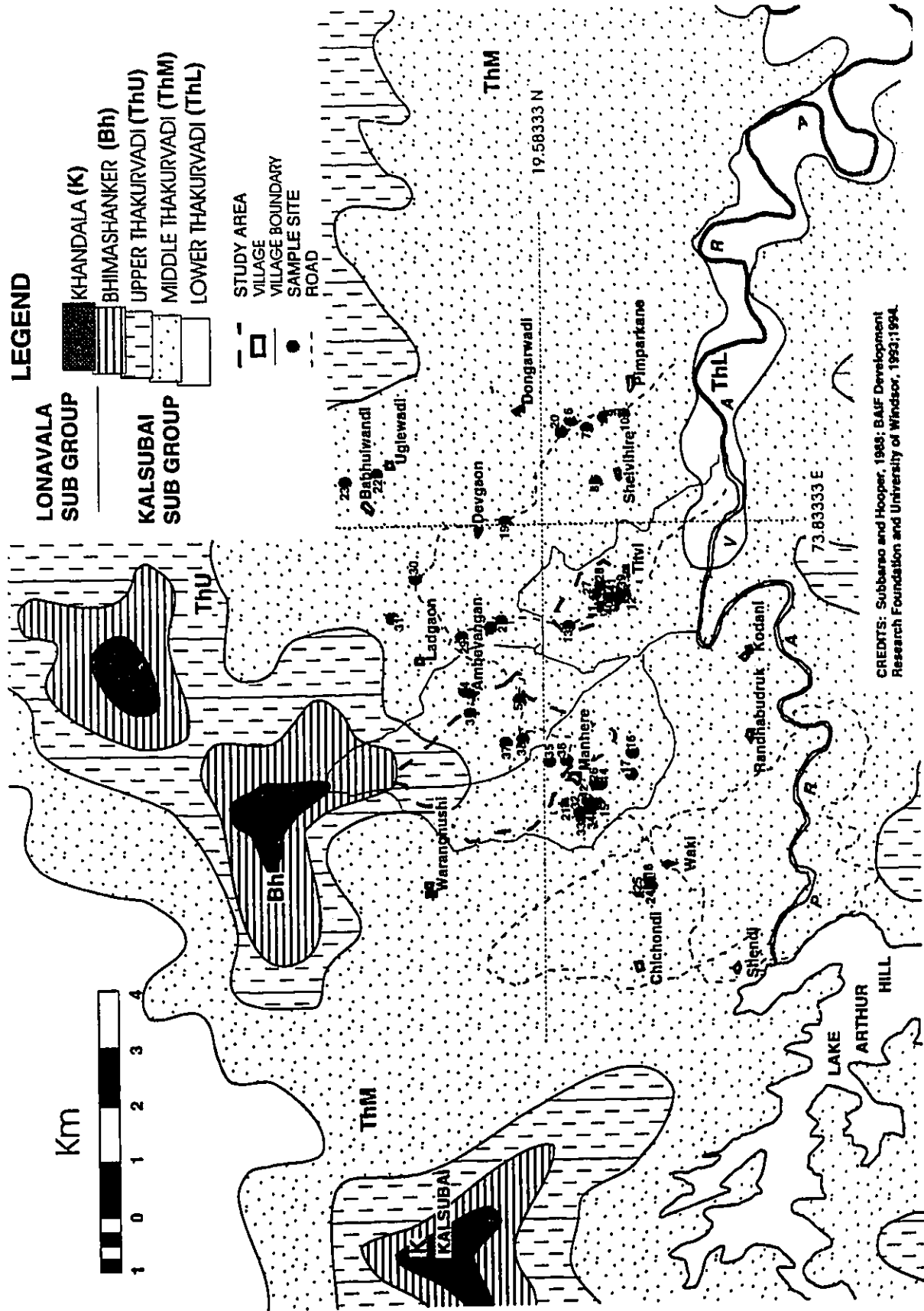


Figure 2- Map of Ahmednagar District showing location of the study area and 47 samples collected for analysis

1.2. Distribution of Deccan Basalts

The Deccan Traps (Deccan comes from a Sanskrit word meaning "south" or "southern"), occupy half-a-million square kilometres of western and central India and southernmost Pakistan (Figure 3). The account of Deccan Trap geology that follows is based to a large extent on the summary papers by Mahoney, 1988; Sukeshwal et al (1981) and; Alexander (1981). The traps rest on, and probably were erupted through the predominantly Archean crust of the Indian Shield. The area covered by lavas originally exceeded 1,500,000 km². Off-shore drilling and geophysical surveys indicate that a considerable portion of the volcanic pile is downfaulted to the west beneath the Arabian Sea (Fig. 3), probably extending to the edge of the continental shelf. Deccan basalt flows have also been encountered to the northwest in southern Pakistan and as far away as Cochin in the south. Deccan outliers are also found beyond the main body of the flows within India. However, recognition of Deccan Basalts in isolated outcrops as far away as Afghanistan is questionable.

The Deccan Trap region is divisible into four subprovinces (Figure 3). The Deccan proper, south of the Narmada River, the Malwa Plateau north of the Narmada River, the Mandla lobe in the northeast, and the Saurashtran Plateau in the northwest. The basalts are nearly horizontal, with dips of 1° or less mainly to the south-east (West, 1959; Raja Rao et al., 1978, in Mahoney, 1988, p. 152).

However, significant departures from the horizontal occur mainly in a zone, extending northward into the Cambay graben, and in an east-west belt along Narmada River,

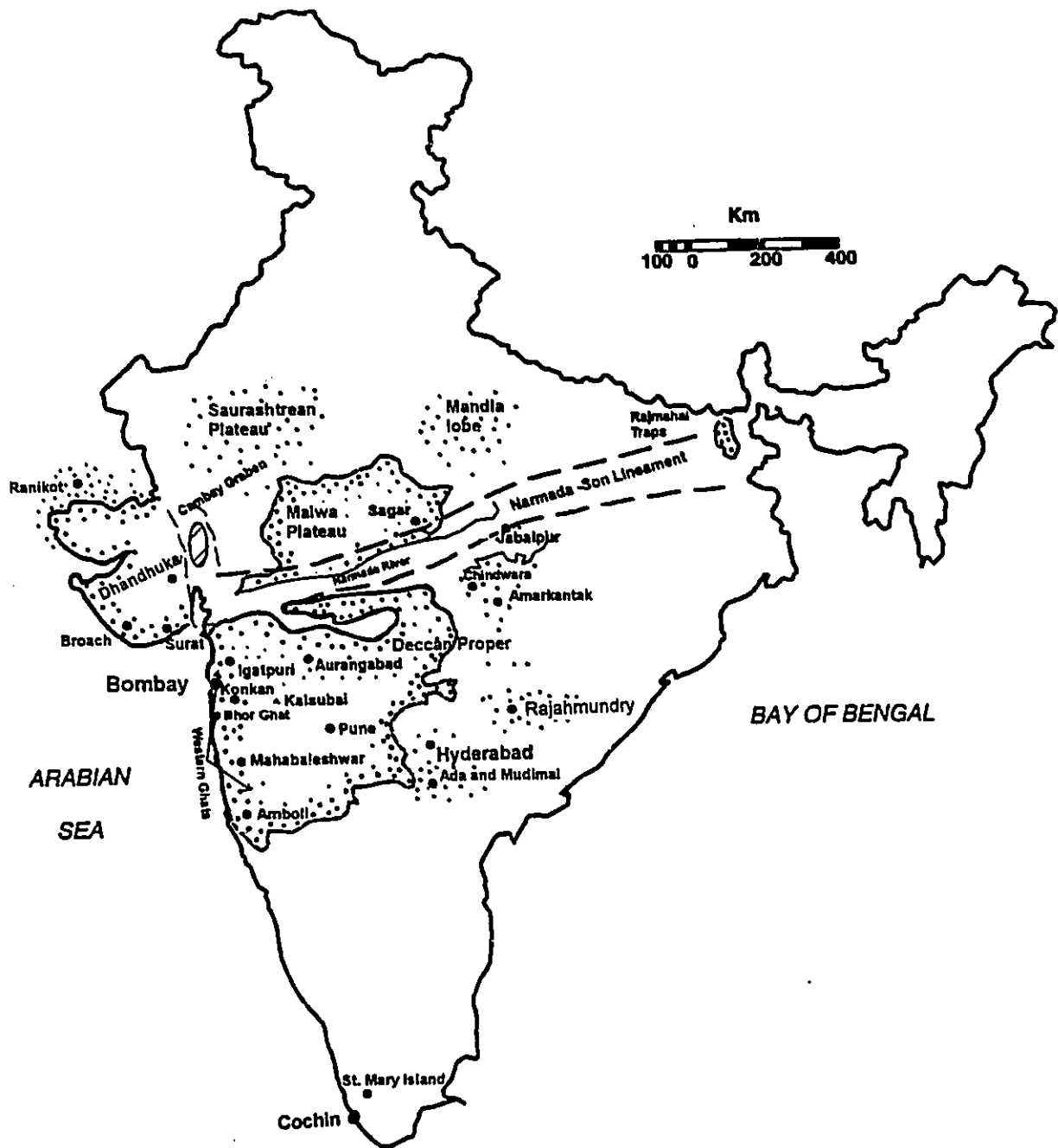


Figure 3- Map of India showing Deccan Traps. The Narmada- Son Lineament and Cambay Graben are sites of positive gravity anomalies. Modified from Mahoney (1988).

known as Narmada- Son Lineament (Fig. 3) both are regions of syn- to post- trappean tectonic activity.

The lava pile is thinnest in the east, thickening westward along the Western Ghats mountain range. Over most of their outcrop area, the traps form a high plateau (about 750 m above sea level) that culminates on its western flank in the ridge that forms Western Ghats. The ridge has an elevation of more than 1200 m in places and drops westward to the relatively flat and narrow Konkan coastal plain. The maximum exposed vertical section is about 1700 m in the Igatpuri area. Around the eastern, northern and southern fringes of the province, exposed thicknesses diminish to 200 m or less and usually account for only a few flows. Recent deep seismic-sounding surveys, running west-east from near the coast across the Deccan Plateau at the latitude of Mahabaleshwar, indicate a maximum thickness of about 1500 m near the coast, which gradually, though irregularly, decreases to approximately 400 m in the central Traps region. This suggests that the main Deccan feeder channels lie in submarine locations near the west coast, and that distal parts of the province were formed mainly by flows travelling large distances (Auden, 1949; West, 1959; Raja Rao et al., 1978; Sethna, 1981). The traps are thought to have been related to the activity of the hot spot, which later gave rise to the Chagos-Laccadive ridge (Mahoney, 1988) and is at present responsible for volcanic activity at Reunion Island.

1.3. Objectives of Investigation

The study area receives virtually all of its precipitation as monsoon rains during June through September; July and August are the wettest months. Annual precipitation ranges from up to 2000 mm in the west of the project area to 600 mm or less in the eastern part. As a result of this extreme variation in rainfall across the area, as well as the vigorous runoff affecting surface waters and high evaporation rates, most tribal people in Akole Taluka face acute shortages of water for domestic use during most of the year.

A research project was initiated by Bharatiya Agro Industries Foundation, Pune, and the Department of Geology, University of Windsor, with the tribal and rural people of Akole Taluka as partners, to develop a methodology for the year-round utilization of surface water and ground water; funding is from the International Development Research Centre, Ottawa.

Accordingly, the purpose of the research presented in this thesis was twofold: 1) to describe and explain the origin of the basalts penetrated by the dug wells in the study area and 2) to establish the geochemical stratigraphy and relations between the rock units present. The investigation employed integration of petrological and geochemical analyses of 47 rock samples, mainly collected from dug wells and blast holes.

Although the weathered bedrock and overlying soil assume greatest importance for the development of ground-water resources within the study area, the project teams from the start took the view that the application of project results in other parts of the Deccan region would require an understanding of how local bedrock geology is related to the regional stratigraphy, elaborated by Beane et al. (1986), Khadri et al. (1988) and Subbarao and

Hooper (1988). There is the additional consideration, not developed further in this report, that the chemistry of the rocks may have health implications for water users. Accordingly, the report also incorporates a brief review of the geohydrologic significance of bedrock features, including considerations of lineaments recognised on satellite imagery.

Chapter 2

2. Regional Setting

2.1. Composition of Deccan Lavas

The basaltic flows occurring in the Ahmednagar District include both pahoehoe and aa types. The pahoehoe type is dominant in the western part. A few of the pahoehoe flows, which are thick, have dark dense rock in the middle section and extend over several kilometres. These are generally altered, softer and purplish, with high volatile content (Geol. Surv. of India, 1976, p.2).

The aa flows generally show a thin zone of basal clinker, a prominent middle section of dark, dense rock and a top section of reddish altered breccia. The breccia comprises angular to rounded reddish amygdules filled with zeolites. The areas with pahoehoe flows exhibit smooth hill slopes, conical peaks and a highly dissected terrain, while an aa flow gives rise to a level terrain and steep cliffs. The tops of hills with aa flows develop plateaux. The soils derived from pahoehoe and flow breccia sections of aa flows are reddish and purplish in colour and incorporate crystals of zeolites. The slopes of Kalsubai exhibit a sequence of eight compound pahoehoe flows and one aa flow. The pahoehoe flows vary in thickness from 29 m to 151 m and the aa flow is up to 24 m (Geol. Surv. of India, 1976, p.2) thick.

Four different rock types have been identified in Deccan volcanism: tholeiite,

rhyolite, alkalic carbonatite and alkali olivine basalt. The rhyolites of the western coastal margin of India came from an independent magma with no genetic link to the tholeiites (Sukeshwala, 1981). Carbonatite/ nephelinite rocks that occur in the Deccan Trap also have no genetic link with the tholeiites of the area. The alkali olivine basalts within the tholeiites have been studied by Sukeshwala (1981), who recorded the occurrence of peridotite nodules in them. Picritic basalts in areas, such as Saurashtra and Igatpuri, represent the parent magma of the Deccan trap lavas. The normal tholeiitic basalts of widespread distribution across the region are derived mainly as a result of differentiation and fractionation of the early crystallizing Mg- rich olivine and pyroxene from the parent magma (Sethna et al., 1988).

Stratigraphic relationships (Beane et al., 1986) show that the Igatpuri basalts (in the north) are older than lava flows occurring further south along the Western Ghats, strengthening the possibility of picrite basaltic magma being the parent type (Sethna et al., 1988). The mineralogical variation in composition for both olivine and pyroxene also support this view (Sethna et al., 1988).

Swanson and Wright (1978) ; Wright and Helz (1979, in Sukeshwala, 1981, pp. 13) suggested that magma compositions were controlled mainly by partial melting. They suggested that mantle from which the tholeiite basalts originated, is not everywhere of the same composition; the basaltic lavas carry a chemical imprint, related to their origin by partial melting in the mantle. Sen (1986) suggested that common Deccan Trap tholeiite are products of crystal-liquid fractionation processes and are derived from primary (or near-primary) magmas generated at a shallow (35-45 km) depth.

2.2. Age of Deccan Traps

The age of the Deccan basalt has been much debated and misunderstood, despite abundant paleontological, geochronological, and paleomagnetic data and good knowledge of the plate- tectonic events involving the Indo-Pakistani subcontinent during Mesozoic through Tertiary time. Opinions differ as to whether the basalts were wholly Tertiary, or wholly or partly Cretaceous. Paleontological evidence such as intercalated *Cardita beaumonti* beds associated with basaltic flows at Ranikot, Sind, suggest volcanic periods before and after Danian time (70 Ma). The Nummulite Beds at Surat and Broach, overlying the traps suggest eruptions in pre-Eocene time, while at Chindwara basalt flows overlying limestone beds suggest post-early Eocene (55Ma) volcanic activity. In the Rajamundari area, basalts overlie marine Cretaceous sandstones and contain sedimentary horizons of Eocene age, indicating that trap extrusions started after Cenomanian time and extended well into the Eocene; hence do not support a short duration of volcanism (Sukeshwala, 1981).

The age of the Deccan basalts, based on the fossil evidence from the infra -strata and intertrappean sediments and on radiometric dating has long been debated. The intertrappean sediments are mostly non-marine, but contain benthonic microfossils at few places. The occurrence of the foraminiferal species *Globotruncana*, *Hetrohelix striata* and *Pseudotextularia browni* suggests that they range in age from Late Cretaceous to Early Eocene (Shastri, 1963). He also suggested that the marine intertrappean sediments along the east coast of India also indicate a Late Cretaceous age, and intertrappean strata found near Rajahmundry indicate a Paleocene-Early Eocene age. Rao and Yadagiri (1979, in

Alexander, 1981, p.252) discovered dinosaurian bones in the intertrappean beds near the villages of Ada and Mudimal in Andhra-Pradesh which also suggest a Cretaceous age for the Deccan lavas. Klootwijk (1979, in Alexander, 1981, p. 252), assigned an Early Cretaceous age (100-105 Ma) to the Rajmahal Traps, on the basis of radiometric data. Thus the Rajmahal Traps are also considered to be as a part of Deccan volcanic episode (Fig. 3).

Agarwal and Rama (1976, in Alexander, 1981, p. 251) presented K-Ar ages for Deccan basalts in Western India from 62.9 to 59.7 Ma, and also from the northeastern corner of the Deccan province, which show an age of 47 Ma (Table 1). Therefore, it has been proposed that the major volcanic episodes in the eruptive history of the Deccan Trap were from 65 to 60 Ma (the main phase) and during 50 to 42 Ma. Flows near the bottom of the sequence at Dhandhuka (Alexander, 1979) were found to be 101.7 Ma in age.

Similarly, K-Ar dating of lavas from different sources such as the acid igneous rocks from St. Mary Island (South Kanara District; Fig. 3) yields a mean of 93.1 ± 2.4 Ma; the Rajmahal volcanics range from 109-69 Ma. This shows that the age of Deccan Trap volcanism extended well beyond the conventionally accepted age range from 65 to 60 Ma span for the total period of active volcanism. However, K-Ar age determinations have not solved the problem of the time range of Deccan volcanism completely, because the distribution of the reported K-Ar ages is very sparse in relation to the enormous volume of Deccan volcanic rocks. A tentative time scale for the evolution of the Deccan Traps is presented in Table 2.

Table 1- Whole Rock K-Ar Ages of Deccan Traps (Modified from Alexander (1981))

<u>Locality/rock-type</u>	<u>K-Ar Age (m.y.)</u>		<u>Reference</u>
A) Mount Pawagarh			
Basalt	65	±5	Rama (1968)
Basalt	60.3	±1.4	McElhinny
	63.2	±1.2	(1970)
Basalt	65.6	±1.7	Kaneoka and Haramura
Ankaramite	66.2	±1.4	-do- (1974)
Basalt	63.5	±2	Alexander (1977)
Rhyolite	43	±2	Rama (1968)
Rhyolite	61.1	±1.2	Wellman and McElhinny (1970)
B) Mount Girnar			
Basalt	59.1	±1.1	Wellman and McElhinny (1970)
Gabbro, diorite, syenite lamprophyre and acid porphyry	56.7	to 64	Paul et al., (1977)
C) Other areas in Western India			
Malad, trachyte	60	±3	Rama (1968)
Andheri, basalt	45	±3	-do-
Mahabaleshwar, basalt	40	to 62	Kaneoka and Harumara
Amboli, basalt	51	to 60	-do- (1973)
Bombay, mugearite	37.7	±0.9	-do-
Bhor Ghat	62.6	±1.5	Agarwal and Rama
Satara, basalt	62.6	±1.7	-do- (1973)
Khandala, basalts	4.2		-do-
Dhandhuka, basalts	62.7	to 101.7	Alexander (1977)
Koyna, basalt	31.1	±1	-do-
Dohad, basalt	37.3	±1.2	-do-
Igatpuri, basalt	63	to 83m.y	Kaneoka (1978)
Bombay, basalt	85		-do-
Mahabaleshwar, basalt	64		-do-
Osam Hill, rhyolite	64		-do-
St. Mary's Islands, acid volcanoes	92		Subbarao (1979)

D. Areas in Central India

Chindwara, Amarkantak, basalts	47		± 1.5	Agarwal and Rama (1976)
Sagar, basalts	41.7	to	50	Alexander (1977)
Manpur, basalts	50.8	to	62.5	Karkare and Singh (1977)

E. Deccan Trap Dykes

Lonawala, Western India	42		± 3	Hama (1968)
Deccan trap dykes, W. India	34	to	63	Agarwal and Rama (1976)
Sardhar dyke, Saurashtra	46		± 1.5	Alexander (1977)

F. Gondwana Dykes

Gondwana dykes	56	to	111	Agarwal and Rama (1976)
Panchmari dykes	61.3		± 2	Alexander (1977)

G. Rajmahal Traps

	81.8	to	109	McDougall and McElhinny (1970)
--	------	----	-----	-----------------------------------

Table 2 - Evolution of Deccan Basalts: A Proposed Time Scale

42-31 Ma	<i>Eocene to Oligocene</i> : Low-intensity volcanism giving rise to some younger flows, and post-trap activity up to Oligocene.
50-42 Ma	<i>Eocene</i> : Another significant episode of Deccan trap activity, which gave rise to Deccan Traps of northeastern and other peripheral areas such as Sagar, Jabalpur, Amarkantak and Malwa.
65-60 Ma	<i>Paleocene</i> : Major episode of Deccan Trap activity, which gave rise to about 2/3 of the Deccan Traps, particularly of the western part.
100 Ma	<i>End of Early Cretaceous</i> : Extrusion of Rajmahal traps (105-100 Ma) and the earliest Deccan Trap flows at Saurashtra (101 ± 3 Ma)
110 Ma	Separation of Africa from India, Australia, New Zealand and Antarctica (Heirtzler, 1958)

Wellman and McElhinny (1970, in Alexander, 1981, p. 252) on the basis of K-Ar dating, proposed that the whole of the Deccan Traps were extruded in just 5 Ma. Paleomagnetic work on the Deccan basalts shows that the vast majority of exposed sections contain no more than one polarity reversal. Paleomagnetic studies demonstrated that only a single reverse-to-normal polarity sequence characterises most of the lava succession, preceded by a much more restricted normal-to-reversed transition. It has been proposed (Pal, 1971, in Alexander, 1981, p. 252) that a single reversal model could be valid for some limited areas of the Deccan province, but cannot be applied to the entire Deccan province.

Kono et al., (1972, in Alexander, 1981, p. 252) rightly limited one reversal model to the Western Ghats. The results of several paleomagnetic studies done lately, suggest that the geomagnetic polarity inversions occurred a couple of times during eruption of the Deccan lavas. The Sagar lava pile, shows two reversals of the geomagnetic field (Sukeshwala, 1981). Pal (1975) suggested that the trappean eruptions continued over a protracted period, probably 70-40 Ma.

A comparison of the Deccan volcanic episode with other flood basalt provinces such as the Siberian traps representing a total time span of 150 Ma, the Karoo basalt of South Africa (190-154 Ma), the Parana province of Brazil (20 Ma), and the Patagonia Plateau of Argentina (70 Ma) duration suggest that the comparatively short period of 5 Ma duration for the eruptions of entire Deccan Trap is an underestimate. It is also believed that the total volume of Deccan basalt erupted is much more than that of the other flood basalt provinces mentioned above (Alexander, 1970). Either the greatest volume is erupted in a short time span, or the rate of eruption must have differed from place to place. There could have been some periods of vigorous extrusion also, and the volcanic activity would have been distinctly episodic rather than continuous.

Basaltic flows, which occur over the entire Ahmednagar District, and form a part of Deccan Trap are considered to be of Upper Cretaceous-Lower Eocene age (Geol. Surv. of Ind., 1976). The dykes occurring at several places are also considered to be of the same period as the flows.

2.3. Sources of Eruptions

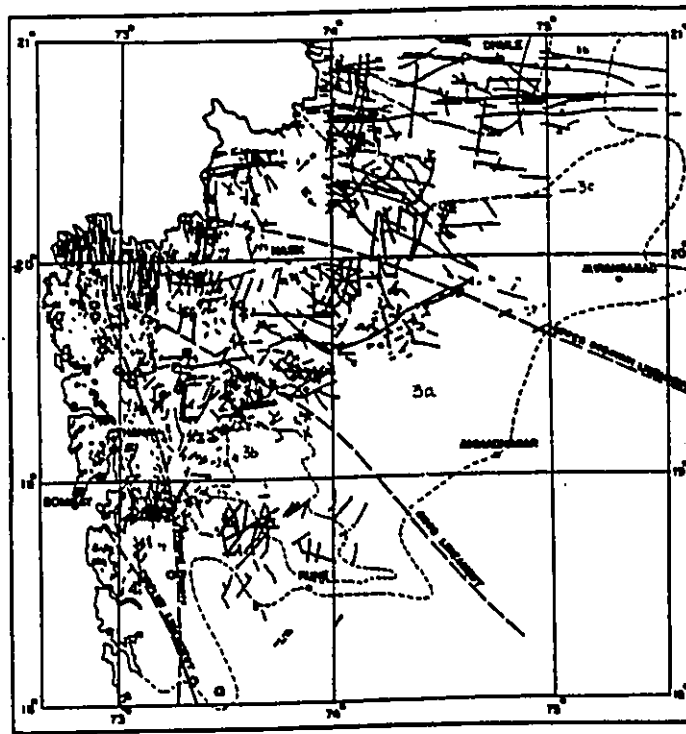
Many workers (Auden, 1949; West, 1959; Wadia, 1966, in Mahoney, 1988, p. 155) proposed that the main Deccan feeder channels lie near the west coast and that distal parts of the province were formed mainly by flows travelling great distances. Many of the eastern and northeastern flows are extensive; the western Deccan on the other hand, appears to contain many flows of restricted extent, implying relatively nearby sources. The Geological Survey of India classified a substantial portion of Deccan into areas dominated by simple flows and by compound flows (Raja Rao et al., 1978) respectively. Compound flows are massive, poorly jointed, and amygdaloidal. They are laterally discontinuous, with ropy structures developed in the upper part. Simple flows, in contrast, are nonamygdaloidal except for vesicular flow tops or flow-top breccias. They may be distinguished in the field by grain size and phenocryst mineralogy. Compound flows includes regions of west coast from south of Bombay to the Gulf of Cambay, and an apex in the central trap near Aurangabad (Fig.3). Compound flows are also common in Saurashtra, west of the Cambay Graben (Raja Rao et al, 1978; Figure 3). Layers of ash and pyroclastics are common in the same areas (Das and Dixit, 1972, in Mahoney, 1988, p. 155; Raja Rao et al., 1978). Both compound flows and ash beds are indicative of relative proximity to the sites of eruption. These provide abundant evidence that places the major eruptive sources in the western part of the province, roughly between Bombay and Cambay.

Because of the flat lying nature of the Deccan Trap lavas and absence of any cone- and- crater structures, it is widely accepted that the Deccan basalts are erupted through

fissures, but whether true Columbia River- type fissure swarms are present in this region remains unknown. Across a large part of Deccan Traps, dykes are not seen. Auden (1949), Agashe and Gupte (1972), and Agarwal and Rama (1976, in Beane et al., 1986, p. 82) reported numerous dykes, many of considerable width and length, present in the Deccan basalt province. For example, on the Malwa plateau, north of the Narmada lineament, dykes extend up to 500 m in length, while in the area of Narmada rift zone they extend up to 750m, but there has been a long-standing question as to whether they represent the feeder system for the main sequence of lava flows.

In the greater part of Deccan Traps, mafic dykes occur in clusters and swarms in tectonic belts parallelling the north-south trending west coast and east-west trending Narmada lineament. Auden (1949) observed that the directions of folding and fractures to which the Deccan Trap have been subjected, coincide with the trends of the dyke systems in this area. Along the west coast, the major trend followed by dykes is north-south to north- northwest - south- southeast and north- northeast - south- southwest, roughly parallel to the west coast, the Western Ghats and the Panvel flexural lineament . In the Narmada - Tapti belt, the majority of dykes are aligned east-west and east- northeast - west- southwest and east- southeast - west- northwest directions parallel to the Narmada-Tapti lineaments.

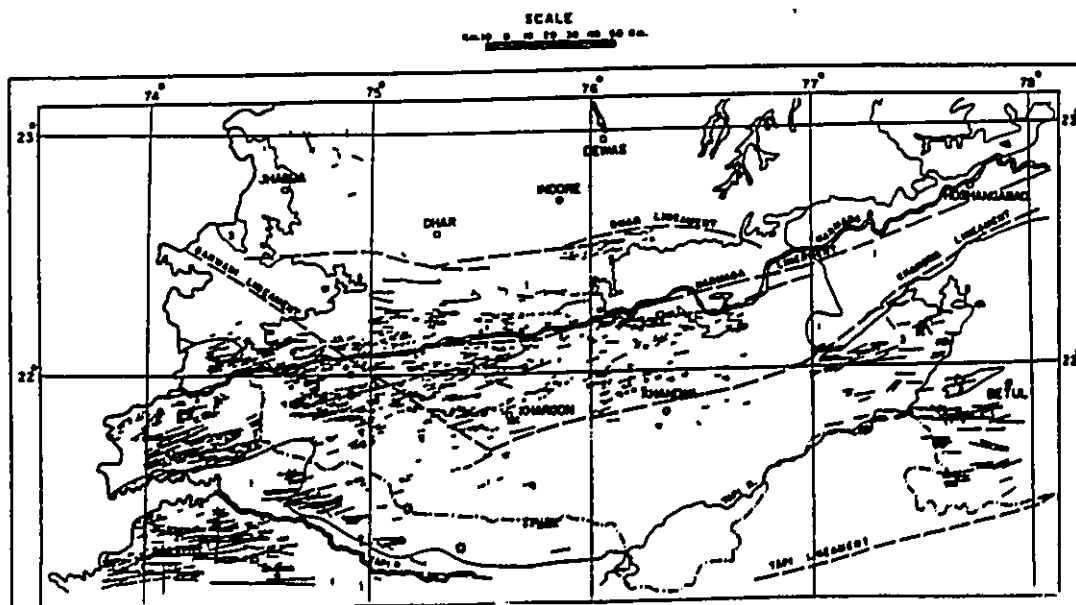
In the region distant from the main dyke swarm, in the plateau area, to the east of the coastal belt, and to the south of the Tapti lineament, dykes are oriented in triangular stellate patterns (Figures 4a,b). Hence four major trends are recognised a) between north- northwest and north- northeast b) west- northwest and west- southwest, c) northwest - southeast, and d) northeast -southwest. The north- northeast - north- northwest trending dykes on the west



- | | | | |
|--|---------------------------------------|---|--------------------------|
| ALLUVIUM | DECCAN TRAP | 5c. Pahoehoe flows with number of AA flows. | AREA OF CARBONATE DYKES |
| BASIC DYKES | 3b. Pahoehoe flows with rare AA flows | 5b. Pahoehoe flows with rare AA flows | AREA OF ULTRABASIC DYKES |
| 3a. AA flows with rare pahoehoe flows. | THERMAL SPRING | AREA OF SILLS | MEGA - LINEAMENTS |
| AREA OF ACID AND ALKALINE DYKES | | | |

Figure 4a- Distribution of dykes over Western Ghats of Deccan Traps. The major trend followed by dykes is N-S to NNW-SSE and NNE-SSW, roughly parallel to west coast.

Figure 4b- Distribution of dykes along Narmada-Tapti Zone. The majority of dykes are aligned E-W and ENE-WSW and ESE-WNW.



coast are younger than those trending in the other direction (Devey et al. 1988).

Most of the dykes cut flows of all ages and appear to represent events late in the eruptive history of the Deccan province. They are unlikely to represent the feeder system for the main sequence of flows forming the Western Ghats. This may point to the post-trap hypabyssal nature of most of the intrusives. Nevertheless, some dykes feeding the flows have been reported (Ghosh and Pal, 1984; Walker, 1967, in Deshmukh, 1988, p. 333). For example, some of these dykes are similar in chemical and mineralogical composition to the main sequence of basalt flows which strongly implies that they are the feeder system by which the Deccan basalt magma reached the surface. The overall ages of dykes and flows (Paul et al, 1977; Agarwal and Rama, 1976; Alexander, 1977; Balasubramanian and Snelling, 1981, in Deshmukh, 1988, p. 333) also suggest that the older dykes may be approximately coeval with the flows and may possibly have fed them.

The basaltic flows of the Ahmednagar District are also intruded by dykes, both of which have a similar mineralogical composition (Geol. Soc. of India., 1976, p. 5). In the north of Godavari, the dykes are up to 12 m in width and run for several kilometres along $N60^{\circ}E-S60^{\circ}W$, NW-SE or $N5^{\circ}$ and $10^{\circ}W$ directions. Several dykes are reported in area NW of Ahmednagar District, where pahoehoe flows are dominant.

Sengupta (1967); Raju et al.(1972, in Mahoney, 1988, p. 154) showed that the Cambay Graben and the Narmada-Tapti and west coast tectonic belts are characterized by positive gravity anomalies, higher gravity and thermal gradients and seismic activity (Kailasram, et al. 1972; Gupta and Gaur, 1984, in Deshmukh, 1988, p. 335). The high gravity gradients are considered to be related to deep-seated regions marking areas of crustal

thinning, upwarping of the asthenospheric shell, and deep-seated, large plutonic bodies and magma chambers. These studies further suggest that in the west coast and Narmada lineament belts, the crustal section is divided into blocks which have moved up and down; hence appears highly fractured and faulted. The major lineaments in the Deccan Traps are also seen to be parallel to the tectonic belts. These lineaments extend for several kilometres and most of the faults; fractures and dykes follow these trends. The lineaments are considered to have been related to deep-seated phenomena, along with some fractures reaching the mantle depths, and thus supplying the material from hot spots for Deccan Trap eruptions.

2.4. Structural Features

Large faults in the Deccan, along with flexures and significant dyke intrusions, are confined mainly to three areas 1) the west coast belt, 2) the Narmada -Son Lineament and the Tapti lineament, 3) the Cambay Graben, Panvel flexure (Auden, 1949; Raju et al., 1972; Raja Rao et al., 1978; Kaila et al., 1979; see Figures 3 and 5). These are broadly the regions where alkalic, ultramafic and acidic rocks respectively occur. The west coast and Cambay Graben are associated with well defined positive gravity anomalies (Glennie, 1951; Takin, 1966; Krishnaswamy, 1981; Quershy, 1981, in Mahoney, 1988, p. 154). Large heat flow¹ have been measured in the Cambay Graben and offshore (Gupta and Gaur, 1984, in Mahoney, 1988, p. 154), with a line of 21 thermal springs running down the west coast. These features, the geometrical arrangement of the three zones, and data on Late Cretaceous

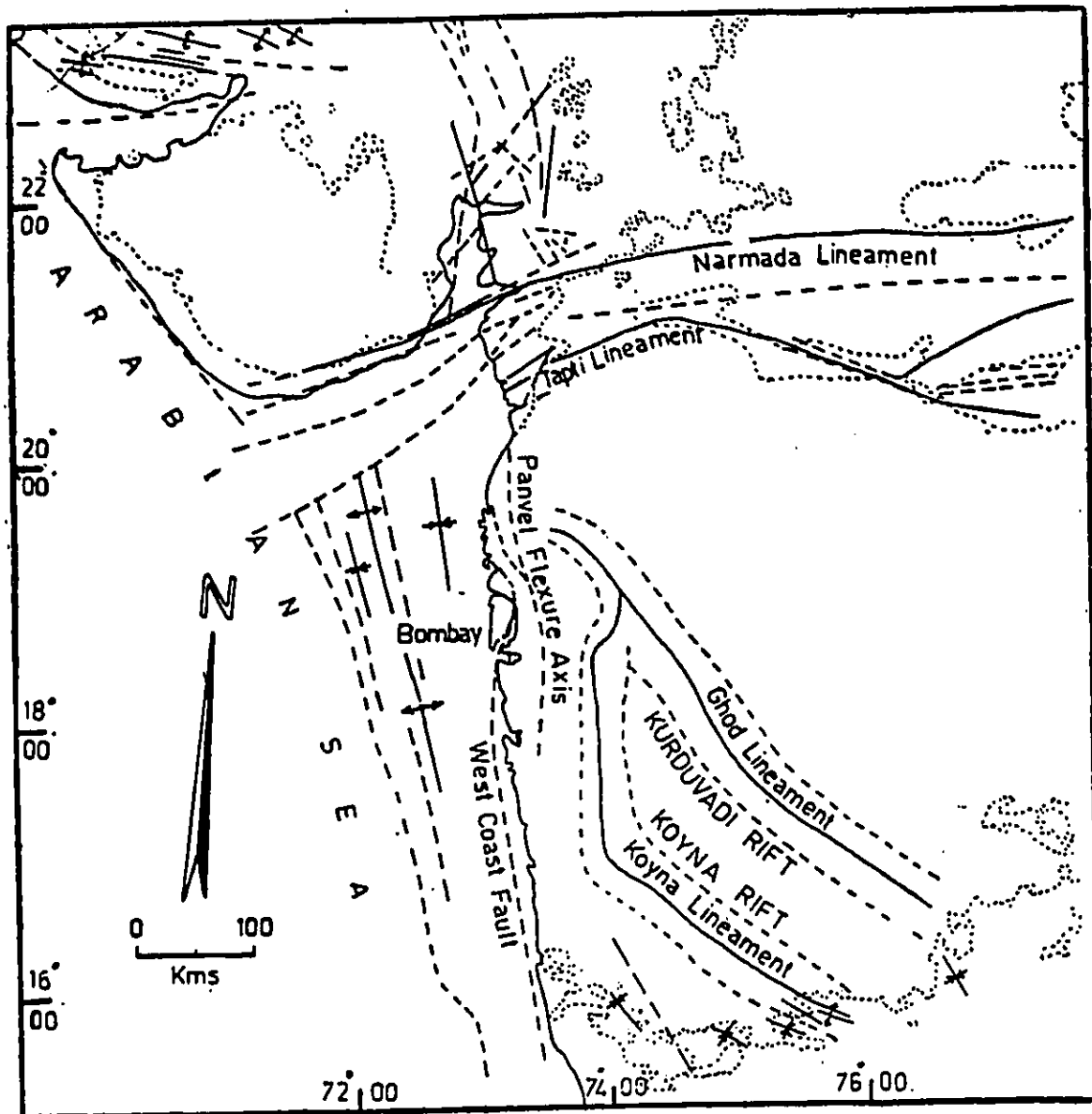


Figure 5- Tectonic framework of the western part of the Deccan Volcanic Province. Modified from Powar (1981).

plate tectonics suggests that a triple junction existed in the Cambay region during the Deccan eruptive episode, with the possibility that the Cambay Graben is a failed rift arm or marginal aulacogen.

In addition to the three tectonically active belts, and block faulting along the parts of Western Ghats, Krishna Brahman and Negi (1973, in Powar, 1981, p. 54) have postulated the existence of basement rifts, the Kurudvadi rift and Koyna rift, in the inland region. Powar (1981) also reported the presence of the Ghod lineament and the Koyna lineament (Fig. 5).

2.4.1. Fold Structures

The fold structures present in the Deccan Traps are explained with reference to the plate tectonic reconstructions for the Indian Ocean and Arabian Sea, which show that India was rifting from the Seychelles Bank at about the time of eruption of the traps (Norton and Sclater, 1979). At the same time, India was moving northwards at between 15 and 20 cm/year (Pierce 1978; Norton and Sclater, 1979; Patriat and Achache, 1984, in Devey, 1986, p. 201). Hence rifting of the western Indian margin; and India's relatively rapid northward movement were probably important factors in the generation of the fold structures seen in the Traps at present. The fold structures of the Deccan Traps are divided into three separate components of dip.

1) The dip of formation boundaries in the west of the Western Ghats, is to the west and south-west, and is generally the steepest amounting to 10° - 20° (Fig. 7). The Panvel

flexure, a coastal monocline with a seaward dipping westerly limb, is present to the north of this area. The axis of the Panvel flexure dies out southwards, and is parallel to the anticlinal axis. Biswas (1982, in Devey, 1986, p. 202) through seismic studies in the Arabian sea off Bombay, proposed that N-S trending structures occur down to the basement; these are probably Deccan or pre-Deccan in age. In addition, relatively steep westerly dips associated with these basalts, are thought to be separated from the gently dipping basalt on the eastern side by a north-south trending fault. It is likely possible that, the Panvel flexure and the anticlinal structure are the results of slight warping of the crust in response to the rifting, or by draping of the basalts over deep trans-crustal faults (Auden, 1949).

2) An easterly dip, about 2-3 ° occurs in the rocks to the east of the Western Ghats mountain chain. Lavas dipping to the east on the eastern side of the Western Ghat ridge suggest that, the ridge- forming event was post eruptive. The strong control of the ridge on the drainage of India, and its large elevation imply that it is a result of uplift of the western margin of India (Devey, 1986). Several explanations for epeirogenic events have been proposed. McKenzie (1984, in Devey, 1986, p. 204) has demonstrated that underplating of the continental crust can lead to permanent thickening of the crust, and hence generate uplift at the surface (Fig. 6). McKenzie (1984) suggested that uplift generated by underplating is permanent, in contrast with other mechanisms, which rely essentially on heating and expansion of the mantle to produce uplift. However, it is unlikely that such underplating could have taken place as far as over a distance of some 1000 km to the south, where no surface expression of volcanic activity is seen. This is further supported by the fact that the Chagos-Laccadive ridge, the postulated trace of the hot spot responsible for the Deccan

magmaism (Morgan 1972; Whitmarsh, 1974, in Devey, 1986, p. 204), separates from the Indian continental shelf at approximately the same latitude as the present- day southerly limit of basalt exposure. Figure 5 summarizes the proposed evolution of the E-W structure in the Deccan region.

3) The southerly dip of Deccan basalts amounting 1-2 °, its relationship to basement, and lateral extent of the formations are all major problems as shown by the N-S section (Fig. 7). From considerations of isostasy, it is very unlikely that the Trap/basement contact located about 1000 m below sea-level (northerly end of the section B-B in Fig. 7) would have existed, when the traps were erupted. There must have been subsidence of a greater magnitude in the north than in the south. Beane et al. (1986) favoured a model involving deposition on the flanks of a migrating volcanic centre to explain the southerly dip, and proposed an overstepping arrangement for the formations. They also suggested that overstepping arrangement of formations, at the same time, allowed the basement contact to subside more in the north than in the south. However, it is important to note that, India was migrating northwards at about 15 cm/year, and this could account for a southward migration of the centre of eruption as India moved northwards. Beane et al. (1986) postulated the migration of a volcanic edifice (cone) at varying rates across land surface. The output of this model is shown in Fig. 8. Each successive cone is offset from the previous one by about 10 % of the diameter of the base, and approximately 70 % of the subsidence of the previous cone occurred before the next one was formed. Beane et al. (1986) assumed that if the contacts between the subsided cones are used to represent the formation boundaries, then the model can be used to account for the southerly dip seen in the lavas. This

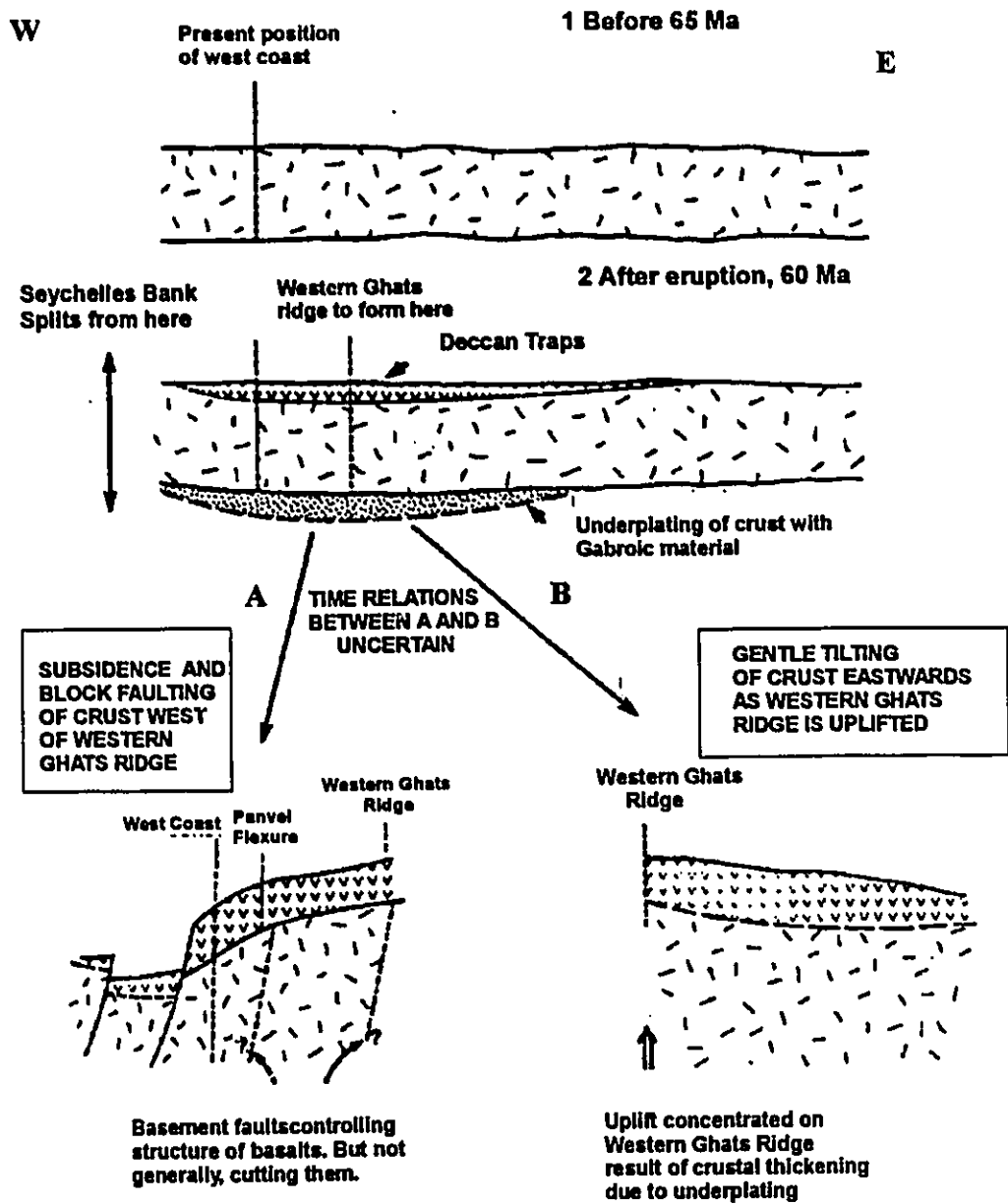


Figure 6- Illustration of evolution of the east-west structure in the Traps with time. Modified from Devey and Lightfoot (1986).

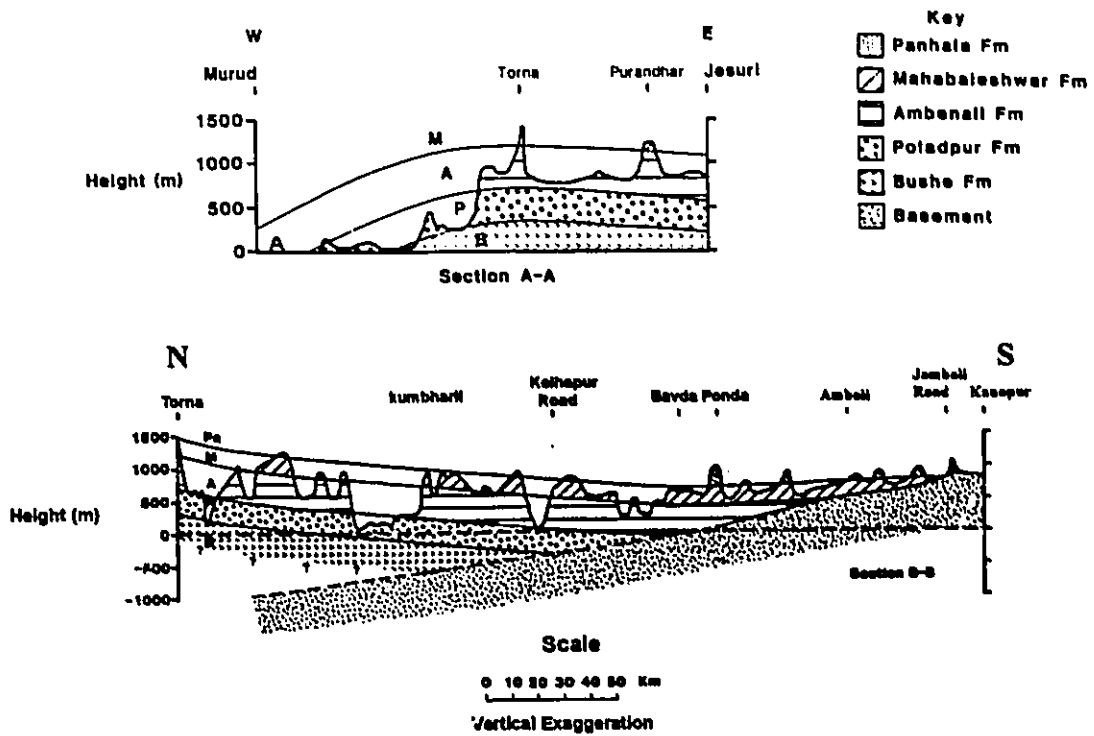


Figure 7- E-W and N-S section through the lava pile across the geological map of southern Deccan Trap. Modified from Devey and Lightfoot (1986).

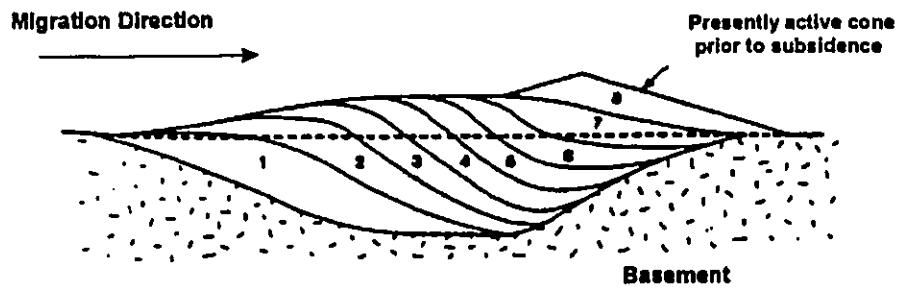


Figure 8- Section across a subsiding volcanic pile erupted from a migrating edifice. Modified from Devey and Lightfoot (1986).

assumption was found to be in accordance with the observation that formation boundaries represent major changes in lava composition, in most cases involving some degree of contamination of the lavas (Cox and Hawkesworth, 1985, in Devey, 1986, p. 204).

One major problem, not apparent from Figure 7, is the appearance of a synclinal structure with an axis perpendicular to the postulated direction of migration of the volcanic cones. This structure arises from the differences in the amount of subsidence which occurs between the centre and the edge of the cone. The possible reason for the lack of any evidence for a synclinal structure could be deposition of a constant thickness of material along any E-W section, so the volcanic edifice at any point would have formed an E-W trending ridge, migrating southwards rather than being conical in shape. This possible morphology; however, suggests more likely that the feeder system trended N-S, rather than in the E-W direction (Auden, 1949).

2.5. Problems of Stratigraphic Correlations

Paleomagnetic work on the Deccan lavas shows that vast majority of exposed sections contain no more than one polarity reversal, making palaeomagnetic correlation difficult without additional controls. Generally they show a reverse-to-normal transition (e.g. Athavale, 1970; Klookwijk, 1979, in Mahoney, 1988, p. 157) and a normal-reverse-normal polarity to the southern flank of the Narmada River (Sreenivasa Rao et al., 1986, in Mahoney, 1988, p.157). Paleomagnetic work in progress also suggests a normally magnetized sequence in the lower part of the Thakurvadi Formation (Khadri et al., 1988).

Thus the implied 40-60 Ma time span between the oldest flows of the stratigraphic column and the youngest remains anomalous and difficult to correlate with the magnetic record. The radiometric work carried out to facilitate stratigraphic correlation has focussed on K-Ar techniques and only subordinately on $^{40}\text{Ar}/^{39}\text{Ar}$, because of the fine-grained nature of the tholeiitic basalts. Problems of Ar loss and K loss or gain, resulting from alteration (e.g. Wellman and McElhinny, 1970; Kaneoka and Haramura, 1973, in Mahoney, 1988, p. 157), as well as extraneous Ar (Balasubramanian and Snelling, 1981, in Mahoney, 1988, p. 157), have also affected geochronological results so far. Because of regional dips of $0.5^\circ - 1^\circ$ in the Deccan lava pile, the paleontological correlations in the field between separate stratigraphic sections of the basalts have also proved unsuccessful in exploring the flow stratigraphy, and it is now generally acceptable that Deccan stratigraphy, based on these criteria, is not well established over vast areas.

However, a comprehensive stratigraphic framework based on geochemical investigations of lithostratigraphic units has thrown new light on these problems (Beane et al. 1986, Subbarao and Hooper, 1988). Geochemical mapping has offered the most satisfactory way of determining flow stratigraphy and has also provided additional information on the petrogenetic history of the Deccan basalts. However, over a limited vertical sequence of lavas, this approach has shown only limited success, as demonstrated in this account (Chapter 5).

2.6. Petrogenetic and Geochemical Aspects of Deccan Traps

Washington (1922, in Mahoney, 1988, p.170) first described the Deccan Basalts as having a monotonous mineralogical and chemical uniformity. Later studies, based on isotopic and geochemical analyses, modified this concept. Krishnamurthy and Udas (1981); Najafi et al., (1981); Mahoney et al., (1982, 1985); Ghose (1983); Paul et al., (1984); Cox and Hawkesworth (1984, 1985); Mahoney (1984); Lightfoot (1985); Beane et al., 1986; and Sreenivasa Rao et al., (1986, in Mahoney, 1988, pp. 170-173) recognized major differences in trace element concentrations and in Nd, Sr and Pb isotopic ratios, as well as some significant ranges in bulk composition, both within and between the sequences. Microprobe work has also demonstrated the existence of a wide range of mineralogical compositions within the Deccan basalts (Muir et al., 1971; Krishnamurthy and Cox, 1977; Sen, 1980, 1986; Lightfoot, 1985, in Mahoney, 1988, p. 166).

Most geologists e.g. (Najafi et al., 1981; Mahoney, 1984; Cox and Hawkesworth, 1985; Lightfoot, 1985, in Mahoney, 1988, p. 173) believe that crystal fractionation is required to explain the petrogenetic character of these basalts. They also believe that besides fractionation, other processes, such as magma mixing, contamination of magma by incompatible elements, mantle heterogeneity and partial melting also have been operative, which could account for the distinctive petrographic features of these basalts.

Chapter 3

3. General Petrography and Mineral Paragenesis

3.1. General Petrography

The rocks are light-grey to greenish grey, porphyritic to microphyric, and aphyric fine- to medium- grained massive basalts. The phenocrysts are optically homogenous and are unevenly distributed throughout the samples. The rocks are mostly amygdaloidal (15-20%), and vesicular (2-3%), and the amygdules are generally filled with zeolites. In some samples, the amygdules are also filled with weathered and altered minerals, while others are partially filled. The vesicles range from a few mm to 2-3 cm in diameter and vary from irregular to regular, spherical and pipe-shaped.

Most samples have weathered surfaces and the common weathering products are chlorite and clays that impart green and brown colours to the surface. A few samples also show superficial oxidized surfaces. Celadonite also occurs in many of the vesicles and forms rims around their boundaries.

3.2. General Description of the Thin Sections

Microscopic analysis shows that the samples are fine- to medium-grained olivine and

olivine-clinopyroxene phyric and microphyric basalts containing 2-15 % phenocrysts.

The olivine phenocrysts occur as isolated, rounded crystals ranging in size from 0.5-2.5 mm in diameter, and are completely altered. The clinopyroxene phenocrysts are usually smaller than olivine phenocrysts, but have greater range of size (1-2 mm), and are unaltered. The plagioclase phenocrysts are usually larger and range from 2-4 mm in diameter. Besides these three major phenocrysts types, some of the samples have magnetite phenocrysts ranging in size from 0.5-1 mm in diameter.

Two suites may be defined according to their phenocryst contents:

Suite No. 1 olivine, plagioclase and clinopyroxene (Figure 9)

Suite No. 2 olivine, plagioclase, clinopyroxene and magnetite (Figure 10)

The groundmass is made up of 30-35 % plagioclase, 25-35% clinopyroxene, 10-15% glass and 2-3% clays. The textures vary from intersertal through intergranular to sub-ophitic and ophitic (Figures 11 and 12), and more than one of these textures may occur in separate domains within the same sample (Figure 13). In some places, the groundmass contains partially devitrified cryptocrystalline glass. The groundmass also shows alteration to green chlorite and a variety of greenish- and brownish clays, possibly smectite.

3.2.1. Petrographic Description of Samples: Suite No. 1

The samples from this suite are generally fine- to medium- grained, with phenocrysts ranging from 2-4 mm in diameter. The principal phenocrysts are olivine, plagioclase and clinopyroxene. The olivine phenocrysts are euhedral to subhedral and are 2-3 mm in

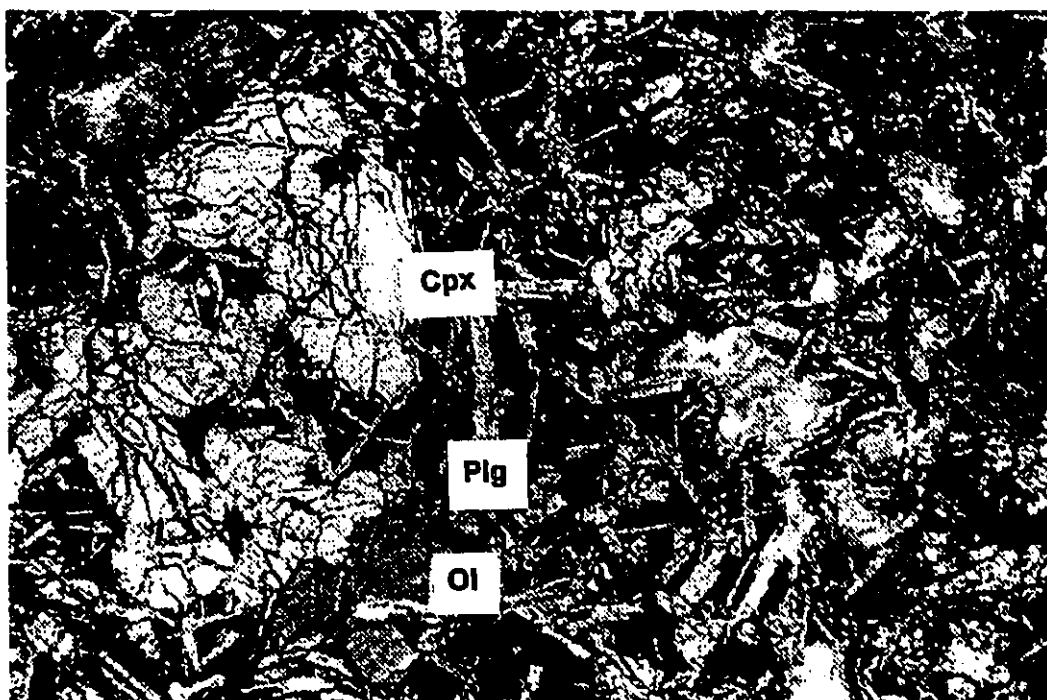


Figure 9- Photomicrograph showing mineral assemblage of ol, cpx, and plg representative of Suite #1. Note that olivine phenocrysts are altered and groundmass is glassy with various percentages of cpx, plg and iron oxides. Field of view is 3.5 mm.

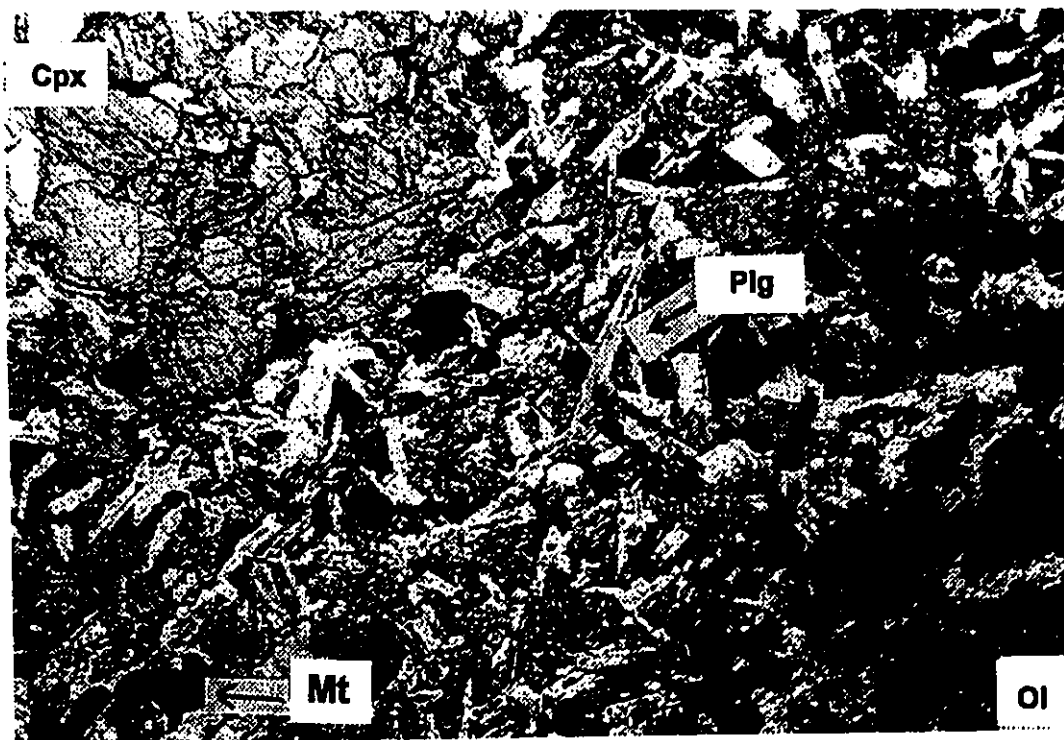


Figure 10- Photomicrograph showing mineral assemblage of ol, cpx, plg and magnetite representative of Suite #2. Note that ol phenocrysts are highly altered. Field of view is 3.5 mm.



Figure 11- Photomicrograph of basaltic groundmass comprising partially devitrified glass, cpx and plg assemblage. Note also the occurrence of intergranular and intersertal texture. Field of view is 3.5 mm.

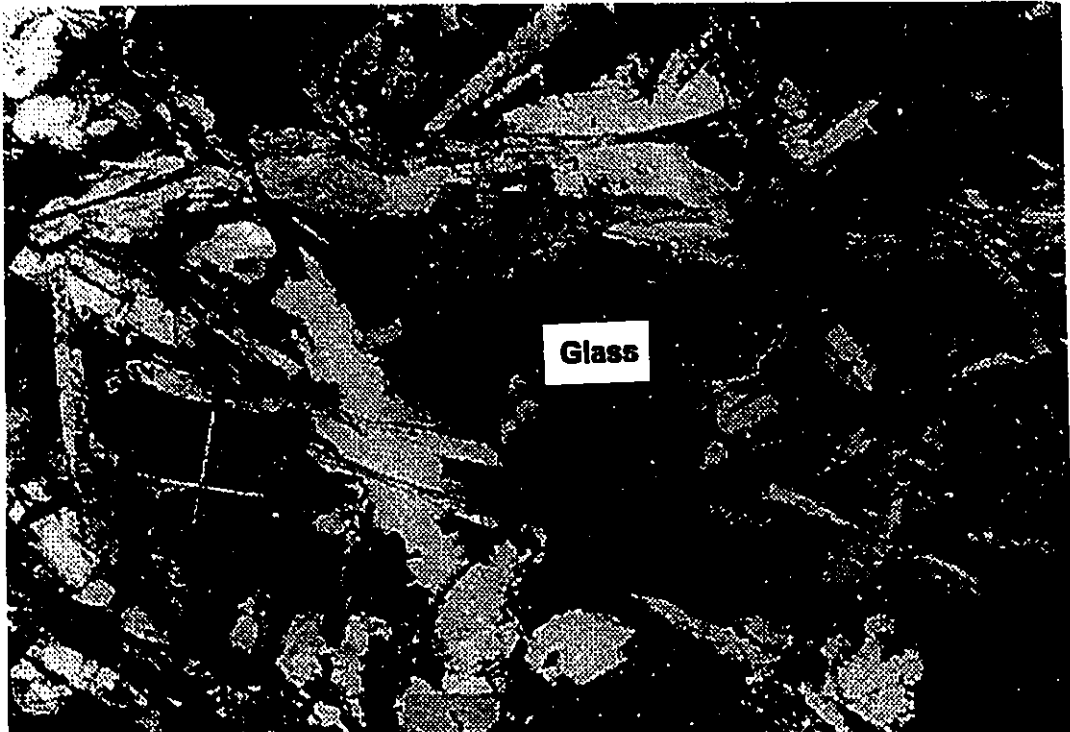


Figure 12- Photomicrograph showing phenocrysts of cpx partially to completely enclosing laths of plagioclase. Note also that intersertal texture is common. Field of view is 2.4 mm.

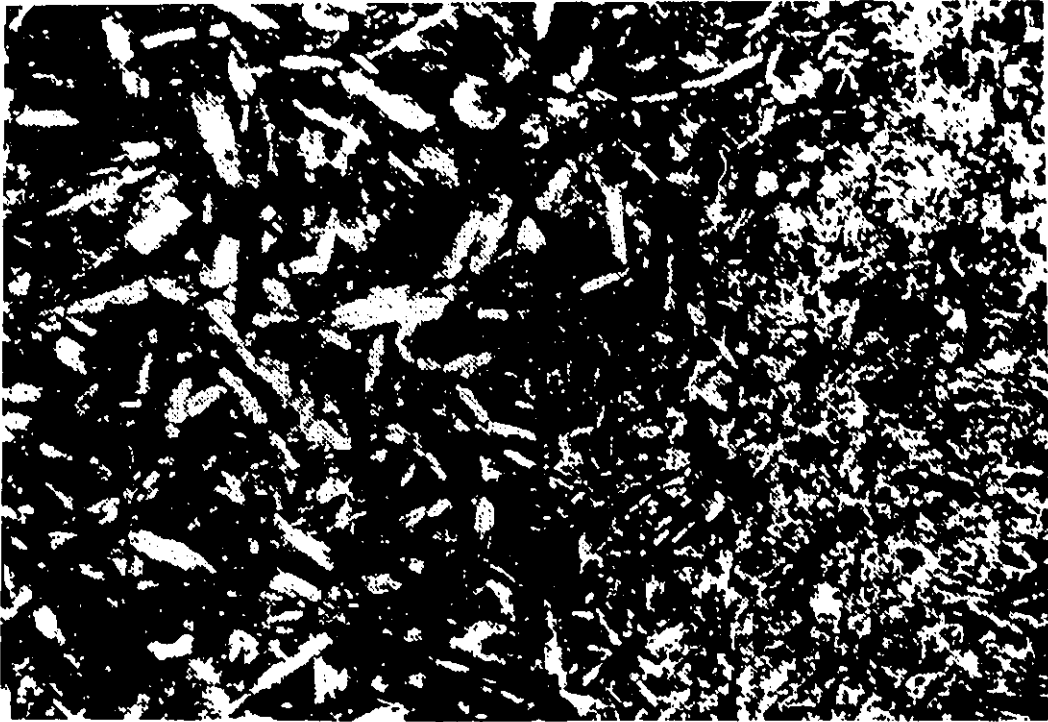


Figure 13- Photomicrograph showing occurrence of textural domains in the basaltic rock. Field of view is 3.5 mm.

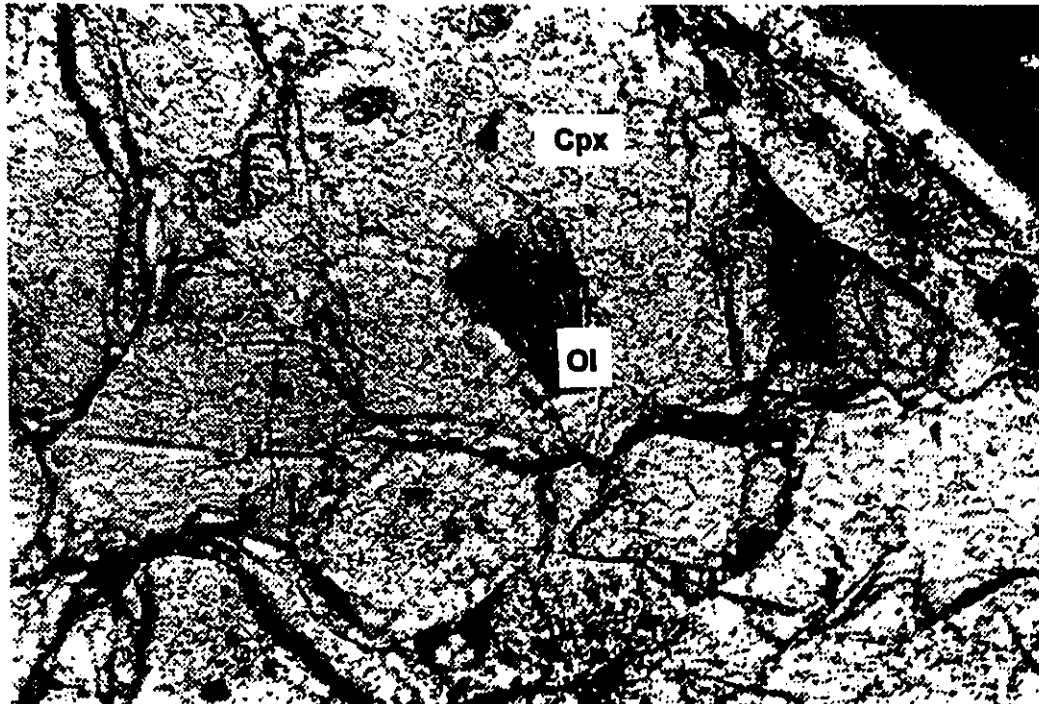


Figure 14- Photomicrograph showing phenocrysts of cpx commonly enclosing olivine. Field of view is 1 mm.

diameter. These phenocrysts are usually hexagonal to prismatic, constituting only 1-2 percent of the rock. They are fractured and occur mainly as isolated crystals. Alteration of olivine to iddingsite, which pseudomorphs almost every crystal, is almost complete, leaving crystal form and fractures as relict features of the minerals. The olivines are oxidised along these crystal forms and fractured zones, which imparts a red colour to the phenocryst surface. Besides iddingsite, some olivine grains also have chlorite and possibly limonite as alteration products on their surfaces. Some of the olivine phenocrysts enclose magnetite grains of the groundmass along their outer margins.

The clinopyroxene phenocrysts are subhedral to anhedral and range from 1-2 mm in diameter; they constitute about 3-5 percent of the rock. These phenocrysts are usually unaltered and have irregular margins. Some of them also include blebs of groundmass in melt channels along the margins. In many cases, the olivine phenocrysts are enclosed completely within clinopyroxene phenocrysts (Figure 14), while magnetite grains 0.5-1 mm in diameter are commonly included in a narrow zone along their margins. Aggregates of clinopyroxene and minor olivine impart a glomeroporphyritic texture to the rocks of this suite.

The plagioclase phenocrysts constitute about 10-12 % of the total rock composition and range in size from 3-4 mm in maximum diameter. These phenocrysts are generally large, as compared to other phenocrysts and show polysynthetic twinning and normal zoning (An₅₅₋₆₀). The phenocrysts have irregular margins, and incorporate some small bodies of the groundmass material along their margins.

The groundmass is made up of 30-35% plagioclase, 25-30% clinopyroxene, 10-

15% glass, 2-4 % iron oxides (magnetite and ilmenite), and 2-5% clays. The plagioclase crystals of the groundmass are 0.05 -1 mm in diameter, clinopyroxene 0.02- 1mm, and magnetite and ilmenite from 0.05 < 1mm. Textures within this suite vary from intergranular and intersertal to sub-ophitic.

The clays constitute 2-5 % of the rock and are uniformly distributed throughout the groundmass as alteration products, affecting partially devitrified glass of cryptocrystalline nature, phenocrysts and groundmass minerals e.g. plagioclase, clinopyroxene etc.

3.2.2. Suite No. 2

The samples from this suite are fine- to medium-grained with variable contents of olivine, plagioclase, clinopyroxene and magnetite as the principal phenocrysts. The olivine phenocrysts commonly occur as euhedral to subhedral, prismatic to rounded, and fragmented crystals, ranging from 1-2 mm in diameter. Complete alteration of olivine to iddingsite is very common. Alteration minerals such as green-brown chlorite can be seen where olivine grains have not been completely altered to iddingsite. The phenocrysts are also oxidised along their margins and fractured surfaces. Some of the olivines enclose magnetite grains near their margins.

The clinopyroxene phenocrysts are euhedral to subhedral, and range in size from 1.5-3 mm. They constitute about 2-4 % of the rock. Most of these phenocrysts are unaltered and have irregular margins. Blebs of groundmass are quite common within these phenocrysts. Clinopyroxene phenocrysts may partially or completely enclose olivine

phenocrysts. Some of them have magnetite phenocrysts enclosed in a narrow zone along their margins.

The plagioclase phenocrysts are euhedral to subhedral comprising about 10-15 % of the rock. The phenocrysts are larger than other phenocrysts and show polysynthetic twinning and normal zoning. The phenocrysts show normal zoning and composition is in the range of An₄₀₋₅₀. They also have irregular margins and incorporate groundmass material along their twin planes.

The magnetite phenocrysts are euhedral to subhedral and range from 0.5-1 mm in diameter, making up 2-3 % of the rock. These phenocrysts are generally scattered throughout the groundmass together with abundant magnetite. A few magnetite phenocrysts, usually euhedral, are partially enclosed in the clinopyroxene along the margins.

The groundmass of this suite comprises 30-35% clinopyroxene, 30-35% plagioclase, 10-15 % glass and 2-4 % iron oxides. The textures of this suite are intergranular, intersertal, and sub-ophitic. The minerals are more oxidised by comparison with the samples from Suite No. 1. Clays constitute 2-4 % of the original percentage of the rock, and show weathering and oxidation. Most of these clays, that are present in the groundmass, replace the partially devitrified cryptocrystalline glass and groundmass minerals such as plagioclase and clinopyroxene. Some of these clays also have replaced the olivine, clinopyroxene and plagioclase phenocrysts.

3.3. Description of Zeolites

The Deccan Trap zeolites in the Akole Taluka District have been identified microscopically and by electron microprobe by Michelle Macdonald at the University of Windsor. The Deccan zeolites occur dominantly in tholeiitic basaltic volcanic rocks and are the product of post-volcanic hydrothermal solutions. Microscopic and probe examination of these zeolites suggest that they are epistilbite, stilbite, harmotome, scolecite, wairakite, and heulandite. The occurrences of these zeolites are shown in Figure 15A-E. The epistilbite and heulandite are the most common zeolite species, while other species occur in minor amounts. Epistilbite occurs as minute, cavity-lining crystals. It occurs as fibrous, radiating needles and also as prismatic crystals. In the majority of samples, epistilbite and green celadonite occur together (Fig. 15A). Heulandite occurs as sheaf-like or radiating bundles of crystals as well as euhedral platy crystals, which show twinning and wavy extinction (Fig. 15B). Granular heulandite crystals rimmed by celadonite have also been observed (Fig. 15C). Heulandite often includes abundant, brownish clay minerals, which may partially or completely hide the mineral optical properties. Zonation of zeolites, in most of the samples, is the result of an increase in grain size of the epistilbite and heulandite crystals, away from the cavity wall. It may also be the result of epistilbite rimming heulandite crystals. Scolecite occurs as thin, acicular, radiating crystals (Fig 15D). It also occurs in association with heulandite (Fig. 15E). Other zeolite minerals include thin radiating sheafs of stilbite (Fig. 15F), and tabular mordenite (Fig. 15G). Rhombs of calcite were found to occur with an isotropic, rhombic, calcic-rich variety of analcime known as wairakite.

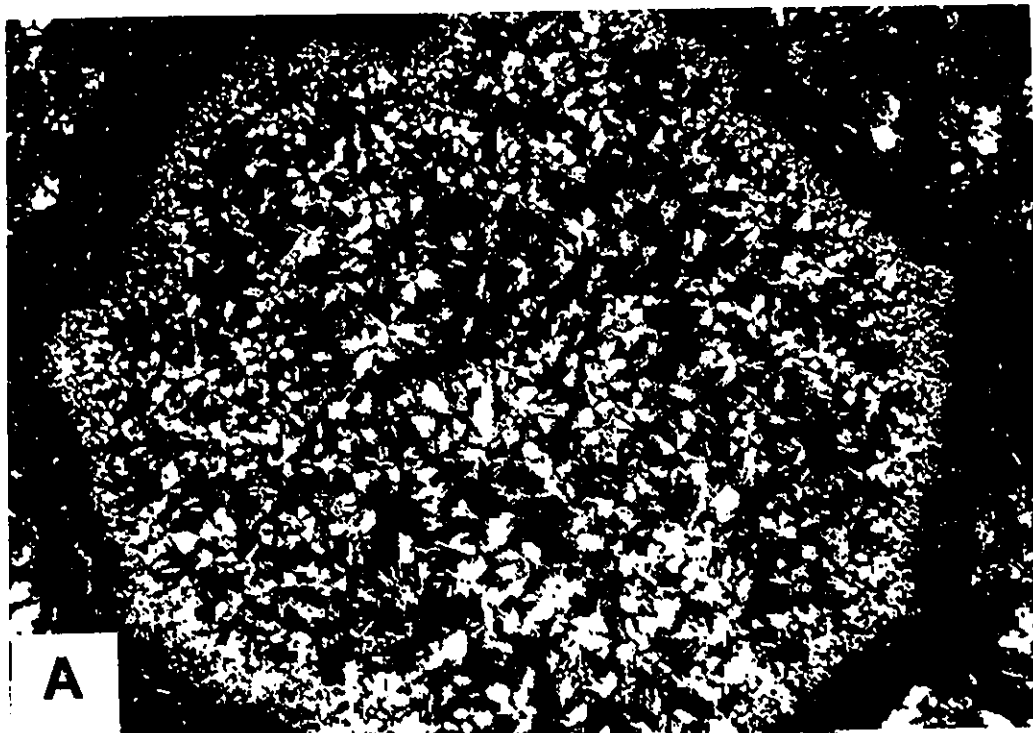


Figure 15A- Zeolite mineral is fine grained radiating crystals epistilbite. Associated mineral is celadonite, the most common zeolite in the Trap. Field of view is 3.5 mm.

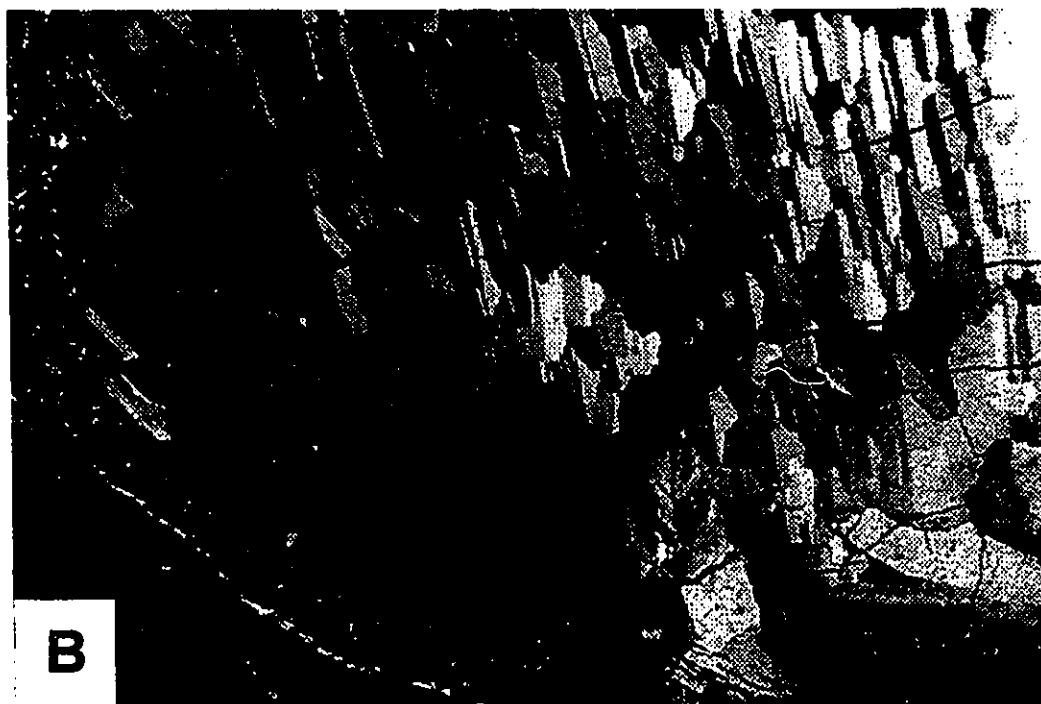


Figure 15B- Zeolite mineral is heulandite (shows twinning). Some show growth of mineral away from cavity lining. Boundary rim of finer heulandite grains is common. Field of view is 3.5 mm.



Figure 15C- Zeolite mineral is heulandite showing no cleavage or twinning (identified using microprobe analysis) bounded by thick cavity lining celadonite. Field of view is 3.5 mm.



Figure 15D- Fractured cavity. Zeolite mineral is scolecite occurring as long radiating fibre with brown interference colours (difficult to identify with microscope). Field of view is 3.5 mm.



Figure 15E- Zeolite minerals are scolecite and heulandite. From outer core celadonite - scolecite - heulandite. Field of view is 3.5 mm



Figure 15F- Zeolite mineral is stilbite showing radiating sheaf like appearance bounded by celadonite. Field of view is 3.5 mm.



Figure 15G- Zeolite mineral is mordenite (tabular form). Field of view is 3.5 mm.

It is suggested that the optical properties of a zeolite species may vary significantly depending upon the degree of hydration. The optical properties may also show overlap among different zeolites species. It is also possible that zeolites, during the preparation of thin sections, may have undergone changes in temperature and moisture, which may have affected the optical properties. Hence, due to the limited number of zeolites identified, a relationship between the mineralogy and its form of occurrence (i.e. pipe-shaped bodies) was not evident.

3.4. Sequence of Crystallization and Mineral Paragenesis

The sequence of crystallization can be deduced from the mutual relationships among the phenocrysts:

Olivine is commonly enclosed completely within clinopyroxene phenocrysts. Plagioclase phenocrysts are partially enclosed, and in some cases completely enclosed, in pyroxene phenocrysts. Thus, olivine is regarded as the first mineral to crystallize upon cooling of the magma, followed by the crystallization of plagioclase phenocrysts. In places, where plagioclase phenocrysts are partially enclosed in clinopyroxenes, simultaneous crystallization of both phenocrysts is suggested i.e. crystallization overlaps.

In Suite 2 magnetite phenocrysts are enclosed in a narrow zones along the margins of the clinopyroxene and a few plagioclase phenocrysts, and are not seen in the cores of either type of phenocrysts. These observations suggest that magnetite represents the last phase to form phenocrysts by slow crystallization under intratelluric conditions.

3.4.1. Mineral Paragenesis

The paragenetic sequence of the crystallizing minerals is represented by the dotted lines shown below. They indicate that olivine was the first mineral to crystallize, followed by the crystallization of plagioclase and clinopyroxene; overlap in the crystallization sequence is indicated at the point of origin of the dotted line. Magnetite represents the last phase of crystallization.

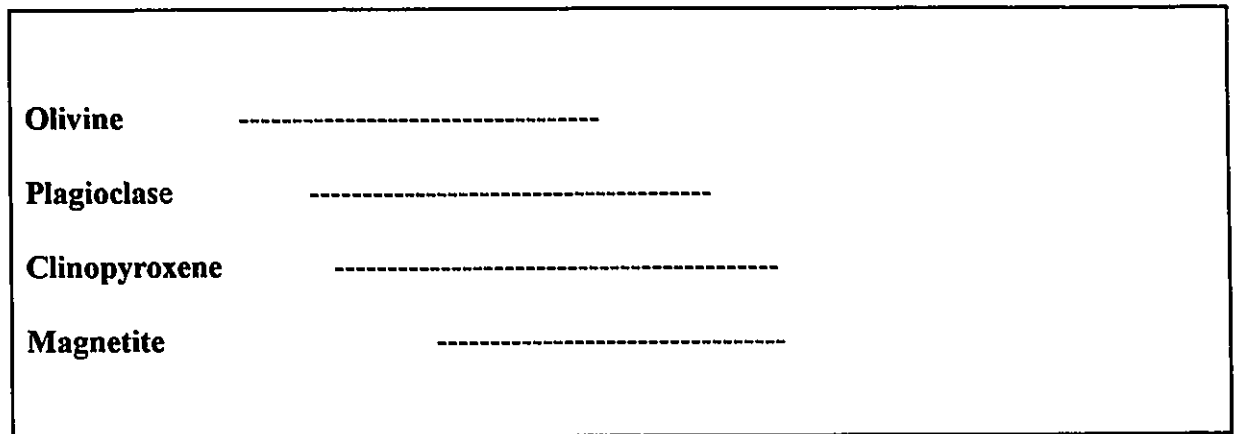


Figure 16- Mineral paragenesis showing sequence of crystallizing minerals

The fine-grained groundmass, comprising various proportions of clinopyroxene, plagioclase, and iron oxides, which occur with or without interstitial glass, suggests sudden decreases in pressure, temperature and increase in viscosity of lavas occurred during their rapid movement to the surface. The vesicular nature of these rocks is due to exsolution of gases from the uprising magma as a result of sudden decrease in pressure.

The increase in albite content of feldspars from An₅₅₋₆₀ in Suite 1 to An₄₀₋₅₀ in Suite 2 and normal zoning can be attributed to the process of fractional crystallization, where diffusion of Ca and Al out of the plagioclase and of Na and Si from the basaltic liquid was not homogenous with the decreases in temperature and pressure.

Observations like intergranular texture is indicative of rapid cooling and suggests mineral compositions were near eutectics; intersertal textures are indicative of very rapid cooling resulting in the formation of metastable glass and also suggest incomplete crystallization of plagioclase. Crystallization of glass, in most places, suggests partial devitrification into a cryptocrystalline mass due to the presence of trapped volcanic gases and/or incipient metamorphism. Replacement of groundmass material, and phenocrysts by alteration products such as chlorite and limonite suggest chemical alteration of basaltic mineral components preferably due to migration of major elements Mg, Na, Ca, Si and K and minor elements, such as Mn, Co, Ni, Cr, Ba and Sr. It may also be possible that these alteration products are formed by the percolation of meteoric waters.

The first mineral to be altered was olivine, producing iddingsite mainly through the expulsion of Mg from the region of alteration and migration of Fe and Al towards the region of alteration. An association of chlorite and limonite was formed, where iddingsitization was incomplete. The alteration of phenocrysts, the groundmass minerals like plagioclase and clinopyroxene to chlorite and limonite, is due to migration of elements. The rims of celadonite around most vesicles suggest a process of alteration, possibly involving hydration reactions. The zeolites can be considered as a product of fluid migration and post-volcanic hydrothermal activity. The fact that some of the rock samples that are completely

oxidised suggests that the hydration-oxidation reactions prevailed, where some parts of the lava completely reacted with the oxygen of meteoric waters to impart a deep reddish-brown colour to a few rock samples. On the other hand, the weathered surfaces suggest that mechanical and chemical weathering, through disintegration, abrasion and solution reactions reduced the surface particles after the rocks were extruded at the surface by an outpouring of lavas.

Chapter 4

4. Geochemistry

4.1. Geochemical Methods

Field sampling was done in the pre-monsoon seasons of 1992 and 1993. A representative suite of relatively fresh samples was collected for analysis. Major element analysis for these samples were done by standard X-ray fluorescence methods (XRF). The 47 samples used were prepared for analysis as follows:

- I Initially, each sample was crushed to 1/5"-1/2" pieces in diameter. A jaw crusher was used to further reduce the sample to less than 1/2" fragments.
- II The sample was then homogenized by rolling on a rubber mat, cone and quartered. A fraction of this sample was pulverised to about -200 mesh size. A representative, 35- 40 g of the pulverised sample was placed in a glass vial.
- III Glass disks were prepared from the rock powders for the major element analysis. Initially, 4 g of sample were dried in an oven at 100° C for several hours to remove the absorbed moisture. About 0.35 g of the dried sample was weighed and placed into a platinum crucible. To this, 1.942 g of flux was added. The flux was prepared from a mixture containing 47% lithium tetraborate, 37% lithium carbonate and 16% lanthanum oxide.

- IV The crucible was heated over a Meka burner until a homogenous melt was formed.
- V The melt was poured into a brass ring lying on a brass plate (preheated to 250° C) and was quickly flattened into a disk using a brass plunger.
- VI The disk was then placed between two asbestos mats lying on a preheated hot plate (250° C), and was allowed to anneal overnight.
- VII The disks were labelled and stored in plastic bags.

The fused glass disk method used in XRF analysis has several advantages. The method eliminates the effects of mineralogical and grain size inhomogeneities, and reduces mass absorption effects. The matrix affects determinations carried out using XRF techniques are based on the application of the linear relationship between the reciprocal of analyte-line intensity and reciprocal of the elemental concentration (Huang and Smith, 1980). This method removes the necessity for mass absorption corrections for major element analysis. Other corrections used during the XRF analysis were dead-time corrections, background corrections and drift. Random errors such as variation in the intensity of the primary X-ray emissions are more difficult to control.

The trace element analysis of these samples was done using an ICP-MS (Inductively Coupled Plasma-Mass Spectrometer). A run of trace elements on the ICP-MS consists of 24 samples. The following procedure was used for the analysis:

- I Twenty four clean dry labelled Teflon screw cap jars, were taken for analysis.
- II The cover was removed and ± 0.1000 g of sample was weighed accurately into each jar. The spatula was wiped with a kimwipe between each sample.
- III About 2 ml of 8N HNO₃ was added and swirled; 1 ml of HF was added and the

cover was replaced, finger tight.

- IV The above solution was then refluxed overnight.
- V Samples were checked to see if they dissolved. For samples that dissolved, the cover was removed carefully and rinsed into a jar with few ml of 8N HNO₃. These samples were then allowed to evaporate at about 80- 100° C until dry. The undissolved samples were refluxed again.
- VI When the jar cooled, another 1 ml of HF and 2 ml of 8N HNO₃ was added. To ensure that complete dissolution of accessory minerals such as zircon occurred, the solution was refluxed for another 2-3 days.
- VII Samples with undissolved material were kept on a hot plate until complete dissolution was occurred.
- VIII The jar was removed from the hot plate, rinsed and covered as before, and samples were allowed to evaporate.
- IX 2 ml 8N HNO₃ and 1 ml boric acid (5000 ppm B) was added and then evaporated.
- X 2 ml 8N HNO₃ was added again and then evaporated. The process was repeated.
- XI The covers were then replaced and 2 ml 8 N HNO₃ was added and warmed gently to get all residue in solution.
- XII Covers were rinsed into jars with Nanopure water.
- XIII Samples were then transferred to clean, dry labelled bottles; jars were also rinsed into bottles. About 2 ml of 0.16 M oxalic acid, 1ml boric acid/ 0.113 M HF solution was added to make up to a final weight of 90 g with nanopure water.

In ICP-MS analysis there are several advantages and disadvantages. It is a technique that combines multi-element capability, speed, and sensitivity. It is a powerful and flexible analytical technique (Riddle et al., 1988; Thompson and Walsh, 1989). Other advantages of ICP-MS include: simple spectra (compared to ICP-optical emission); capability of determining isotopic ratios; rapid scanning ability; moderate installation costs; ICP-MS, like Spark-Source Mass Spectrometry (SMSS) and Thermal Ionization Mass Spectrometry (TIMS), can be used to analyze small samples. However, one of the major disadvantages of ICP-MS is the requirement to introduce the sample in solution. The need to get a sample into solution brings with it problems, including: the potential for incomplete dissolution, increased sample preparation costs (technicians and laboratory). Another potential disadvantage of ICP-MS is operating cost. Fixed costs per sample for an ICP-MS are at least 6 times higher than XRF analysis. The other problems are matrix effects, drift and interferences. A variety of procedures exist to solve these problems (Riddle et al., 1988; Hall, 1989). The most common technique involves a number of calibration strategies (external, surrogate and standard addition) to determine elemental sensitivity and to correct for matrix effects.

The precision of the analysis for ICP-MS was calculated by taking percent average standard deviation for each element determined 3 times for analysis. A check of precision values associated with these elemental determinations was found to be $\pm 5\%$ of trace element concentration, which indicates that counting rate has not adversely affected the analytical precision for any of these elements. The check of precision and accuracy values for the trace elements is given in Table 3 and 4.

Table 3- Precision values for ICPMS analysis.

Suite #1

Sample #1	Average SD in %
V	2.4
Li	3.6
Co	4.0
Ni	1.8
Cu	1.8
Rb	2.8
Sr	2.2
Y	2.1
Zr	2.0
Nb	2.5
Yb	8.4
Ba	4.7
La	3.1
Ce	2.1
Pb	16.6
Pb	13.3
Th	12.9

Suite # 2

Sample #	Average SD in %
V	1.0
Li	2.3
Co	3.0
Ni	2.7
Cu	1.7
Rb	1.9
Sr	2.3
Y	2.6
Zr	1.9
Nb	2.0
Yb	3.9
Ba	6.3
La	4.0
Ce	2.0
Pb	4.1
Pb	11.3
Th	6.4

Table 4- Accuracy values for ICPMS analysis.

Element	BHVO-1a		BHVO 1-a		Accuracy		DNC-1a		DNC-1a	
	Mean ppm	literature	Mean ppm	literature	Mean ppm	literature	Mean ppm	literature	Mean ppm	literature
V	322	317			101.6		165	148		111.5
Li	4.47	4.6			97.2		4.16	5.1		81.6
Co	45.73	45			101.6		60.8	54.7		111.2
Ni	134.95	121			111.5		266.05	247		107.7
Cu	131.57	136			96.7		92.7	96		96.6
Rb	10.75	11			97.7		4.47	4.5		99.3
Sr	394.43	403			97.9		149.4	145		103.0
Y	26.36	27.6			102.8		18.69	18		103.8
Zr	174.9	179			97.7		34.47	41		84.1
Nb	19.03	19			100.2		1.99	3		66.3
Yb	1.34	2.02			66.3		1.16	2.01		57.7
Ba	150.41	139			108.2		114.5	114		100.4
La	22.1	15.6			139.9		5.62	3.8		147.9
Ce	32.17	39			82.5		6.5	10.6		61.3
Pb	3.1	2.6			119.2		7.91	6.3		125.6
Pb	2.99						7.39			
Th	1.17	1.08			103.3		0.48	0.2		240.0

4.2. Alteration

As noted above many of the samples analyzed have undergone post-magmatic mineralogical alteration which may be accompanied by chemical alteration. Beswick and Soucie (1978) devised a method to identify the type and intensity of chemical alteration affecting volcanic rock suites during metasomatism and metamorphism. They show that unaltered igneous rock suites all plot within well defined fields on log molecular ratio plots (LMPR) as suggested by Touminen (1964). On these plots, basaltic rocks plot farthest from the origin and rhyolitic rocks plot closest to the origin. Two initial assumptions are used in this method; firstly, the altered rocks had original compositions which would plot within the trends defined by similar, but unaltered rock types. Secondly, Al_2O_3 remains immobile during alteration as suggested by Carmichael (1969) and Fisher (1970).

The method involves plotting three components X, Y, and Z on a graph that has axes of $\log X/Z$ versus $\log Y/Z$. Should alteration have affected any of the components, the samples will not plot within the fields defined by the unaltered suites. If alteration affects the X component, the samples will be shifted parallel to the X/Z axis. If the Y component is affected, the samples will be shifted parallel to the Y/Z axis. If the Z component is affected, the samples will be shifted along a line with a slope of 45° . If more than one of the three components are altered, the samples will plot along a vector that is the resultant of two or

three components. As more than one component can be altered, a single plot will not allow for a unique solution of the alteration taking effect; hence a series of plots is necessary (Beswick and Soucie, 1978).

The method for the determination of alteration effects was applied to the samples from Maharashtra, which are tholeiitic basalts with SiO_2 content ranging from 48-50 %. Their chemical composition are plotted on Figures 17 A-G. On each plot, most samples from the two suites fall along a single well defined trend of Beswick and Soucie (1978) indicated by parallel lines. The samples extend from the field representative of basaltic rocks, to the field representative of rhyolitic rocks (Fig. 17).

In Figure 17 A-E, most samples lie within the field defined by the modern unaltered rocks of Beswick and Soucie (1978). Samples that lie to the lower left of each diagram closest to the origin are likely to have undergone K_2O enrichment. These trends suggest that Z metasomatism has dragged down some of these tholeiitic samples into rhyolitic field, which is represented by the movement of samples along a line of constant slope of 45° . However, such rocks may also show progressive increase in SiO_2 and CaO contents, but as observed on these plots, their $\text{CaO}/\text{K}_2\text{O}$ and $\text{SiO}_2/\text{K}_2\text{O}$ ratios decrease. This is due to more rapid increase in K_2O contents during metasomatism as compared to CaO, SiO_2 and FM, while Al_2O_3 was assumed immobile.

In Figures 17 A-E four samples, TCSM1-1, WA1-1, UP1-1 and TPZ1-1, plot away from well defined linear trends. The plots indicate that these four samples have undergone a depletion in CaO. Figures 17 F and G are another set of LMPCR plots, with Na_2O as the

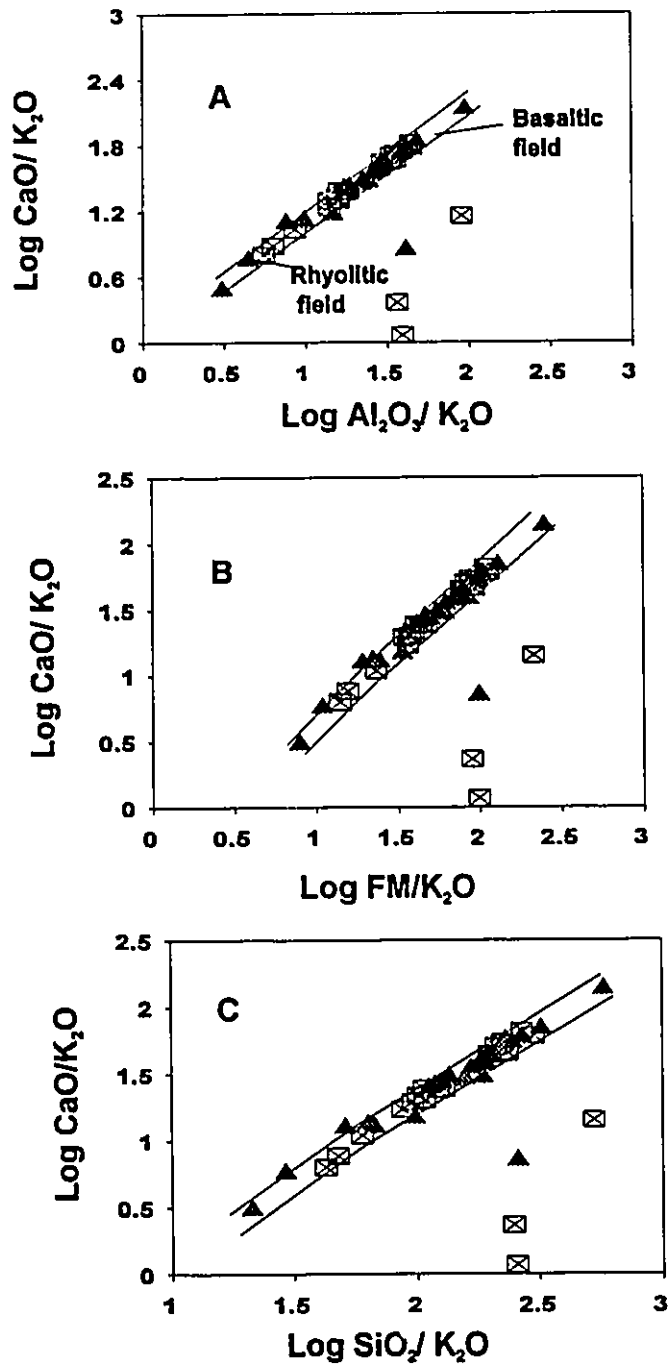


Figure 17- Log Molecular Proportion plots normalized to K₂O and Na₂O, where FM is (FeO+MgO+MnO). Symbols are; crossed boxes- Suite #1; filled triangles are samples from Suite #2. Both suites initially fall along well defined trends of Beswick and Soucie (1978), indicated by parallel lines.

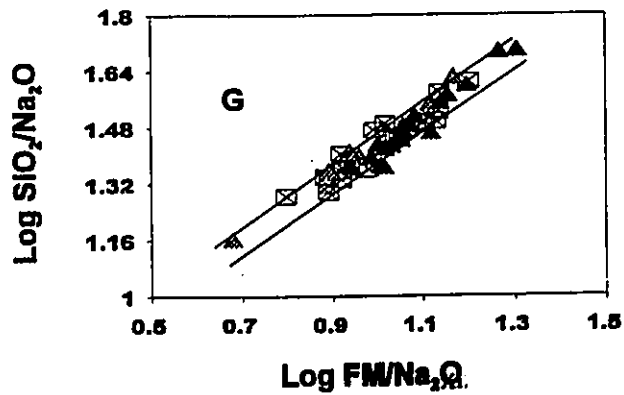
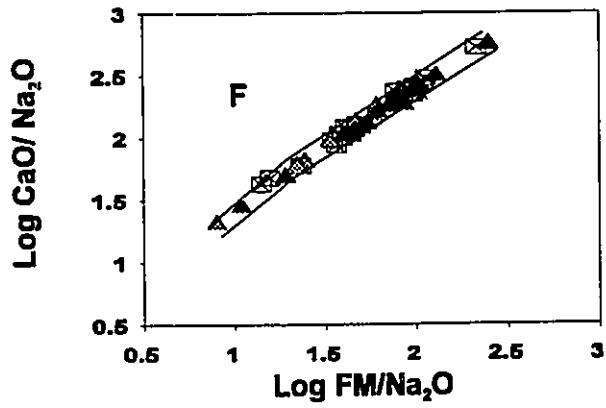
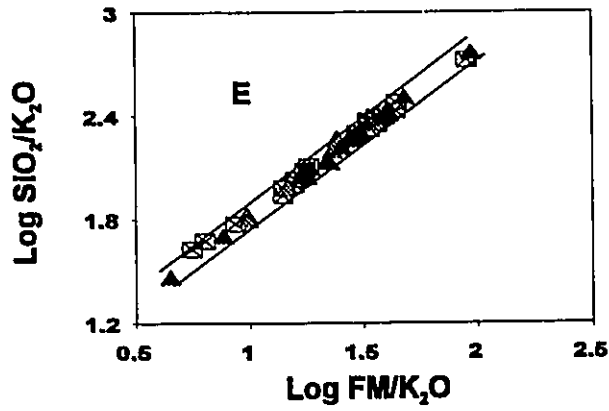
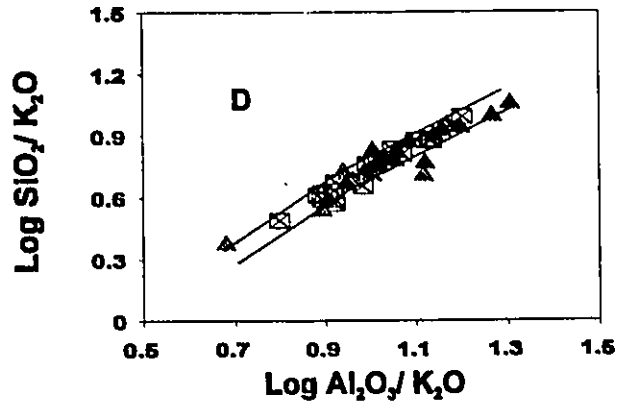


Figure 17-continued.

normalizing factor. Similar but less well-defined trends are apparent. This suggests that Na_2O metasomatism is not as pronounced as that for K_2O . In Figures 17 B-D and F as the origin is approached, the well defined linear trend of rocks, curves downward, deviating from the 45° slope seen at the top of the curve. The alteration of samples which plot along this curve can be attributed to erratic changes in K_2O and Na_2O .

Thus, plots based on oxide molecular proportion ratios suggest that there have been changes in the composition of the rock. These include changes in K_2O and Na_2O contents. The plots also suggest that the SiO_2 , FM and CaO contents (except for the four samples named above) were relatively unaffected by alteration. It is also possible that these elements were present in zeolites, in a different proportion from that of the original composition of the rock; hence the presence of zeolites may have also imparted non-uniform distribution of these elements in the rocks.

4.3. Geochemical Variations

The results of XRF and ICP-MS analysis are given in Table 5 and 6. No linear trends with Mg as a differentiation index are obtained; hence the major and trace elements are plotted on variation diagrams against Zr for each petrographic suite; Zr is chosen as differentiation index because of its incompatibility with the mantle minerals and the fractionating mineral assemblage, and its immobile nature during metamorphism. As K_2O and Na_2O have been shown to be altered during metasomatism; uneven distribution of Ba, Rb,

Table 5- Major Element Chemistry, Weight Percent.

SUITE # 1

SAMPLE #	TCN-2	MIMC1-1	MK1-1	WHM1-2	MSSB-4	MGG-1	ARKD1-1	TP1-2	MGG-2	MMD2-1	TCN3
SiO2	50.94	52.3	50.92	49.86	47.79	48.24	47.97	48.7	48.02	47.13	50.56
TiO2	1.68	2.53	1.59	1.65	1.72	1.72	1.68	1.75	1.73	1.73	1.59
Al2O3	12.76	11.51	12.32	12.58	12.65	13.29	13.05	12.46	12.22	12.87	12.35
Fe2O3	11.15	14.06	10.47	11.12	11.57	11.89	10.94	12.22	12.18	11.65	10.78
MnO	0.15	0.14	0.18	0.22	0.14	0.15	0.13	0.15	0.14	0.16	0.13
MgO	6.32	4.34	5.93	6.9	6.64	7.1	7.83	7.09	6.84	6.55	5.94
CaO	8.93	7.23	9.26	9.49	9.6	11.03	8.8	10.38	10.01	10.67	9.38
K2O	0.74	1.92	0.34	0.28	0.74	0.28	0.86	0.71	0.38	0.35	0.65
P2O5	0.14	0.25	0.13	0.11	0.15	0.14	0.17	0.14	0.13	0.14	0.13
Na2O	2.41	2.13	1.77	2.49	1.64	1.61	2.15	1.5	1.47	1.72	1.69
LOI	4.5	2.38	8.5	4.27	5.98	5.04	5.8	5.3	6.97	6.8	6.27
Total	99.72	98.78	99.41	98.92	98.62	100.49	99.38	100.4	100.09	99.77	99.47

Suite # 1 continued...

SAMPLE #	ALDK1-1	DPK-1	TP-1	DP-1	PCT1-1	WHM1-1	WA1-1	U1-1	UP1-1	TCSM1-1
SiO2	47.26	47.39	50.21	50.19	49.84	52.49	48.94	49.61	47.15	48.93
TiO2	1.76	1.75	1.65	1.74	1.76	1.7	1.68	1.64	1.72	1.66
Al2O3	13.02	12.72	12	12.23	12.31	11.8	12.69	12.7	13.76	12.15
Fe2O3	12.34	11.55	11.45	11.27	11.61	11.13	11.23	11.22	11.99	11.34
MnO	0.2	0.14	0.14	0.15	0.16	0.14	0.17	0.16	0.17	0.16
MgO	7.29	6.55	6.52	7.29	6.13	5.81	6.96	7.38	6.76	6.1
CaO	10.56	10.63	8.92	8.52	9.52	7.86	0.21	9.22	1.19	0.43
K2O	0.33	0.33	0.61	1.31	0.81	1.72	0.3	0.33	0.14	0.31
P2O5	0.13	0.17	0.13	0.17	0.14	0.14	0.15	0.16	0.14	0.15
Na2O	1.55	1.2	2.29	2.41	2.22	2.81	1.78	2.59	1.55	1.33
LOI	5.65	7.44	5.46	4.1	5.15	4.28	5.89	4.19	4.47	7.08
Total	100.09	99.87	99.38	99.38	99.65	99.88	100.04	99.2	99.04	99.64

Table 5- Continued..

Major element chemistry

SUITE # 2

SAMPLE #	PK1-1	MMC2-1	PTV1-1	MSSB2	MSSB3	ABRB1-1	LRNB1-1	MR1-1	PKS1-1	LPB1-1	AKB1-1	UC1-1	MCOD1-1
SiO2	50.33	49.02	50.68	52.37	50.19	49.72	47.25	48.84	49.57	49.19	48.50	50.39	47.29
TiO2	1.72	1.83	1.73	1.7	1.71	1.73	1.87	1.68	1.64	1.67	1.78	1.68	1.64
Al2O3	12.5	12.88	12.44	11.57	12.7	12.18	12.69	12.87	13.32	12.66	13.6	12.53	12
Fe2O3	11.23	12.14	11.28	11.38	11.58	11.67	11.99	11.35	10.17	11.26	12.04	11.49	11.45
MnO	0.21	0.18	0.12	0.18	0.14	0.15	0.15	0.14	0.18	0.18	0.18	0.17	0.16
MgO	6.72	6.93	6.94	5.72	5.82	6.21	7.97	5.72	5.97	6.5	6.83	7.02	6.04
CaO	9.02	10.58	7.01	8.08	7.28	9.12	11.19	9.93	9.72	9.33	10.48	9.68	11.29
K2O	0.5	0.34	3.73	0.44	0.8	1.18	0.32	1.21	0.58	2.63	0.58	0.42	1.45
P2O5	0.14	0.13	0.13	0.18	0.14	0.16	0.12	0.13	0.15	0.11	0.12	0.12	0.13
Na2O	1.91	1.88	1.49	3.71	2.27	2.05	2.09	1.2	1.98	1.02	1.86	2.25	1.81
LOI	5.27	2.7	3.9	4.57	7.15	5.3	3.48	6.09	5.76	4.37	2.87	3.8	5.48
Total	99.55	98.59	99.45	99.88	99.58	99.45	98.92	99.16	99.02	98.92	98.88	99.55	98.74

SUITE # 2 continued..

SAMPLE #	DT1-1	MMD1-1	FS1-1	MCN1-1	TGNM1-2	TGNM	MSSB-1	UF-1	PC1-1	LPB-1	TPZ-1	MMC3-1	MMC3-2
SiO2	48.18	49.54	49.18	47.85	48.92	47.7	48.84	48.18	48.28	49.28	51.23	48.49	49.08
TiO2	1.76	1.68	1.78	1.68	1.7	1.72	1.86	1.78	1.69	1.61	1.73	1.73	1.88
Al2O3	12.45	12.58	13.22	12.29	12.7	12.08	12.84	13.38	12.03	12.21	13.82	13.18	12.69
Fe2O3	11.52	12.2	12.21	11.02	11.42	11.63	12.29	12.32	11.68	11.68	11.95	11.49	12.37
MnO	0.16	0.15	0.19	0.17	0.15	0.15	0.18	0.17	0.17	0.16	0.16	0.13	0.19
MgO	6.45	7.21	6.73	6.98	6.45	6.98	6.51	7.68	6.87	6.87	7.03	6.2	6.45
CaO	10.32	10.2	10.28	9.15	9.97	10.27	10	10.93	10.01	10.52	1.35	10.48	10.4
K2O	0.28	0.24	0.31	0.39	0.48	0.38	0.38	0.13	0.6	0.65	0.31	0.68	0.42
P2O5	0.15	0.13	0.15	0.15	0.14	0.15	0.14	0.17	0.11	0.14	0.11	0.12	0.18
Na2O	1.33	1.83	1.92	1.69	1.65	0.98	2.03	2.11	1.25	1.43	1.73	1.53	1.72
LOI	7.16	3	2.79	6.47	6.73	6.79	3.9	2.4	6.67	5.58	0.5	6.09	4.76
Total	99.86	98.72	98.74	99.7	100.29	98.81	98.97	99.25	99.34	100.11	98.92	100.12	100.14

Table 6- Trace Element Chemistry

suite #1

Sample #	TCR-2	MMS1-1	JK1-1	WMM1-3	MSSB4-A	MGG-1	ARMD1-1	MGG-2	MMD2-1	TCR-3	ALDX1-1	DPK1-1
P	0.0011	0.0004	0.0003	0.0005	0.001	0.0003	0.0003	0.0004	0.0034	0.001	0.0003	0.0005
Tl	0.0048	0.0088	0.006	0.0174	0.0126	0.0045	0.0079	0.0046	0.0042	0.019	0.0133	0.0177
V	347	352	314	325	327	354	371	324	325	313	336	375
Li	14.39	10.63	6.16	7.33	7.61	7.37	9.46	6.62	5.43	6.21	6.92	3.78
Co	50.75	43.74	42.10	51.17	49.52	50.81	50.33	50.48	48.33	44.71	51.71	49.91
Ni	97.59	84.06	96.51	111.2	126.48	107	118.68	104.4	98.97	118.89	108.54	130.4
Cu	149.19	227.42	128.27	150.76	158.86	133.08	99.15	132.15	131.9	134.3	155.54	142.02
Rb	17.7	72.77	11.94	6.7	21.98	8.2	25.42	15.73	15.03	23.42	7.25	9.78
Sr	434.48	232.23	135.86	301.48	234.96	152.65	259.32	101.36	130.18	295.74	149.23	143.47
Y	26.27	38.15	25.31	23.21	26.01	26.83	26.05	27.62	26.88	22.46	26.58	25.51
Zr	125.06	195.01	118.23	111.63	128.52	131.33	130.97	127.62	127.73	107.72	127.73	118.57
Mo	8.15	12.57	8.02	7.54	8.89	8.44	11.03	8.43	8.52	7.46	8.37	8.36
Yb	1.82	1.76	0.93	0.6	1.08	1.05	1.26	1.13	1.21	0.89	1.23	1.12
Ba	229.57	202.43	111.08	107.76	173.73	101.97	192.51	150.6	179.44	89.16	83.46	111.49
La	17.11	30.27	17.74	15.34	17.91	20.25	21.51	20.2	20.3	13.91	19.09	17.2
Ce	29.36	37.91	21.32	18.56	21.35	24.04	27.58	24.35	24.53	16.92	24.33	20.53
Pb	3.61	6.93	4.53	3	4.93	5.62	4.91	5.28	4.91	2.87	4.91	3.85
Bi	3.5	7.05	4.54	3.24	4.42	5.79	5.06	5.75	5.06	2.76	4.91	4.09
Th	2.89	5.04	2.9	2.07	3.2	2.94	3.23	3.23	3.29	2.17	3.23	2.67

suite #1 continued

Sample #	TP-1	DP-1	PCT1-1	WMM1-1a	WMM1-1b	WA-1	U1-1	UPT-1	TCSM-1
P	0.0007	0.0014	0.0011	0.0003	0.0004	0.0005	0.0005	0.0001	0.0002
Tl	0.0049	0.0193	0.006	0.016	0.0181	0.0112	0.0111	0.0291	0.0049
V	356	338	330	310	300	320	375	335	325
Li	12.97	5.38	9.06	7.94	6.91	10.52	5.77	6.66	-0.25
Co	51.55	49.92	49.88	46.95	42.54	50.18	52.07	55.47	54.23
Ni	129.08	107.92	106.01	91.78	86.34	119.45	96.65	101.35	288.76
Cu	149.16	141.46	154.11	107.3	104.83	143.4	126.93	140.3	143.41
Rb	47.46	17.54	14.46	35.32	32.79	-3.6	-5.34	1.95	8.95
Sr	185.92	239.18	186.08	88.69	89.25	301.04	291.65	146.54	331.29
Y	26.23	25.62	26.3	24.98	24.56	26.44	26.29	26.44	25.23
Zr	123.16	117.65	127.65	117.7	118.12	116.17	113.93	126.36	121.42
Mo	8.02	8.49	8.52	7.45	8.01	7.92	7.17	7.92	8.23
Yb	1.63	0.97	1.51	1.82	1.72	1.54	1.9	1.58	1.69
Ba	140.26	162.03	181.58	269.03	286.54	142.13	106.29	85.19	205.03
La	17.07	17.83	16.11	16.34	16.83	16.36	15.47	18.56	17.4
Ce	28.32	21.26	27.83	25.68	26.59	25.65	26.08	29	28.1
Pb	4.83	4.04	3.61	4.39	4.68	3.37	1.67	4.85	5
Bi	4.38	3.66	3.44	4.23	4.16	3.08	2.53	4.32	4.61
Th	3.01	3.04	2.95	3.46	3.57	3.08	1.09	3.41	2.92

Table 6- continued

Suite # 2

Sample #	PRT-1	MNCS-1	PTVT-1	MNCS-2	MNCS-3	ARCS-1	LEMS-1	ML-1	PIST-1	LPHAD-1	AUB-1	MCD-1	DT-1	MOT-1	PST-1	MCH-1	TCMCH-1	TCMMS-1
P	0.0007	0.0002	0.0005	0.001	0.0008	0.0005	0.0006	0.0007	0.0007	0.0003	0.0002	0.0004	0.0006	0.0002	0.0005	0.0003	0.0002	0.0004
T1	0.0038	0.0058	0.0044	0.0084	0.0097	0.0143	0.0004	0.0046	0.0043	0.0043	0.0137	0.0041	0.0189	0.0062	0.0036	0.0047	0.0048	0.0047
V	319	335	337	314	302	332	368	323	316	323	304	303	328	341	343	319	334	349
LI	7.36	6.7	5.71	5.19	8.18	6.18	8.97	4.38	5.61	6.12	7.1	6.59	3.11	6.63	9.14	8.96	0.76	4.1
CO	49.11	57.17	46.46	49.15	50.59	45.01	58.2	42.94	47.64	47.55	46.11	47.59	47.67	49.48	51.84	49.13	50.81	52.37
MS	101.19	80.85	83.44	83.29	83.44	83.29	176.42	100.82	101.06	96.7	103.21	91.63	98.73	111.25	106.77	118.09	83.78	110.82
CU	157.99	138.75	139.08	196.02	125.12	135.22	96.96	137.62	139.45	135.69	131.37	149.69	152.25	125.47	135.69	131.04	147.08	114.82
RD	14.85	7.45	62.3	12.28	27.48	26.17	4.95	50.08	22.84	26.34	17.29	35.9	14.02	7.26	10.57	12.46	10.76	14.83
BR	577.45	276.12	136.99	240.53	284.1	518.83	281.14	372.81	297.41	146.91	197.36	189.36	171.92	236.21	185.65	177.63	203.45	257.92
Y	25.58	26.68	25.13	27.28	27.7	27.48	25.05	24.69	24.29	24.51	26.01	26.92	26.01	25.02	26.45	27.56	26.16	26.03
Zr	125.66	130.3	122.15	121.25	128.87	128.46	122.2	118.81	116.67	118.31	125.99	120.10	122.55	121.7	128.39	126.84	122.29	122.02
MO	8.38	8.5	7.9	8.64	8.63	8.31	10.83	7.96	7.77	7.65	8.24	7.82	8.4	7.68	8.69	8.44	8.16	7.88
YB	1.76	1.3	1.48	1.02	0.99	1.17	1.68	1.48	1.29	1.39	1.17	1.06	0.88	1.04	1.94	1.14	2.08	1.75
BA	186.19	113.05	278.05	204.82	261.43	363.8	179.98	164.85	171.67	310.29	120.23	356.38	122.08	92.98	95.84	153.82	146.8	176.99
LA	17.51	20.12	17.17	19.95	20.24	19.58	18.3	16.02	16.18	16.53	18.54	19.41	17.76	17.64	17.99	19.11	17.91	18.42
CA	27.19	25.11	26.92	23.22	23.39	25.85	29.73	25.72	25.71	26.36	24.89	23.44	21.59	22.56	22.96	23.96	29.06	29.83
PB	3.87	3.78	3.06	3.81	3.96	4.61	4.61	2.28	2.96	4.25	5.12	5.12	4.54	5.72	4.46	5.89	4.72	5.96
A	3.94	4.54	4.03	4.54	4.54	3.42	3.42	3.49	3.42	3.43	5.32	5.32	4.86	5.33	3.7	5.62	3.83	3.85
TH	3.03	3.29	2.83	2.87	3.24	1.53	1.53	2.89	2.61	2.75	5.01	5.01	3.04	2.89	3	5.01	2.83	2.7

Suite # 2 continued

Sample #	UPT-1	PCT-1	LPB-1	TPZ-1	MNCS-2	MNCS-3	UCT-1
P	0.0008	0.0005	0.0004	0.0003	0.0005	0.0005	0.0002
T1	0.0038	0.0038	0.0042	0.0121	0.0056	0.0053	0.0129
V	378	324	318	299	351	316	351
LI	6.46	6.81	5.99	5.44	7.86	5.96	7.18
CO	57.23	49.94	49.68	49.1	51.4	47.44	57.34
MS	132.38	105.91	84.35	123.79	96.64	93.37	107.39
CU	133.32	134.78	129.4	131.36	146.66	145.15	150.51
RD	0.66	13.46	15.71	5.77	14.18	24.59	1.53
BR	278.78	327.65	149.66	371.17	165.81	185.41	267.48
Y	25.1	24.05	24.23	24.12	28.35	26.91	27.06
Zr	119.75	117.23	110.79	110.79	138.51	127.24	123.95
MO	7.55	8.16	7.55	6.5	9.33	8.66	8.68
YB	1.56	1.58	1.64	1.12	1.72	1.09	1.99
BA	89.91	245.5	127.35	110.79	153.93	188.05	145.31
LA	16.03	15.53	15.64	16.04	20.86	20.35	18.28
CA	26	25.65	26	25.21	25.96	24.92	28.93
PB	2.06	5	4.02	5.44	3.91	3.85	3.47
TH	2.78	4.15	3.8	4.35	4.47	4.05	4.67
TH	0.88	3.12	2.74	2.73	3.46	2.99	3.69

Sample #	DMC-1A	DMC-1B	EHYD-1B	EHYD-1B
P	0.0003	0.08	0.0014	0.27
T1	0.0012	0.48	0.0077	2.71
V	165	168	375	317
LI	4.16	5.1	15.57	4.6
CO	60.8	54.7	55.59	45
MS	266.05	247	138.96	121
CU	92.7	96	152.84	136
RD	4.47	4.5	10.65	11
BR	149.4	145	399.84	403
Y	18.69	18	29.49	27.6
Zr	34.47	41	177.98	179
MO	1.99	3	19.7	19
YB	1.16	2.01	1.62	2.02
BA	114.5	114	155.08	134
LA	5.62	3.8	20.25	15.8
CA	6.5	10.6	37.21	39
PB	7.91	6.3	2.8	2.6
TH	7.39	6.3	3	3
TH	0.48	0.2	1.18	1.08

Sr also indicate that their concentrations have been modified during metasomatism, they are not considered for the present study.

4.3.1. Major elements

The major element data are shown in Table 5, and are plotted on Figure 18. Suite No. 1 altogether has relatively large range of Zr (107-131 ppm); SiO₂ (47.13-52.49) and CaO (7.23-11.03 wt.%), except for three samples (0.21 wt. %; 0.43 wt.%; 1.19 wt.%). The other elements show a more limited range; Fe₂O₃ (10.47-12.34 wt.%), TiO₂ (1.59-1.76 wt.%), except for for one sample (2.53%); P₂O₅ (0.14- 0.17 wt%), except for one sample (0.25 wt%) and; MnO (0.13-0.22 wt. %). This suite shows very poorly defined trends of decreased Fe₂O₃, Al₂O₃ and MgO with decreasing Zr.

One sample (MMC1-1) which has been assigned to Suite 1, on the basis of its phenocryst assemblage is very different in chemical composition. It shows much higher concentrations of TiO₂ value (2.53 wt %), while those of other samples lie within (1.59-1.76 wt %); Zr (195 ppm); Fe₂O₃ (14.06 wt %); P₂O₅ (0.25 wt %). In addition to this, three other samples TCSM1-1, UP1-1, WA1-1 previously described in the section of alteration show low CaO values.

The Suite No. 2 samples have a relative wide range of Zr (111-138 ppm); SiO₂ (47.25-52.37); CaO (7.01-11.29), except for one sample (1.35 wt. %); P₂O₅ (0.11-0.18 wt.%) and limited ranges of other elements. The variation diagrams show poor linear trends of decreased TiO₂ and Al₂O₃ with decreasing Zr, and show no significant trends for other major

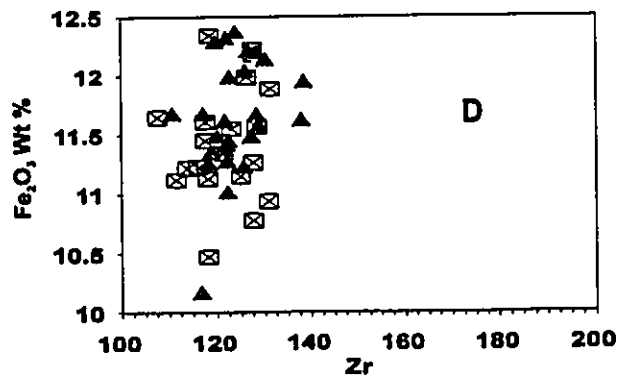
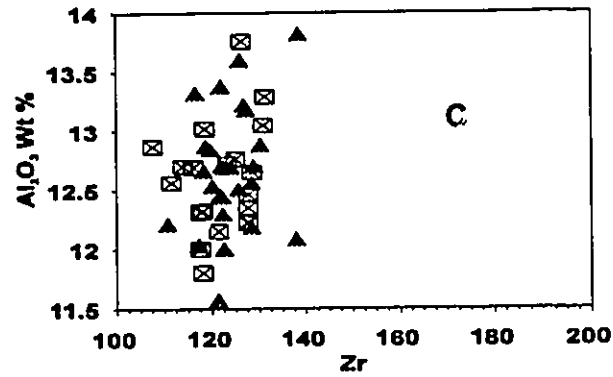
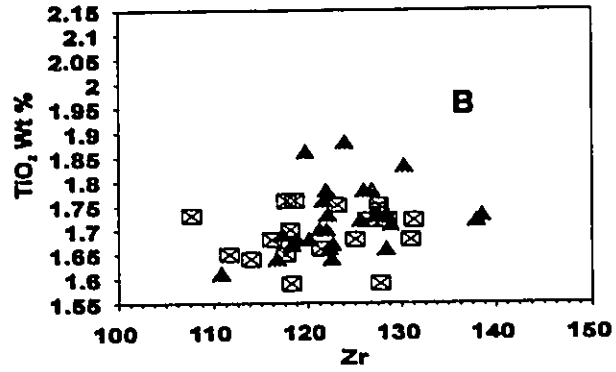
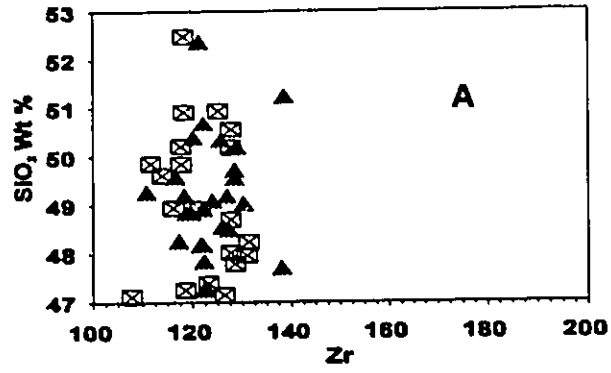


Figure 18- Major element variation plots versus Zr (ppm). Symbols are; crossed boxes- Suite #1; filled triangles- Suite #2.

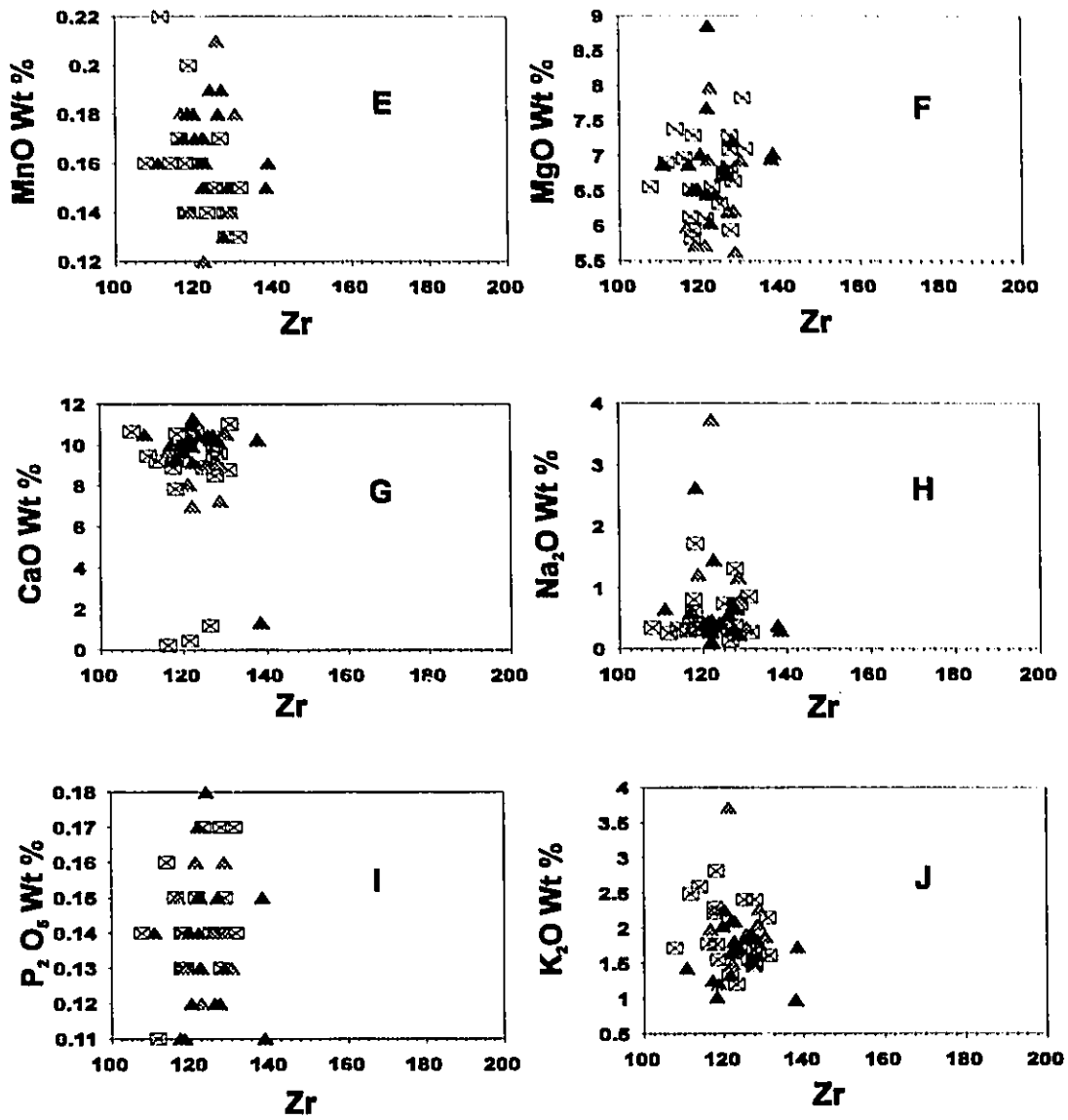


Figure 18-continued.

elements against Zr.

The major elements that show complete overlap between the two suites are Fe_2O_3 , CaO , P_2O_5 , and MnO (approx). The other elements that show partial overlap are SiO_2 , TiO_2 , Al_2O_3 , and MgO ; hence the compositional range of Suite 2 lies within that of Suite 1.

4.3.2. Trace elements

The trace element data are presented in Table 6, and are plotted on Figure 19. The Suite No. 1 samples have relatively large ranges of V (300-375 ppm), except for one sample (571 ppm); Ni (84-298 ppm); Cu (99-227 ppm). They show more limited ranges of Li (5-14 ppm), except for one sample (0.25 ppm); Co (42-55 ppm); Y (22-38 ppm); Nb (7-12 ppm); Yb (0.6-2 ppm); La (16-30 ppm); Ce (16-37); Pb (2-7 ppm) and; Th (2-5 ppm). They show poor trends of decreased Cu, Ce, Pb-1 with decreasing Zr, while Y, Nb, La, Pb-2 and Th show well defined decreased trends with decreasing Zr (Fig. 19).

One sample (MMC1-1) previously discussed also shows a difference in trace element chemistry. High values are observed for Cu (227 ppm); Rb (72 ppm); Yb (38 ppm); Nb (12 ppm); La (30 ppm); and Pb (7 ppm).

The Suite No. 2 samples with wide ranges of elements are V (299-378 ppm); Ni (83-132); Cu (100-153 ppm). The samples show limited range of Li (3-9 ppm), except for one sample (0.76 ppm); Co (43-58 ppm); Y (24.0-28 ppm); Nb (6-11 ppm); Yb (1.0-2.0 ppm); La (16.0-20 ppm); Ce (21-30 ppm). The elements of this suite show poor linear trends of decreased V, Cu, Yb, Ce and Pb-1 with decreasing Zr, while Y, Nb, La, Pb-2 and Th show

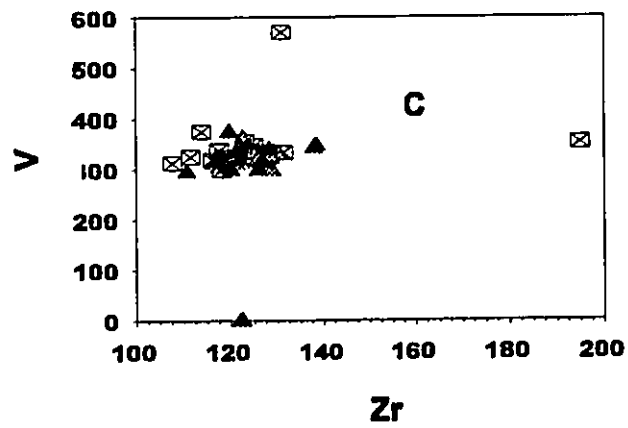
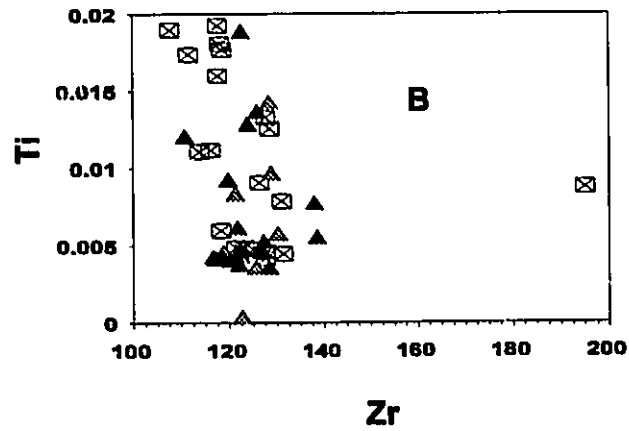
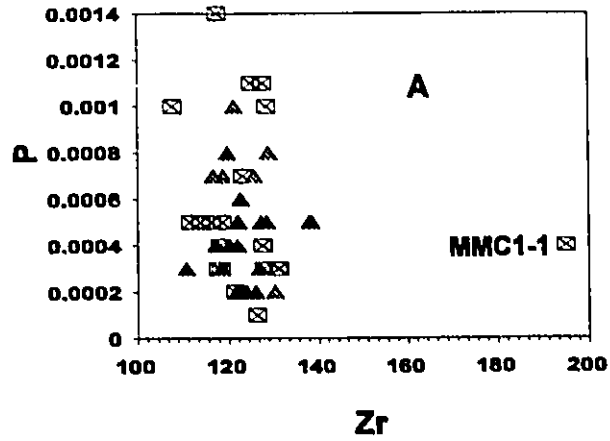


Figure 19- Trace element (ppm) plots versus Zr (ppm). Symbols are; crossed boxes- Suite #1; filled triangles are samples from Suite #2.

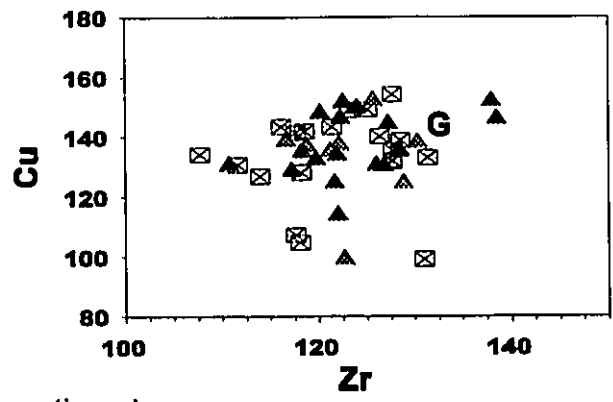
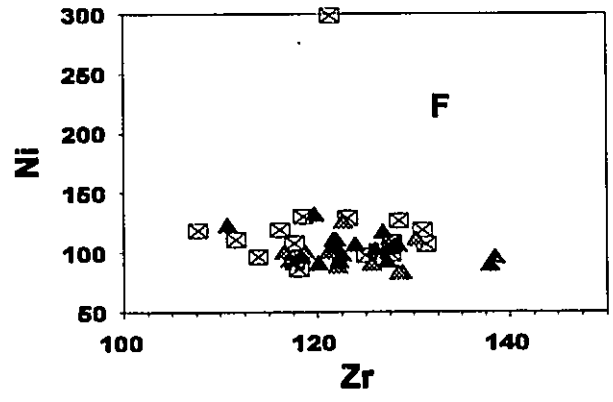
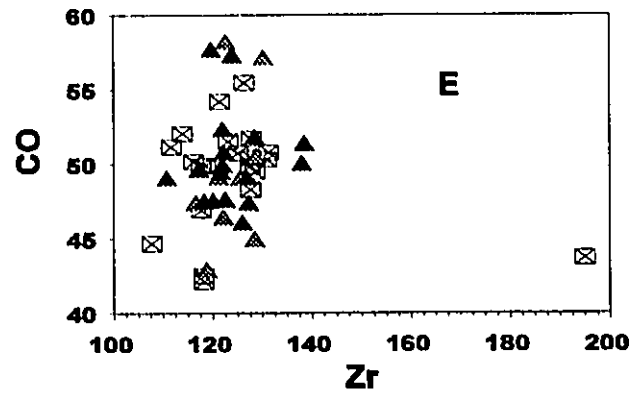
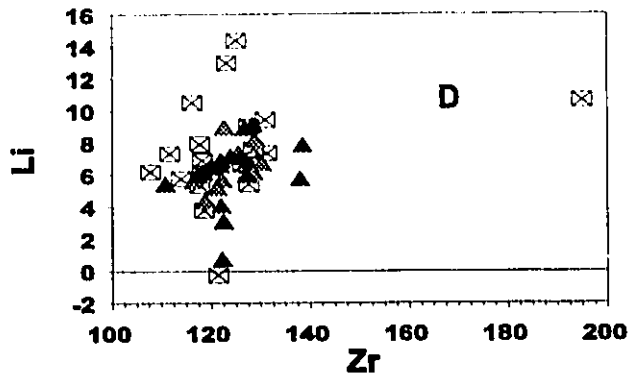


Figure 19- ...continued.

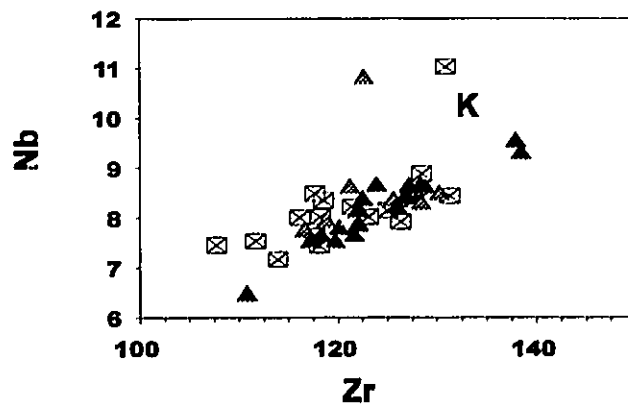
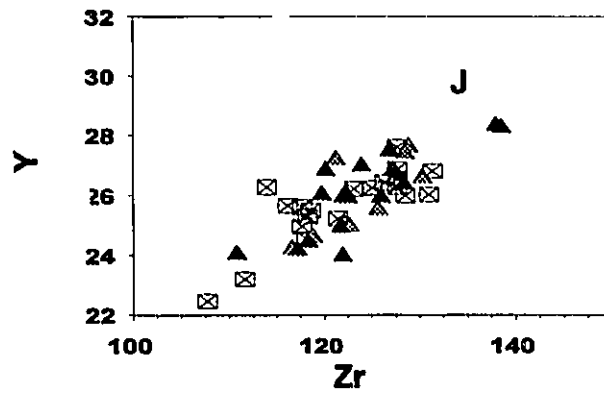
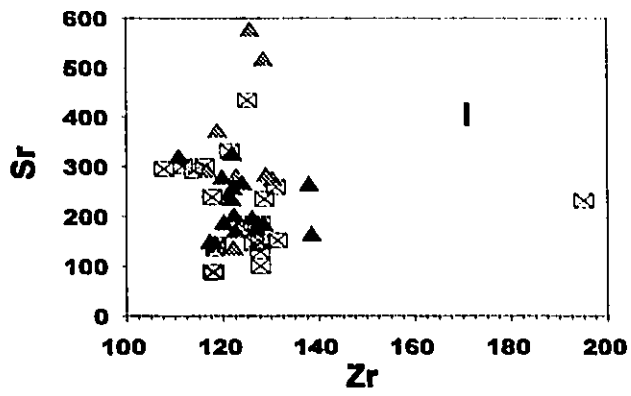
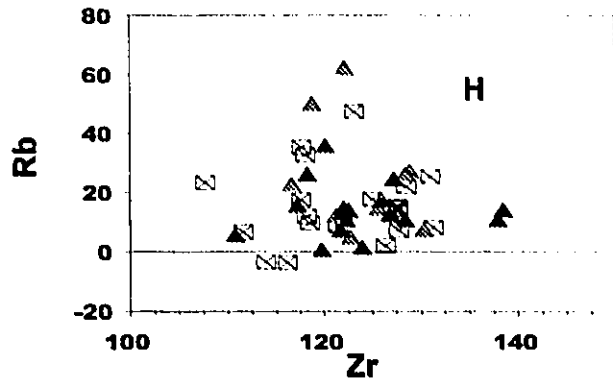


Figure 19-continued.

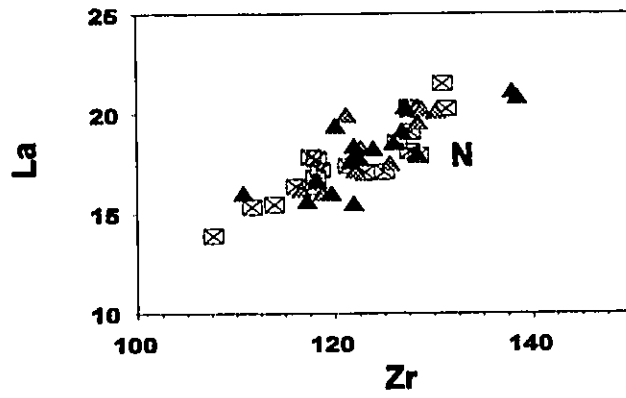
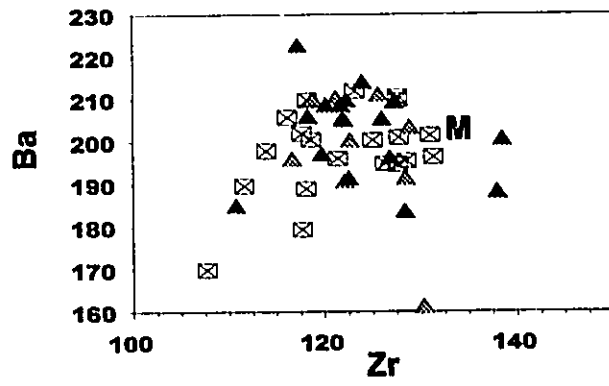
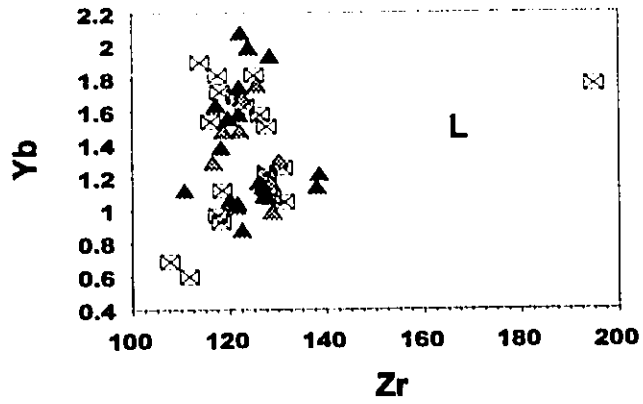


Figure 19-continued.

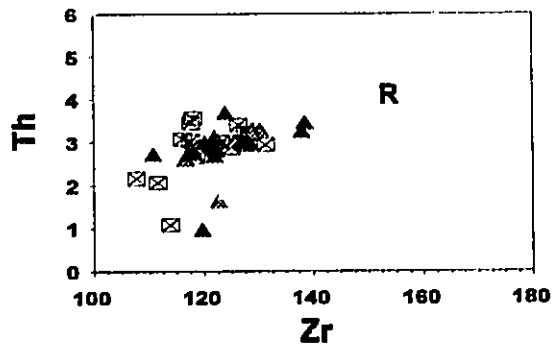
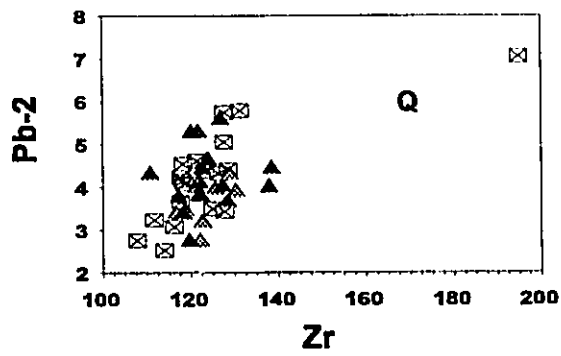
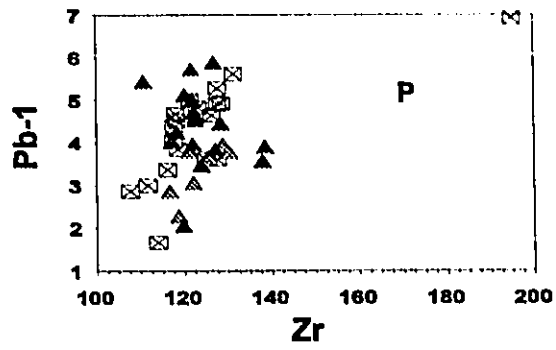
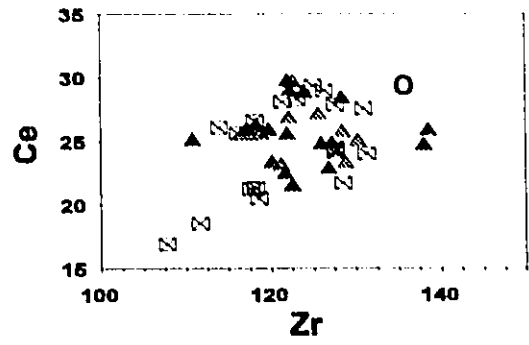


Figure 19- ...continued.

well defined decreased trends with decreasing Zr. However, Ni shows poorly defined increased trend with decreasing Zr (Fig. 19F). The elements that show complete overlap between two suites are Cu, Y, La, Ce. The other elements that show partial overlap are V, Ni, Li, Co, Nb, Yb, Pb-1, Pb-2 and Th. Once again, the range of all Suite 2 traces lies inside Suite 1 ranges with minor exceptions.

As discussed above, the two petrographic suites are chemically similar. Within suite variation is exhibited by the samples MMC1-1, TCSM1-1, UP1-1, and WA1-1 in Suite No 1. and TPZ1-1 in Suite No 2. The other differences shown by the two suites are: Suite No. 1 shows poorly defined increasing trends of Fe_2O_3 , Al_2O_3 and MgO, Yb, Pb-1, Pb-2, while Suite No 2 shows increasing trends for TiO_2 , V, Cu and Ce Vs. Zr. Suite No.1 also has a wider and higher range of Zr (108-137 ppm), On an average, Suite No 1 also shows lower contents of TiO_2 , MgO, Cu, Co, Y, Yb, Ce, Pb-1 and Pb-2 as compared to Suite No 2, while the rest of the elements are higher in Suite No. 2. These chemical variations within each suite can be attributed to the original mineralogy. For example, increasing trends for Al_2O_3 and Fe_2O_3 in Suite No. 1, and TiO_2 in Suite No. 2 suggest both suites were originally dominated by pyroxene. Similarly, the decrease in trends of Ni vs. Zr, indicate removal of olivine in both suites.

The poorly defined trends of elements when plotted against Zr imply that fractional crystallization and/or partial melting may have occurred during lava genesis. For example, Fig 19F shows depletion of Ni vs Zr; which suggests that, the initial crystallization sequence was largely dominated by olivine.

As discussed above, the two petrographic suites do not show much chemical

difference apart from four samples (MMC1-1, TPZ1-1, UP1-1, WA1-1), which show their higher values of TiO₂, P₂O₅, CaO, V and Li. Thus, due to absence of significant variation in the chemistry of major and trace elements, the variation diagrams plotted against Zr are found to be of limited value in interpreting the petrogenetic history of the Deccan Trap.

4.4. Petrogenesis

The aim of petrogenetic modeling is to explain observed geochemical variations within an igneous rock suite using processes of differentiation which are thought to occur in the earth's crust and mantle (Cox et al., 1979; Hanson, 1980). The two most significant differentiation processes are partial melting and fractional crystallization.

The simplest and most widely applied model for partial melting is batch melting or equilibrium melting. In this model liquids generated by fusion remain at the site of melting, and are in chemical equilibrium with the solid residue until a single homogenous batch of liquid is mechanically extracted. During this study, the simple batch melting model was applied rather than applying Rayleigh melting or a dynamic melting model because of lack of more complex elemental behaviour (Cox et al., 1979).

In addition to these two major differentiation processes, features such as magma mixing, magma contamination and source inhomogeneity are also likely to contribute to the geochemical variation in the given suite. However, in this study, no evidence of mixing and contamination was encountered; hence it is excluded from consideration.

4.5. Fractional Crystallization Model and Partial Melting

Fractional crystallization represents a major differentiation process that can be used to model geochemical variations in igneous systems. The most common crystallization process is the Rayleigh crystallization process i.e. crystals formed during the cooling of primary magma are separated from the liquid instantaneously. It is, however, unrealistic to apply the fractional crystallization model rigidly to geological processes, but it does provide a limit to possible chemical variations produced by crystal fractionation. The systematic increases and decreases in the trends of elements observed are indicative of mineral melt equilibria process, either fractional crystallization or partial melting. Major element variation diagrams show poor trends and are not useful in defining the petrogenetic history of these rocks. However, the MgO-FeO diagram of Hanson and Langmuir (1978; Fig. 20) can be used to evaluate the petrogenetic history of mafic volcanic suites. The samples used in the present study plot on a sub-horizontal trend outside the liquidus field (Fig. 20). There is no evidence that partial melting influenced this trend, which can be explained in terms of fractional crystallization of olivine \pm plagioclase \pm clinopyroxene. This is in agreement with the original mineralogy and petrography of these rocks discussed in Chapter 3, where crystallization of olivine is followed by plagioclase and clinopyroxene.

The fact that two petrographically distinct suites show overlap in chemistry can be argued reasonably by the fact that magmas were derived from the same source and followed a similar fractional crystallization history. The petrographic variations observed in the phenocryst assemblages may be due to differences in the redox potential of the magmas. At

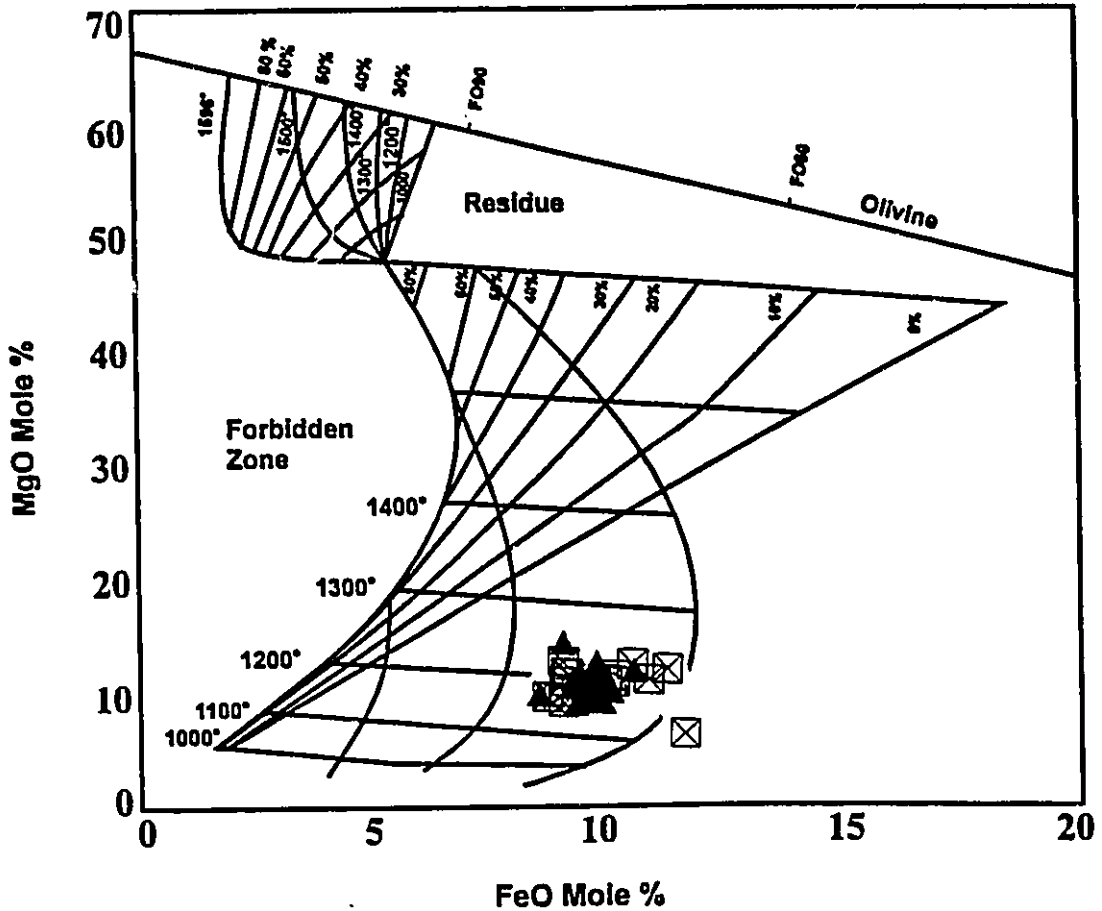


Figure 20- MgO versus FeO sail diagram of Hanson and Langmuir (1978). The curves indicate fractional crystallization of olivine from melts at one atmosphere. The melt field is shown by different degrees of melting lines. Symbols are; crossed boxes- samples from Suite #1; filled triangles are samples from Suite #2.

a higher redox potential, magmas with magnetite phenocrysts are evolved, while at a lower redox potential magmas with no magnetite phenocrysts are evolved.

Pearce and Norry (1979) used the high field strength elements Ti, Zr, Y and Nb for modelled vector diagrams to interpret trace element variations, in particular the changes in crystallizing phases. High field strength elements are not usually transported in aqueous fluids, except when these fluids contain high activities of certain complexing agents such as F-, and tend to remain unaffected in rocks which have suffered metasomatic alteration. Thus, this approach has provided a useful way of investigating volcanic suites which are too altered for the more conventional studies to be applicable.

Mineral vectors on Zr/Y plot (Figure 21) show how melt composition would change in a closed system during fractional crystallization and/or partial melting of a single phase and typical multiphase assemblage (ol, cpx, plg). Magmas must be formed by partial melting, and may then evolve by fractional crystallization. On the Y-Zr diagram, the mineral vectors predict that for basic magmas most crystallizing phases will leave a residual liquid enriched in both Y and Zr. Figure 22A represents fractionation trend, which is similar to the fractionation trends observed for magmas of basic and basic-intermediate composition, corresponding to a combination of olivine-plagioclase-clinopyroxene \pm magnetite as crystallizing phases. The mineral vectors on the Ti-Zr plot (Fig 22B) suggest that the observed trend is consistent with a crystallizing assemblage of olivine-clinopyroxene-plagioclase and magnetite. The mineral vectors on the Nb-Zr plot (Fig. 22C) suggest that for all phases these elements increase during fractional crystallization. This feature is consistent with the trends where olivine, feldspars, clinopyroxene and magnetite are the main

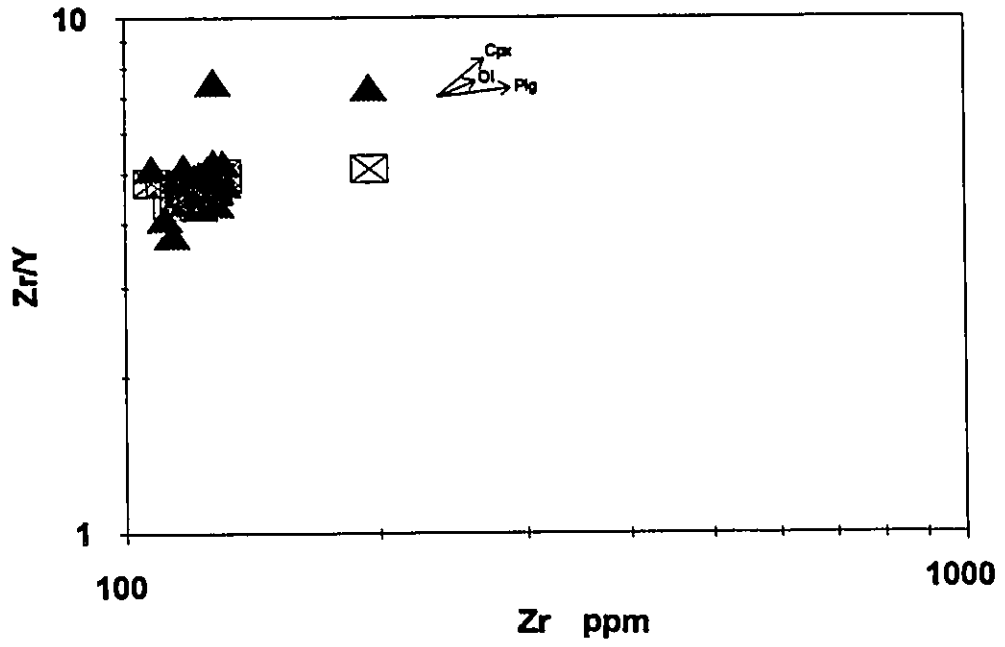


Figure 21- Zr/Y versus Zr fractional crystallization plot. Symbols are; crossed boxes- Suite #1; filled triangles are samples from Suite #2.

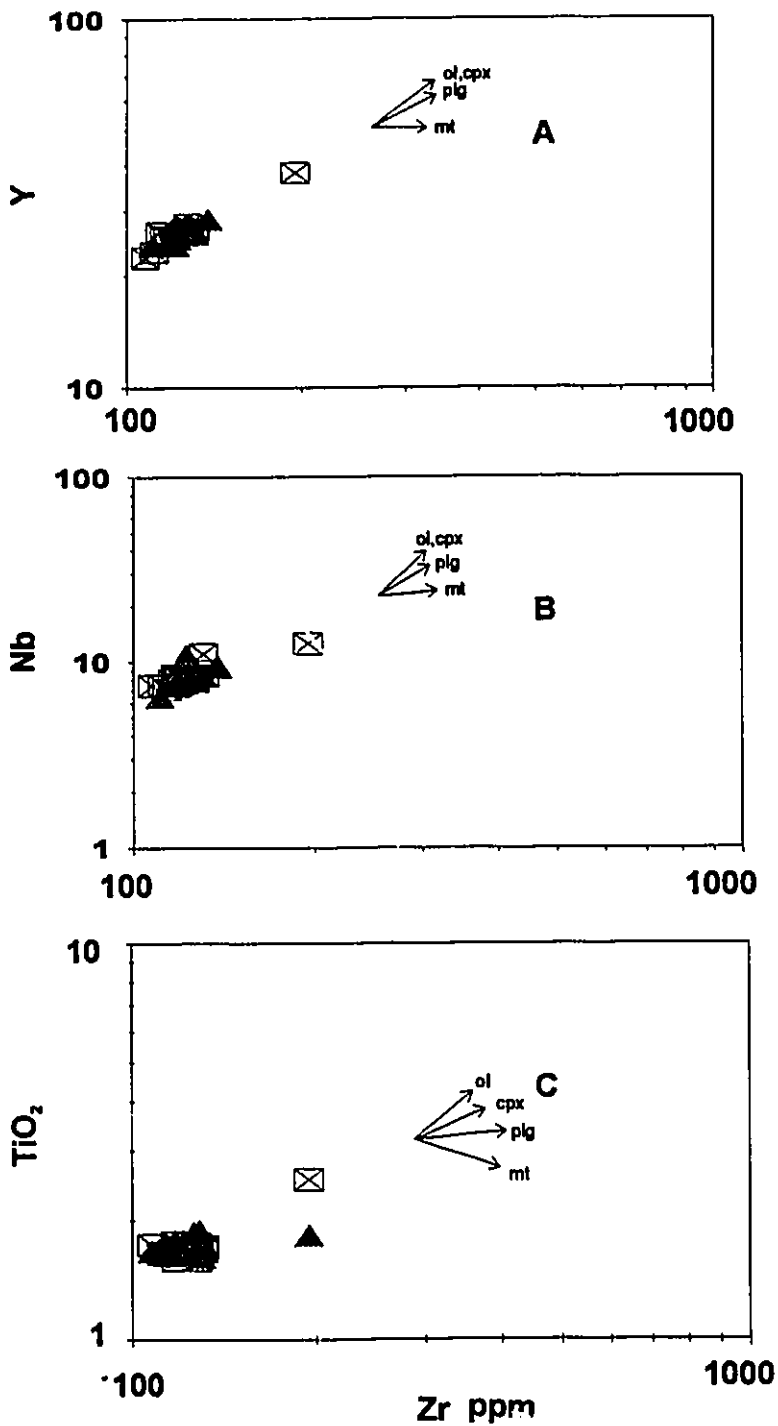


Figure 22- Y (ppm), Nb (ppm), TiO₂ (wt %) versus Zr (ppm) crystallization plots of Pearce and Norry (1979). Symbols are; crossed boxes- Suite #1; filled triangles are samples from Suite #2.

crystallizing phases. To determine the precise explanation of fractional crystallization or partial melting, in each case requires use of other elements, namely Cr and Ni. For example, the Ni concentration varies little during partial melting, but in the present study Ni concentration decreases with increased Zr. The different degrees of partial melting can be discarded by the limited range shown by Zr (100-140 ppm). Thus fractional crystallization (ol, cpx, plg) is the dominant phase to explain the observed within-suite chemical variations and petrogenetic evolution of these rocks.

Chapter 5

5. Geochemical Stratigraphy

5.1. General Stratigraphy of the Deccan Traps

Beane et al. (1986), Lightfoot (1985), Cox and Hawkesworth (1984), and Mahoney (1984) first proposed a four-fold lithostratigraphic subdivision for the basalts of the Trap area in the Mahabaleshwar region. Later Khadri et al. (1988) proposed a three-fold stratigraphy of the Traps. The Deccan Basalt Group of the Western Ghats was later subdivided into three subgroups and 12 formations (Subba Rao and Hooper, 1988) (Table 7), on the basis of a combination of field mapping with petrochemical and isotopic studies. The distribution of the eleven main formations along the Western Ghats is shown in Figures 23 and 24.

The areal extent of each formation and the variation of their thickness provide some idea of the physical nature of the volcanic event. No detailed mapping of the Jawahar and Igatpuri Formation has been carried out; however, the units are assumed to be thicker in the north than in the south (Bodas et al., 1984). The Neral Formation dies out to the north and south of Damdamia, with a maximum thickness of 145 m at Bivpuri, and was presumably erupted as a large lens from a centre in the Western Ghats. The Thakurvadi Formation is very much thicker in the Kalsubai (about 600m) and Igatpuri areas than in the southern part

GROUP	SUB-GROUP	FORMATION
DECCAN BASALT	WAI	Amboli Panhala Mañabaleshwar Ambenali Poladpur
	LONAVALA	Bushe Khandala
	KALSUBAI	Bhimashanker Upper Thakurvadi Middle Lower Neral Igatpuri Jawahar
	Basement	

Table 7- Reconnaissance subdivision of Deccan Basalt Group in the Western Ghats, India. Compiled by K.V. Subbarao and P.R. Hooper (1988)

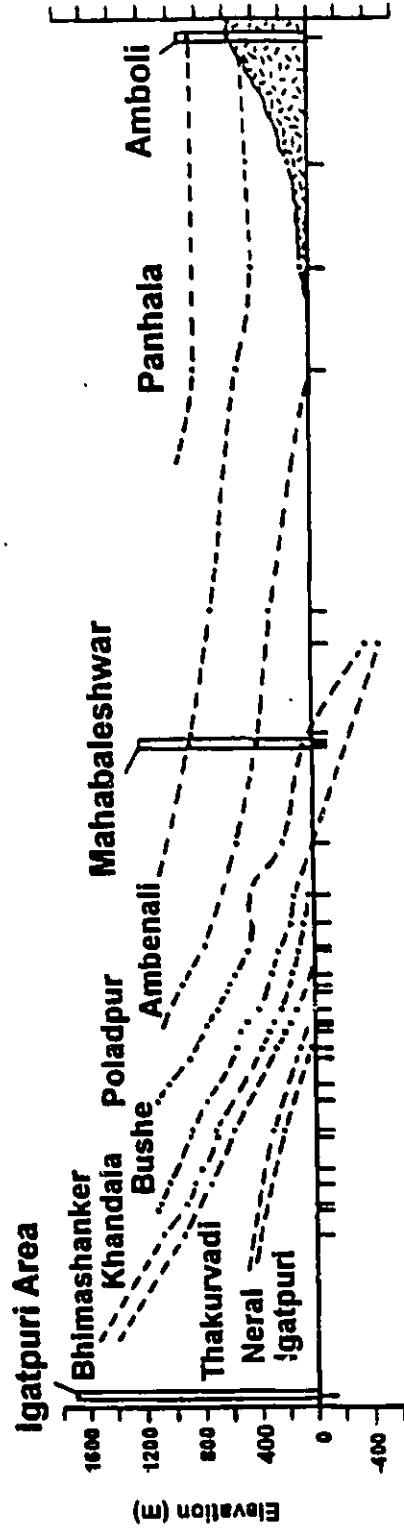


Figure 23- Stratigraphic cross-section along the Western Ghats. Formation boundaries are indicated by dashed lines. Black dots represent contacts between formations. Lowermost Jawahar Formation is not shown. Modified from Mahoney (1988).

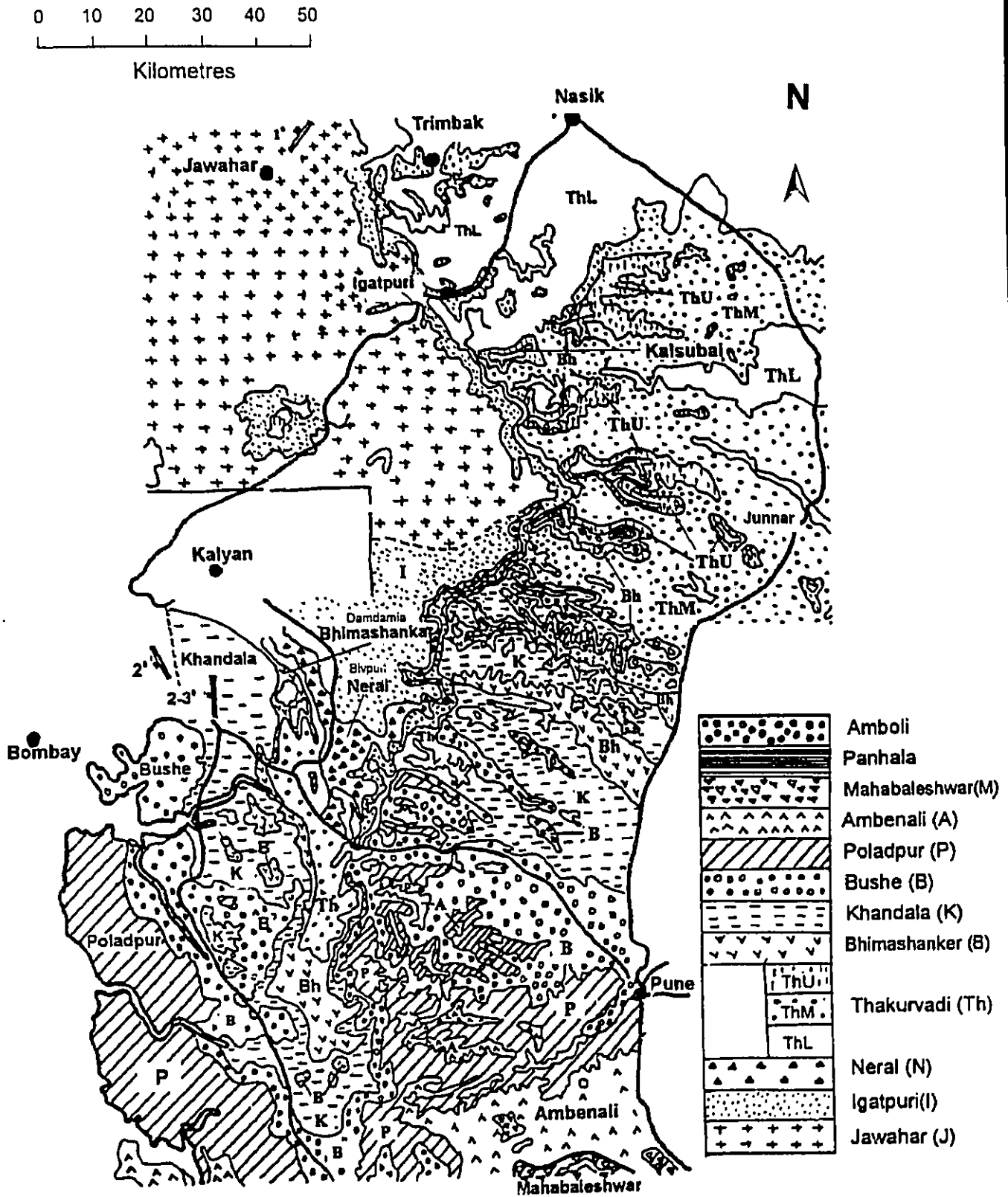


Figure 24- Geological sketch map of the Western Ghats showing distribution of different formations between Nasik and Pune. Study area is shown by dotted line. Modified from Hooper et al. (1988).

of the Western Ghats (Mahoney 1984; Bodas et al. 1984; Khadri et al., 1988); its eruptive centre presumably lay within that northern area. The relatively thin Bhimashanker Formation is also thicker in the north (140 m) than in the south (20-60 m) and accordingly may be assumed to have erupted in the north. The overall thickness of the Khandala Formation remains fairly constant (140 m), but many of the flows have a restricted lateral extents suggesting eruption at nearby sources (Beane et al., 1986). The Bushe Formation, with an overall thickness of 325m thins to the north (50 m) and south, where most of the lower part of the formation is missing. This lens probably had its eruptive source in the centre of the Western Ghats (Beane et al., 1986).

The Poladpur Formation displays quite abrupt changes in thickness. The chemically distinct upper Poladpur Formation thins abruptly from Poladpur northeast to Pune (Bodal et al., 1986). The lower Poladpur Formation shows no apparent variation in thickness (400m) over the same distance. Little information is available on the thickness of the Ambenali Formation, but like the lower Poladpur Formation it appears to maintain the same thickness (400m) from Poladpur to Pune. Finally, the Mahabaleshwar Formation is reported as thickening significantly southward from Mahabaleshwar (Lightfoot, personal communication 1983, in Beane et al., 1986, p. 81).

The uplift of Kalsubai by 1500-2000 m relative to the area of basalt farther south has been suggested as a response to permanent crustal thickening due to underplating (McKenzie, 1984, Chapter 2). Deep seismic studies by Kaila et al. (1981) also indicate that Deccan basalts to the south of Mahabaleshwar extend about 500-1000 m below sea level. For example, the base of the Bushe Formation, missing in the north, is found to be at 450

m below sea level. This can only be explained by a drastic reduction in thickness of lava flows from north towards south, followed by the post-trappean activity. This also explains the presence of the entire Khandala Formation and over 2000 m of the Kalsubai Subgroup.

The distribution and variation in thicknesses of these formations strongly suggest a regional trend in which the older formations are thicker in the north, the middle formations have a broad lenticular shape thinning both to the north and south in the centre of Western Ghats, while the younger formations increase in thickness farther south. This suggests that the present configuration of the flows is mainly a primary volcanic edifice, and supports a southerly migration of the main volcanic centre. This structure is modified locally around the margins and particularly along the west coast by post-volcanic deformation. Such a volcanic structure could be explained by hot-spot activity related to the northward-moving Indian plate (Cox, 1980). If one assumes plate motion was constant, then the rate of magma eruption probably waned following the initial outpouring of amygdaloidal basalt.

However, Mitchell and Widdowson (1991) proposed two models of eruption. In their first model, the centre of eruption remains essentially fixed throughout the Deccan episode, giving rise to annular and concentric flow units. The second model involves the southerly migration of the volcanic centre as mentioned above. The authors suggest that the present distribution, variation in thicknesses, and the observed overstep arrangement of these formations (Fig. 8) could have been the result of either model. However, the updated geochemical information (Cox and Hawkesworth, 1985; Najafi, 1981; Beane, 1986; Mahoney, 1988, etc.) supports the migration model, as the picritic and K-rich basalts are restricted to the northern Deccan and the southern regions are characterized by thick

tholeiitic sequences.

5.2. Flow Stratigraphy of Thakurvadi Formation.

Khadri et al. (1988), on the basis of extensive study of the western Deccan basalt province, presented a revised flow stratigraphy of the 650 m - thick Thakurvadi Formation; originally proposed by Beane et al (1986). Their study was mainly based on field observations, petrographic and mineralogical work, and bulk geochemistry of both major and trace elements; computer-aided statistical analysis using a large set of chemical variables proved to be useful in the subdivision of otherwise indistinguishable flows.

Beane et al. (1986), on the basis of petrographic and chemical studies, first proposed the concept of chemical types (CTs). They suggested CTs may be repeated at different stratigraphic levels. Each chemical type is characterised by its own set of physical characteristics, with a range of variation in chemical composition. Beane et al. (1986), also divided the Thakurvadi Formation lying South of Junnar into five members; the number of members was later increased to eight (Beane, 1987).

Khadri et al. (1988) in their study to the north of Junnar, plotted major and trace element contents against ground elevations above mean sea level, to demonstrate the variation of chemical composition with the stratigraphic position of the flows. They believed these plots to be extremely useful in dividing the complete Thakurvadi Formation into members and CTs. Khadri et al. (1988) proposed that the Thakurvadi Formation represents nine CTs. In order to maintain uniformity of nomenclature, they retained the

names of the sequences proposed by Beane et al. (1986). In addition they used the names of local villages or towns in designating new members. The different chemical types as described by Khadri et al. (1988) are shown in Table 8.

Table 8- Nine chemical types as described by Khadri et al. (1988)

Chemical Types	Petrographic Characteristics	Chemical Characteristics
9. Manhar GPB	<ul style="list-style-type: none"> • Coarse- grained matrix • Phenocrysts of Ol and Plg 	<ul style="list-style-type: none"> • MgO < 6% ; TiO₂ < 3% • P₂O₅ > 0.3% • Ni < 100 ppm
8. THHINI	<ul style="list-style-type: none"> • Medium- to coarse- grained ol phyric; alteration to iddingsite is common. • Less Cpx 	<ul style="list-style-type: none"> • MgO = 8-9.5 % • TiO₂ = 1.4-1.9%; • P₂O₅ = 0.18-21% • Cr = 300-900 ppm • Ni = 140-170 ppm
7. RGD	<ul style="list-style-type: none"> • Massive plg phyric basalt with mafic microphyric bands. • This can be separated from MGT by its coarse grained mafic-phyric (Ol+Cpx), and chemical nature. 	<ul style="list-style-type: none"> • MgO > 7 % • TiO₂ < 2.3 % • P₂O₅ < 0.23 % • Ba < 120 ppm • Ni > 130 ppm • Cr > 220 ppm
6. MGT	<ul style="list-style-type: none"> • Compact, fine-grained, Plg phyric, amygdaloidal basalt. • Microphenocrysts of Ol. • 15-20 % modal plg composition • Twinning and zoning 	<ul style="list-style-type: none"> • MgO < 6.2 % • TiO₂ > 2.4 % • P₂O₅ > 0.2-0.3% • Cu > 190 ppm

<p>5. PICRITE</p>	<ul style="list-style-type: none"> • Coarse-grained Ol phyric (25-30%) • Picritic basalt with Ol and Cpx phenocrysts • Separated from overlying middle Thakurvadi by physiographic break and sudden changes in chemical composition to overlying THHINI 	<ul style="list-style-type: none"> • MgO >10% • TiO₂ >1.65 • P₂O₅ <0.2 % • Cr >500 ppm • Ni 300 ppm • Ba <150 ppm • Zr <140 ppm • MgO content increases in the middle as compared to the top and bottom
<p>4. THLONI</p>	<ul style="list-style-type: none"> • Fine-grained ophitic basalt • Dominant Plg and Ol phenocrysts; occasional Cpx phenocrysts • Granular fine grained groundmass with small grains of Fe and Ti oxides 	<ul style="list-style-type: none"> • High TiO₂ and P₂O₅ than UBHADE; THHICR and; THINNI • Less MgO, Ni, Cu than THHICR • TiO₂ > 1.75-2% • P₂O₅ > 0.20-26% • MgO < 7% • Ni = 100-180 ppm
<p>3. UBHADE</p>	<ul style="list-style-type: none"> • Medium- to coarse-grained • Abundance of Ol and Cpx phenocrysts 	<ul style="list-style-type: none"> • MgO < 7% • P₂O₅ <0.25% • CaO <10.5% • TiO₂ < 1.7% • Distinguished from THLONI by its smaller proportion of TiO₂ (<1.75%) and P₂O₅ • Distinguished from THHICR by its smaller proportion of TiO₂, P₂O₅, MgO <7%
<p>2. THHICR</p>	<ul style="list-style-type: none"> • Compact, massive Olaphyric basalts of coarse grained matrix. • Subophitic texture • Abundance of Cpx and Ol microphenocrysts 	<ul style="list-style-type: none"> • Higher MgO and Cr • Less K₂O and Ba, Ni than other CTs • MgO >7% • CaO = 10-11% • TiO₂ = 1.65-1.8% • K₂O = 0.41% • Ba = 138 ppm • Ni = 100-200 ppm

1. JP-3	<p>▶ Highly evolved</p>	<p>• MgO < 4.1 % • P2O5 = 0.29-0.36% • TiO2 = 2.5-2.8% • Ba = 260-415 ppm • Ce = 49-54 ppm • La = 21-38 ppm • Zr = 180-220 ppm • Sr = 300-490 ppm</p>
JP-2 JP	<p>▶ Coarse-grained, generally unaltered with fresh Ol and Plg phenocrysts.</p>	<p>• MgO = 5.8 % • K2O = 0.32-1.2 % • P2O5 = 0.20-0.30 % • TiO2 = 2-2.6 % • Ba = 100-300 ppm</p>
JP-1	<p>▶ Phyric amygdaloidal basalts</p>	<p>• MgO = 6-7 % • TiO2 = 1.6-1.94% • P2O5 = 0.18-0.23%</p>

These chemical types show an overall compositional range of MgO 3.5-17 %; TiO₂ 1.3- 3.3 %; P₂O₅ 0.12-0.30 %; and CaO 7.47-12.5 %. Each chemical type (CT) consists of one or more flows with distinctive field characters, phenocryst assemblages and chemical variation, associated with major or minor breaks. In addition to the physiographic and chemical breaks in the stratigraphic sequence, giant plagioclase phenocryst basalt (GPB) horizons may occur at or near the formation boundaries (top or bottom of the flow; Karmarkar et al., 1972 in Subbarao, 1988, p. 236). These boundaries have been used as marker horizons to distinguish between different formations (Beane et al., 1986). They found that these chemical types represent the repetitive eruption of these lavas at different stratigraphic levels.

5.3. Results of Present Study

In the present study, an attempt is made to establish a stratigraphic sequence for the 40 rock samples within the Thakurvadi Formation. Table 9 represents the range of elevation from the bottom of the sequence towards the top. In order to achieve uniformity of approach with regard to previous investigations, the trace element chemistry and the petrographic features of each sample are also plotted against the elevation on this table. The lowest elevation recorded is about 720 m and the highest elevation is about 920 m above mean sea level. All the samples from the study area fall within this range. In Table 9 the samples are arranged in the increasing order of elevation. Seven intervals have been designated, and each interval consists of the samples within that range in elevation. In order to maintain

Table 9. Elevation versus chemical and petrographic features of the samples from the Deccan Traps.

Height Metres	Sample #	MgO	TiO ₂	CaO	P ₂ O ₅	Mg	Ba	Zr	Y	Sr	OI	CDX	PIQ	MF	c.Mass	Height In m
820	UP1-1	7.68	1.78	10.93	0.17	132	90	159	26	279	X	X	X	X	M-C	970
845	DP1-1	7.29	1.74	7.29	0.17	108	162	117	26	239	X	X	X		F	860
to	ADK1-1	7.83	1.68	8.8	0.17	118	192	131	26	259	X	X	X		M	860
875	U-1-1	7.58	1.64	9.22	0.166	96	106	174	26	291	X	X	X		M	860
810	ALDK	7.29	1.76	10.56	0.13	108	83	128	27	149	X	X	X		M	820
to	MSSB-3	5.62	1.71	7.26	0.14	83	261	129	28	284	X	X	X		M-F	800
845	MSSB-1	6.58	1.66	10	0.14	90	216	121	27	240	X	X	X		F-M	800
790	MSSB-2	5.72	1.7	8.08	0.16	101	204	121	27	240	X	X	X		M	800
to	MSSB-4	6.64	1.72	9.6	0.15	126	174	128	26	235	X	X	X		M	800
810	LRMB-1-1	7.79	1.67	11.19	0.12	126	130	123	25	281	X	X	X		C-M	800
	PST1-1	6.73	1.78	10.26	0.15	107	96	128	26	185	X	X	X		F	800
	ABR-1	6.83	1.78	10.48	0.12	103	120	126	26	197	X	X	X		F	780
	UPRAD1-1	6.5	1.67	9.33	0.11	97	310	118	24	147	X	X	X		C-M	780
	AFRE1-1	6.21	1.73	8.12	0.16	83	364	128	27	519	X	X	X		M-F	780
775	TCHM1-1	6.1	1.66	6.45	0.15	289	205	121	25	331	X	X	X		F	780
to	MCG-1	7.1	1.72	11.03	0.14	107	102	131	27	152	X	X	X		F	780
790	MCG-2	6.84	1.73	10.01	0.13	104	150	127	28	101	X	X	X		F	780
	MBC1-1	6.2	1.66	10.48	0.12	93	198	195	38	232	X	X	X		M	780
	MAD01-1	7.21	1.66	10.2	0.13	99	92	122	25	236	X	X	X		M-F	780
	DT1-1	6.45	1.76	10.32	0.15	99	122	122	26	172	X	X	X		M-F	780
	MACE-2	6.45	1.88	10.4	0.18	96	154	135	28	166	X	X	X		M-F	780
	MCD1-1	6.03	1.64	11.29	0.13	91	356	120	27	166	X	X	X		M-F	760
750	PCT1-1	6.13	1.76	9.52	0.14	106	181	127	26	186	X	X	X		F	760
to	TCH-2	6.32	1.68	8.93	0.16	95	229	125	26	434	X	X	X		M	760
775	PC-1-1	6.87	1.69	10.01	0.11	106	245	121	24	328	X	X	X		F	760
	TCHM1-2	6.45	1.7	9.97	0.14	94	147	122	26	205	X	X	X		M	760
	MCR-1-1	8.86	1.66	9.15	0.15	118	154	127	27	178	X	X	X		M	760
	TCH-3	5.94	1.59	9.38	0.13	119	89	108	22	296	X	X	X		F-M	740
	VMNT-1	5.81	1.7	7.86	0.14	92	3	118	24	89	X	X	X		C-M	740
	MRT-1	5.93	1.59	9.26	0.13	96	111	118	25	136	X	X	X		F-M	740
720	PBST-1	5.97	1.64	9.72	0.15	101	171	116	24	292	X	X	X		M-F	740
to	PR1-1	6.72	1.72	9.02	0.14	91	196	123	25	577	X	X	X		M	740
750	PTV1-1	6.54	1.73	7.01	0.13	89	278	122	25	157	X	X	X		M-F	740
	MR-1-1	5.72	1.68	9.93	0.13	101	165	119	25	373	X	X	X		F	740
	TCHM	6.96	1.72	10.27	0.15	111	177	122	26	258	X	X	X		M-F	740
	DPRT-1	6.55	1.75	10.63	0.17	150	111	178	25	133	X	X	X		M-F	740
	TP21-1	7.03	1.73	13.57	0.11	124	111	110	24	321	X	X	X		M	720
720	WAT-1	6.69	1.68	8.21	0.15	119	142	116	26	301	X	X	X		F-M	720
	TP-1	6.52	1.65	8.92	0.13	119	140	123	26	186	X	X	X		M	720

uniformity of approach, the criteria for choosing these intervals is based on the previous investigations. The interval boundaries are mostly taken at differences in elevation of 20-30 m, to observe possible variation in the chemistry and petrography of the samples falling at different intervals. Three samples lie in the lowest interval at 720 m. All three samples show similar chemical features, except for variation in CaO for WA 1-1 and TPZ 1-1. These samples have been discussed as altered in the previous section. Petrographically, sample TPZ 1-1 falls in Suite No. 2 and has magnetite as one of the principal phenocrysts.

Nine samples fall in the next level upwards. These samples show little variation in MgO (5-7 %), TiO₂ (1.59-1.75) and P₂O₅ (0.13-0.17 %). One sample PTV 1-1 shows a marked difference in Ba and Ca values which could have been due to mobility of these elements. The majority of the samples that lie at this level belong to Suite No 2.

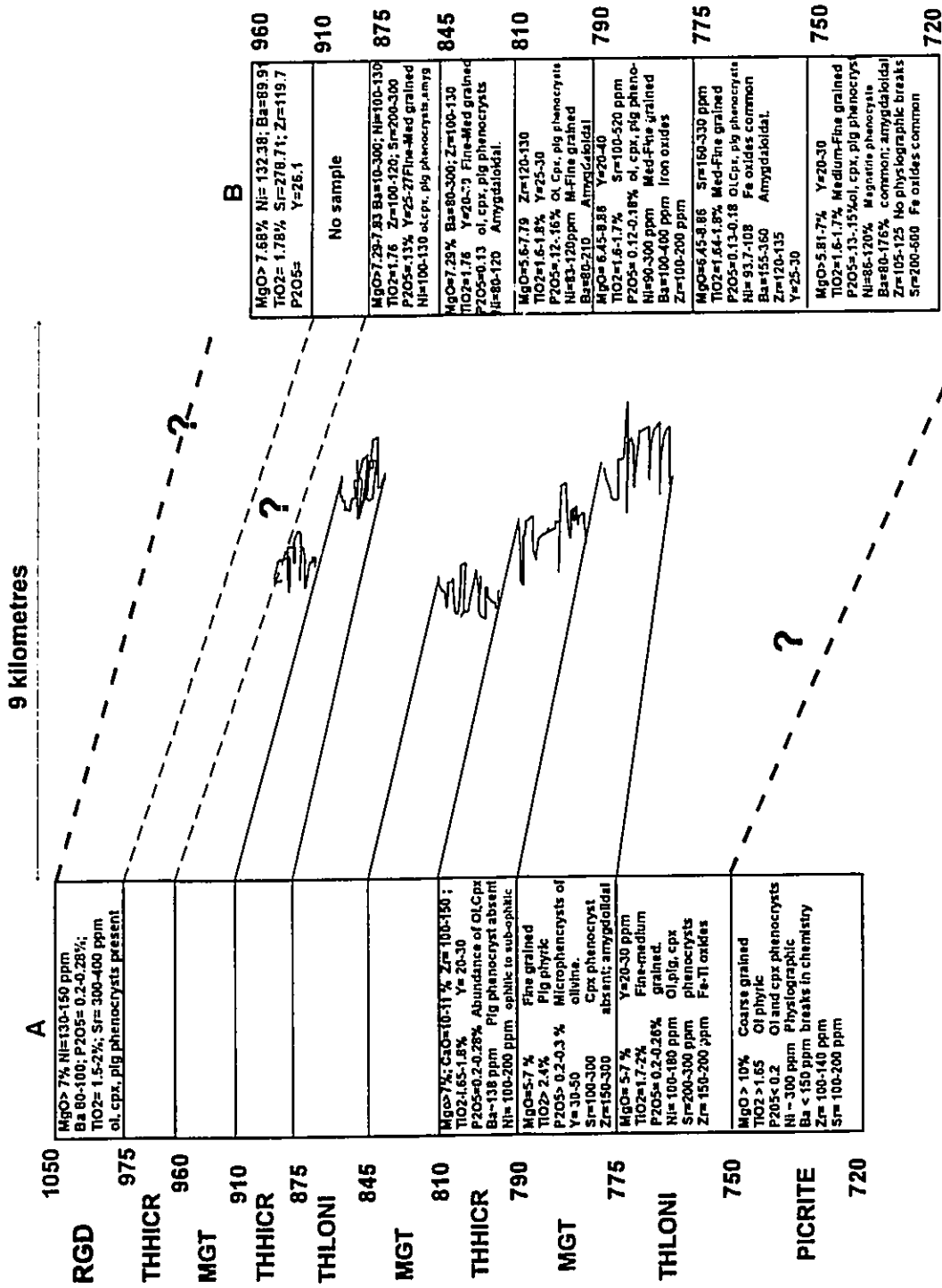
At elevations 760 m and 780 m., most samples show only minor variation in rock chemistry, except for the Ba and MgO values for sample # MCN1-1. Samples falling at this level are from two different petrographic suites. The samples from 780 up to 820 m also do not show major variation in rock chemistry. Three samples that lie at the elevation 860 m show higher values for MgO content and a very little enrichment in P₂O₅ as compared to other samples. One sample, UF-1, lies at the highest elevation of 920 m. It shows similar chemistry to those at 860 m, except for being medium- to coarse- grained.

Therefore, on the basis of the field observations, major and trace element analysis and petrography, the above observations lead to the fact that, most of the samples from the study area belong to flows that are chemically similar rather than distinct. No physiographic breaks in the chemistry of the present samples were observed. Marker horizons such as

Giant Plagioclase Basalts with larger concentration of high field strength incompatible elements, differences in size, shape and abundance of phenocrysts were not observed. Hence, no distinct boundary and/or intra-formational sub-divisions are recognised in the present study area.

A comparison of the present study with the work of Khadri et al. (1988) is shown in Figure 25. In the stratigraphic cross-section of the Thakurvadi Formation, originally described by Khadri et al. (1988), between 600-1200m elevation, the present study samples fall in a limited range of elevations (720-920 m). Four out of nine chemical types (CTs) should occur at these elevations. The reference section of Khadri et al. (1988) is about 9 kilometres west of the study area and lava flows in the study area dip less than 0.5° E, it is possible that the whole lava sequence may have been displaced by 70 -80 m from the reference section of Khadri et al. (1988). Hence direct comparison of lavas above mean sea level in the same height interval is not successful. Therefore, in order to correlate the present study area with that of the previous workers, the characteristic features of all the chemical types described by previous workers, that occur in the middle Thakurvadi, are compared with the chemical data and petrological observations of the present study (Fig. 25).

In Figure 25, the chemical type "PICRITE" occurs at the base of the type section, at elevations 720-750 m. On comparing samples of the present study with this chemical type, the following differences were observed: MgO (5.8-7 wt%); P_2O_5 (0.13-0.15 wt%); Zr (105-125 ppm) and Ni (86-120 ppm) values are found to be lower than the values reported by the previous workers. Study samples show high values of Sr and Ba. No breaks in the chemistry were observed. The samples are amygdaloidal. The phenocryst assemblage



(A) Reference section (Khadri et al. 1988)

Figure 25- Chemical types in Thakurvadi Formation of the reference section compared with geochemical and petrological analysis of basalt samples from Akole Taluka. The study area comprises flows representative of the chemical type THLONI, while chemical types MGT, THHICR and PICRITE pinched out before reaching the study area.

(B) Present study

comprises olivine, plagioclase, clinopyroxene, and magnetite, with iron oxides. On the other hand, the samples of Khadri et al. (1988), representative of the chemical type "PICRITE", are non-amygdaloidal and show phenocryst assemblages of olivine and clinopyroxene. No plagioclase phenocrysts in this chemical type have been reported by them. However, on comparing the chemical and petrographic features of the present study samples at this elevation with other chemical types of Khadri et al. (1988), the chemical type "THLONI" corresponds closely than the chemical type "PICRITE".

At the second stratigraphic interval, between 750 and 775 m, most samples from the study area show chemical variations, such as MgO from 6-8 %; TiO₂ (1.64-1.8 %) and; Zr (120-135 ppm); Sr (130-330 ppm); Ni (93-110 ppm). The samples are amygdaloidal. Phenocryst assemblages consist of olivine, clinopyroxene, plagioclase and magnetite, with a medium- to fine-grained groundmass. These chemical and petrographic characteristics, except for P₂O₅, are very similar to those of the chemical type "THLONI" of Khadri et al. (1988). At the interval between 775 and 790 m most samples from the present study show lower values for TiO₂ (1.6-1.7 %); P₂O₅ (0.12-0.18 %); Zr (100-200 ppm) than the values of the chemical type "MGT" observed by Khadri et al. (1988). On the other hand MgO (6.5-8.9 %) and Sr (100-520 ppm) show higher range than that of the chemical type "MGT". The samples from this range of elevations are amygdaloidal and show phenocryst assemblages of olivine, clinopyroxene, plagioclase and magnetite, with medium-to fine-grained groundmass. These observations were found to be closer to the chemical type "THLONI" of Khadri et al. (1988), but inconsistent with the observations of "MGT" or any other chemical type of the middle Thakurvadi.

At heights of 790-810 m, TiO₂, Zr, Ni values of the study samples are lower than that of the ranges described by the previous workers, while Ba shows high range for the chemical type "THHICR". Samples are amygdaloidal and show phenocryst assemblages of olivine, clinopyroxene, plagioclase and magnetite, with a fine- to medium- grained groundmass. These features are found to be consistent with the petrography and chemical characteristic of the chemical type "THLONI" rather than that of "THHICR" as reported by previous workers. At elevations between 810 and 845 m the previous workers have reported the repetition of the chemical type "MGT". From the study samples, only one sample falls at this interval and the chemical and petrographic features of this sample is consistent with that of the chemical type "THLONI" not "MGT". Three samples fall at the interval of 845-875 m, which represents the repetitive phase of the chemical type "THLONI". Chemical and petrographic features of these samples are in general agreement with this chemical type, except for P₂O₅ and MgO. None of the samples from the study area falls at the next interval between 875-910 m, which represent the chemical type "THHICR" by Khadri et al. (1988). Hence there is no evidence in favour of either the presence and absence of this chemical type, or any other chemical type, in the middle Thakurvadi Formation.

Only one sample falls at the interval between 910-935 m, which should fall under the chemical type "MGT" of Khadri et al. (1988). The petrographic and chemical features of this sample are not in accordance with the characteristic features of MGT (Fig. 25), but were found to be in general agreement with the chemical type "RGD" of Khadri et al.(1988).

Thus, from the present research it is concluded that, the details shown in the Figure 25 of the present study do not correspond with the regional lithostratigraphic subdivision as

proposed by Khadri et al. (1988). The four CTs described by them at the given elevations of 720-920 m do not match to the petrographic and chemical observations made during the present study. However, the majority of samples occurring in the study section are similar to the chemical type "THLONI". This leads towards the conclusion that, rocks from the study area probably belong to flows that show petrographically two distinct suites, but show similar chemistry.

5.4. Discussion

Although lava flows between 150-200 m in thickness have been reported in the Sagar area by previous workers (Mahoney, 1988), in the light of present study, it seems highly unlikely that a single flow could reach about 200 m in thickness as its presence would require a special explanation in terms of petrogenesis. Had this been the case, the petrogenetic assemblages of minerals occurring would have shown the phenomenon of crystal settling with olivine at the bottom. However, this phenomenon seems implausible as olivine was found at all elevations; hence no evidence(s) of the crystal settling was encountered.

Secondly, it is also possible that the presence of zeolites in the Deccan basalts may have affected the whole-rock chemistry, which may further cause problems in geochemical correlations. The elements K, Na, Ba, Sr, and Rb are present in the Zeolites (previously discussed) and impart non uniform distribution of these elements. However, zeolites will not have much effect on elements like Zr and Ni, as the presence of abundant zeolites would

only cause reduction in the concentrations of elements not in their ratios.

Kale et al. (1991), on the basis of the three-dimensional geometry of the lava flows, their lateral continuity, and the order of superposition, questioned the validity of correlation of the chemical types. They suggested that the lateral continuity of an individual flow (the basic stratigraphic unit in Deccan basalts) is difficult to trace in regions where compound flows are dominant. The compound and simple lava flows show interfingering; hence lateral pinching out of flows and deep weathering present limitations on tracing individual lava flows laterally. Hence in a vertical cross section of a few kilometres, a flow may occur in one region and could easily be missed in the other part.

Thus it seems reasonable that lava flows representative of the chemical types PICRITE, MGT and THHICR present in the reference section of Khadri et al. (1988) may have pinched out before reaching the present study area, while lava flows representative of the chemical type "THLONI" appear to be distributed over larger areas, including the study area.

An attempt has been made to correlate the chemical types of Khadri et al. (1988) with those of the present study (Figure 25). The chemical type "PICRITE" that occurs at the base of type section, is missing from the study area. An alternative explanation to pinchout, for its absence can be argued on the basis of vertical drop of 70-80 m of the study area due to regional dips of $< 0.5^\circ$; therefore, an approximate correlation is suggested (Fig. 25).

One sample, UF-1, occurs at the highest elevation (920) m in the present study area. It correlates very well with the chemical type "RGD" that occurs at the elevation of 970-1050 in the reference section of Khadri et al. (1988; Fig. 25).

Mitchell and Widdowson (1991) suggested that, in order to acquire the mapability criteria, it is important to have lateral continuity of each formation (lava packages, each consisting of numerous flows) representing the basic stratigraphical unit. They suggest by considering packages of lava flows characterized by similar chemical signatures rather than single flow units (as suggested by Kale et al. 1991) problems such as lateral pinchouts, changes in phenocryst content and other lithological variations, which makes the lava flow based stratigraphy difficult, can be avoided. These authors also proposed that the question of scale is another important criterion in interpreting the regional structure. They suggested local details can be of significance in a small-scale study, whereas on a larger scale, such local details may not affect the regional interpretation.

While considering the current discussion on the debate of chemical stratigraphy by Mitchell and Widdowson (1991) and Kale et al. (1991), some suggestions have been made for the present study area. A chemical type comprising a lava package, each consisting of one or more flows, with similar chemical and petrographic signatures, is considered as the basic unit of stratigraphic subdivision in the study area. However, the results of the present study suggest that not only a single lava flow, but also a lava package of a certain chemical type comprising several flows, may also show pinchouts. These lava packages or chemical types may avoid the problems of lateral pinchouts, changes in phenocryst contents and lithology on a large scale (Mitchell and Widdowson, 1991), but in a small scale study such as that done by Kale et al. (1991) and, to some extent, the present work, the lava geometry such as interfingering of simple and compound flows, can not be avoided.

Chapter 6

6. Bedrock Geohydrology

In Maharashtra State the areal extent of basaltic flows is about 230,000 km². During the past two decades various factors such as climate, structural controls and hydrogeological conditions have affected the occurrence of groundwater. The state has suffered three severe droughts since 1965, as more and more land is approaching desertic conditions due to depletion of groundwater. Climatic factors, topography and hydrogeological conditions have also affected the groundwater regime so far.

As a result, millions of people from the rural sector are facing acute scarcity of water. Despite receiving heavy rainfall, the area remains dry, particularly in the summer months, due to heavy surface runoff and high evaporation rates. Hence, the purpose of this chapter is to discuss some aspects of bedrock geology that affect the groundwater regime of the Deccan Traps.

6.1. Lava Flows

Nicholas (1936, in Lindholm, 1988, p. 49) introduced the concept of flow units for a basaltic flow and stated that many lava flows are divisible into flow units. Within the Deccan Traps, each flow is characterized by an upper part that cooled and solidified before

another flow unit was superimposed upon it. Thus the term "compound flow" was proposed for a lava divisible into flow units, and "simple flow" for that which is not divisible. In some cases, no significant cooling of a unit occurred before it was buried. In this case, the whole assemblage of lava layer then cooled as a single cooling unit, known as "multiple flow". If there existed an interval of time between two superimposed lava flow units, weathering of the top of one unit took place before next unit buries it. Hence one lava flow is commonly separated from another by a weathered zone or soil horizon. Hence interpretation of features in an individual flow, is restricted to regions where surface weathering is less pronounced.

From bottom to top an individual flow consists of a flow base, a colonnade and an entablature (Lindholm et al., 1988; Fig. 26). The thickness of each of these depends on the total flow thickness. The flow base is vesicular basalt and constitutes < 5 % of the total flow thickness. Sometimes the presence of pillow structure indicates flow interaction with water. The colonnade averages about 30 % of the total flow thickness. It consists of 3-8 sided columns of basalts, less vesicular than base. The columns commonly range in size from 1 m in width to 7.5 m in length (Swanson and Wright, 1978, in Lindholm, 1988, p. 40). Columns may also be cut by a system of joints. The denser entablature, which averages about 70% of the total flow thickness, consists of basalt columns less than 0.5 m in diameter. Cross joints in the entablature are less consistently oriented and connected than in the colonnade; hackly joints are also common. The upper part of the entablature is commonly vesicular, rubbly and clinkery. This vesicular upper part of the entablature, in combination with a superposed flow base, constitutes an interflow zone.

Thin bedded basaltic lavas, with diverse porosity-permeability features form the most

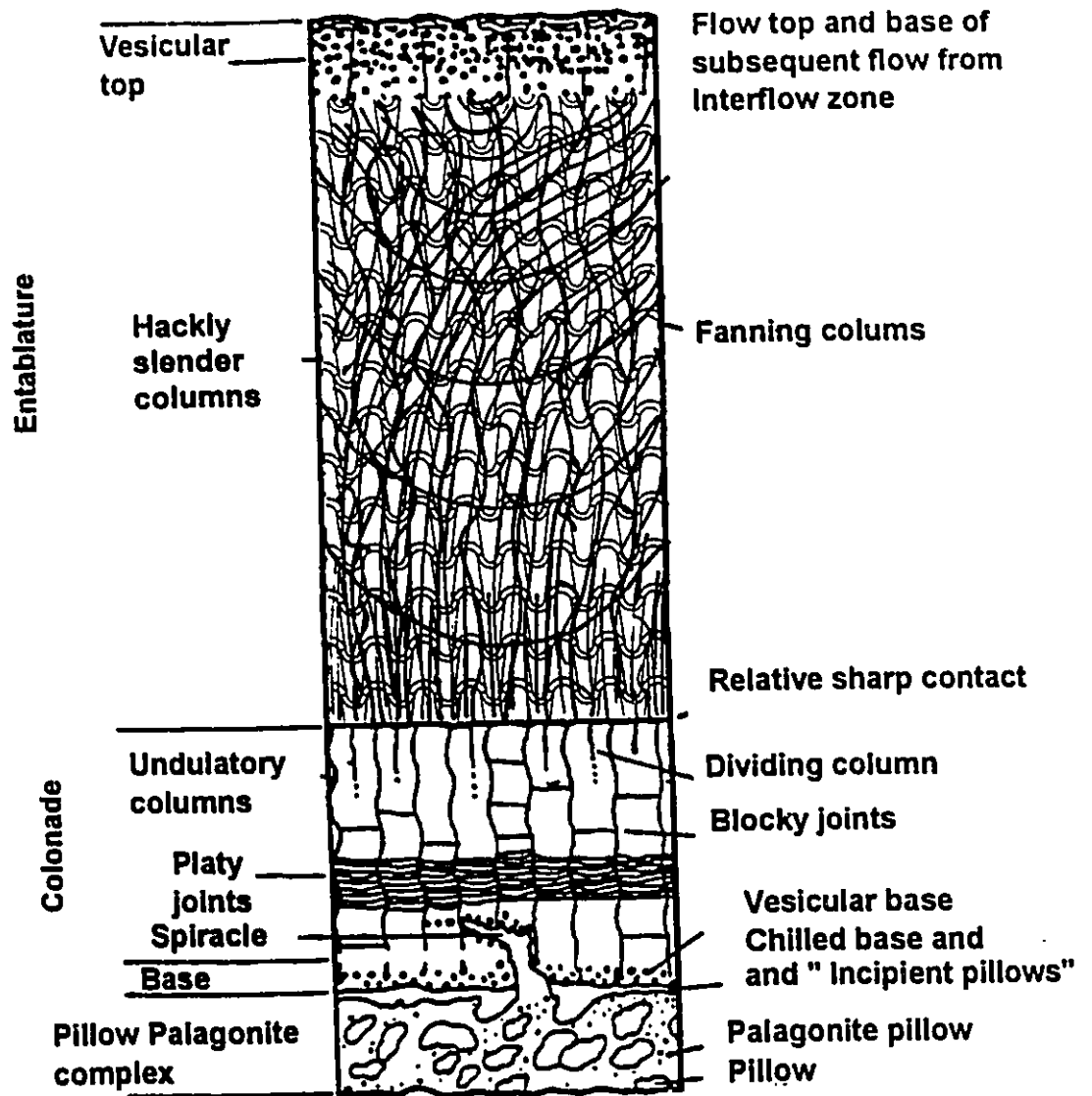
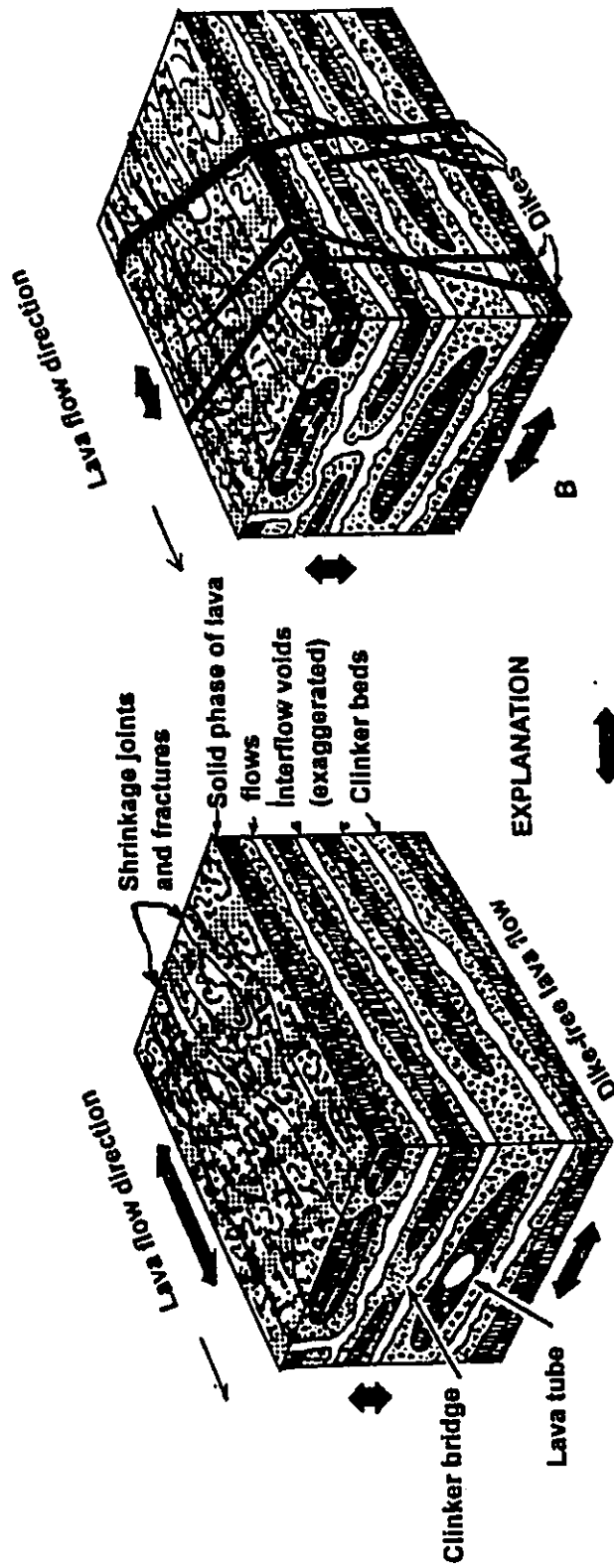


Figure 26- Intraflow structure in basalts. Modified from Lindholm (1988).

productive aquifers as compared to thick bedded flows with reduced porosity permeability features (Hunt et al., 1988). Figure 27 gives details of various permeability features in a typical sequence of such lavas. These are fracture permeability (joints and cracks); intergranular permeability (beds of clinkers and rubbles); and cavernous permeability (lava tubes and interflow voids).

Basaltic flows are generally characterized by aa and pahoehoe flow units (Figure 27). An aa flow unit unlike that of pahoehoe, is characterised by a dense aa core a meter or more in thickness, with fragmental clinker beds both on top and bottom of the dense part. This typical of aa unit exerts a strong layering control on flow of groundwater. The clinker fragmental layer is the main water producing zone in aa lavas. Sometimes vertical bridges of clinker at the lateral margins of aa flows provide important avenues for the vertical movement of water. Gas vesicles are common in both aa and pahoehoe lavas and may impart a high bulk porosity to both of them. The vesicles generally are not connected and do not contribute appreciably to effective porosity and hydraulic conductivity. A sequence of thin bedded lavas containing many individual pahoehoe and aa flows have greater areal extent, with near horizontal bedding, shows that they are anisotropic, with greater horizontal than vertical hydraulic conductivity (Hunt et al., 1988).

Previous workers (Deshpande, 1975; Singhal, 1973; Adyalkar, 1976; Thigle and Zambre, 1982, in Thigle, 1983, p. 323) proposed that the vesicular portion of basaltic flows and the weathered and jointed areas in massive flows are favourable sites for the occurrence of groundwater, under unconfined conditions. In addition, the cross-cutting dykes act like underground dams restricting the movement of groundwater.



Length of arrows denotes relative magnitude of hydraulic conductivity in direction of arrows

Figure 27- Features associated with lava flows. Hydraulic conductivity is highest in lava flow direction (A); hydraulic conductivity is lowered by dykes intruded at right angle to the lava flow direction (B). Modified from Hunt (1988).

6.2. Interflow Beds and Soil Horizons

In the western part of the Deccan Province the basalt flows are often separated by fine-grained pyroclastic material such as ash and tuff beds. These constitute fine-grained, clayey material predominantly red in colour. They are often referred to as red boles, and vary from a few tens of centimetres to 2 m in thickness.

The Deccan basalts of eastern and southern parts of the province are sometimes separated by sedimentary beds commonly known as inter-trappeans. They are composed of chert, limestone, calcareous sandstone, shales and pyroclastics. These inter-trappeans can also account for movement of groundwater between two flow units. However, the amount of water occurring in inter-trappeans is variable and depends upon primary porosity and areal extent (Powar, 1988). The erratic changes in temperatures during the summer and winter seasons, may also give rise to soil and saprolite through weathering. The basaltic saprolite has a homogenous structure that may include preferred zones of water movement and retention. In dyke complexes, where dykes are numerous and intersect at various angles, the net effect is overall reduction in porosity and hydraulic conductivity (Takasi and Mink, 1985, in Hunt, 1988, p. 260).

It is recommended that the search for ground water in the study area, based on the possible sites discussed above, should concentrate on the vesicular and weathered portion of the basaltic flows. No evidence of other possible sites was encountered.

6.3. Lineaments

Badgley (1962, in Thigle, 1983, p. 324) noted that remote sensing techniques can provide valuable information regarding the structural fabric of lithologically homogeneous terrains that have been subjected to mild, non-orogenic types of diastrophism. Keeping this view in mind, a hydrogeomorphological map of Akole Taluka, Ahmednagar, Maharashtra (Space Application Centre, Ahmedabad), in the Deccan Trap was used to delineate the structural fabric and the lineaments occurring in it.

Tjia (1971, in Molano, 1987, p. 172) suggested that lineaments are expressions and images on areal photographs of subsurface discontinuities in the rocks. They are surface expressions of deep-seated crustal fractures propagated upwards through the overlying consolidated and unconsolidated materials (Gay, 1972, in Molano, 1987, p 173). Molano (1987) suggested these discontinuities are potential sites of groundwater accumulation. For example, the longer a lineament, the higher is the probability of groundwater accumulation. Localities where long lineaments intersect are also likely to be potential sites of groundwater accumulation.

Satellite data from IRC 1A imageries (LSSII FCC); SPOT (MLA FCC); and SPOT (PLA B/W) on a scale of 1:25,000 were obtained covering the Akole Taluka, Ahmednagar district (Space Application Research Centre, Ahmedabad).

The length and orientation for each lineament was recorded and the data obtained were grouped into 6 azimuth ranges with 30° intervals. A length- azimuth frequency diagram (Figure 28) was then prepared for the data collected. A rose diagram for the

frequency of the lineaments was also plotted to identify the primary and secondary directions of orientation of these lineaments (Fig. 30).

As previously discussed (Chapter 2), the main tectonic features within the Deccan Traps are the Narmada lineament (east-west), the Tapti lineament, the Panvel flexure, and the west coast fault (north-south). The Kuruvadi rift, Konya rift, the Ghod lineament and the Konya lineament were later reported by other workers. In the present study, it is noted that the lineaments were predominantly zones of structural weakness along which fractures developed. The lineament map obtained from the satellite data is shown in Figure 29. Rose diagram (Fig. 30) shows that the maximum concentration of lineaments, is in range of $N 150^{\circ}$ to 180° . The secondary direction of the lineaments is observed at an interval of 120° - 150° . The principal resultant vector direction of these lineaments, was found to be 122° .

The lineaments form a structural pattern dominated by a north- northwest - south - southeast trend; with a secondary northwest - southeast trend. The lineaments that show north- northwest - south- southeast and northwest - southeast trends are oriented almost parallel to the west coast fault and Panvel flexure lying in north - south directions. A few lineaments that occur at an interval of $N 60^{\circ}$ - 90° are parallel to the regional Narmada and Tapti lineaments. In Bombay and surrounding areas, dykes are also oriented in north-south direction (Auden, 1949). Thus the concentration of these dykes was found to be parallel to the concentration of lineaments in range $N 150^{\circ}$ - 180° and orientation of major structural elements, the west coast fault and the Panvel flexure. Some of the lineaments, on the hydrogeomorphological map, are also parallel to the valley fills filled with unconsolidated sediments. All these features suggest that the emplacement of dykes and fractures been

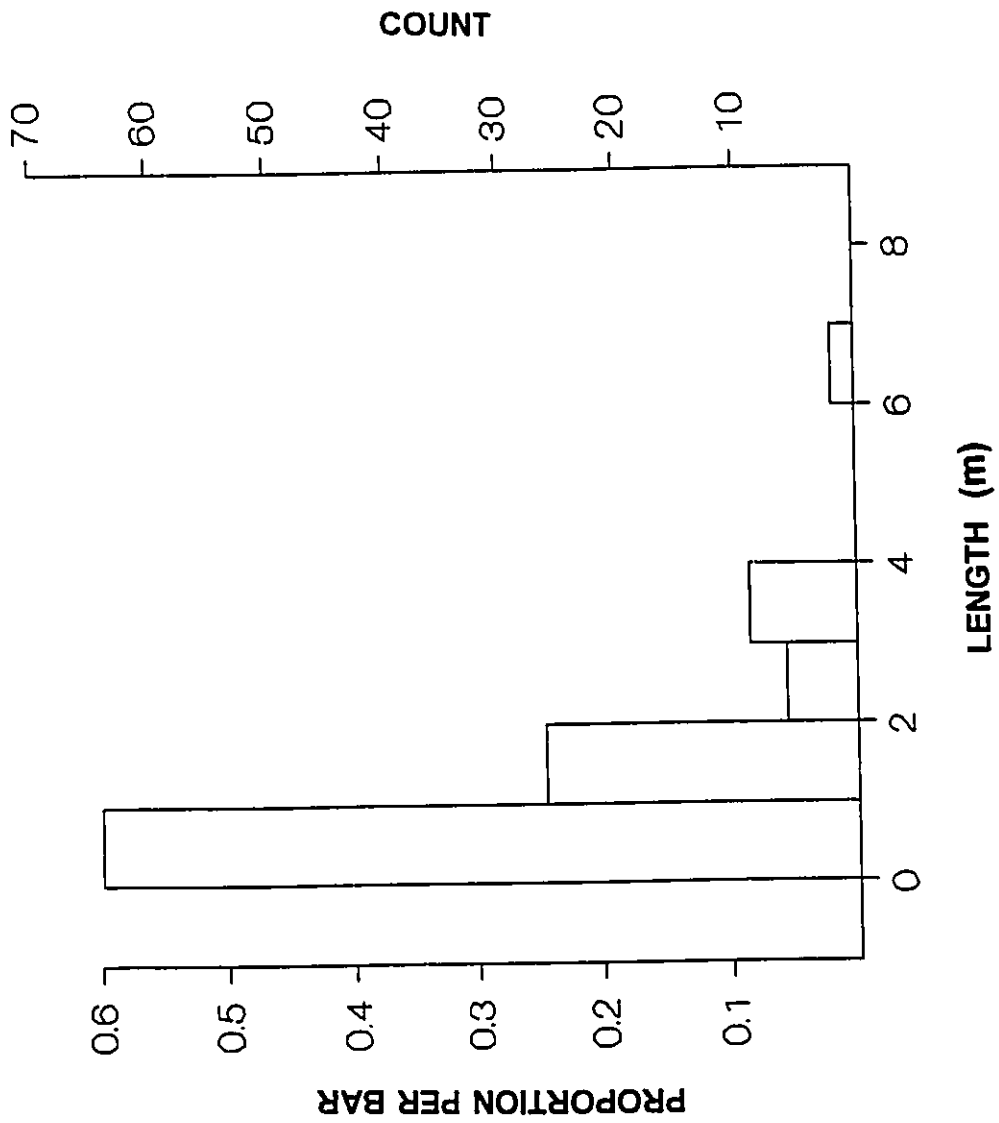


Figure 28- Length histogram for the lineaments in Akole Taluka.

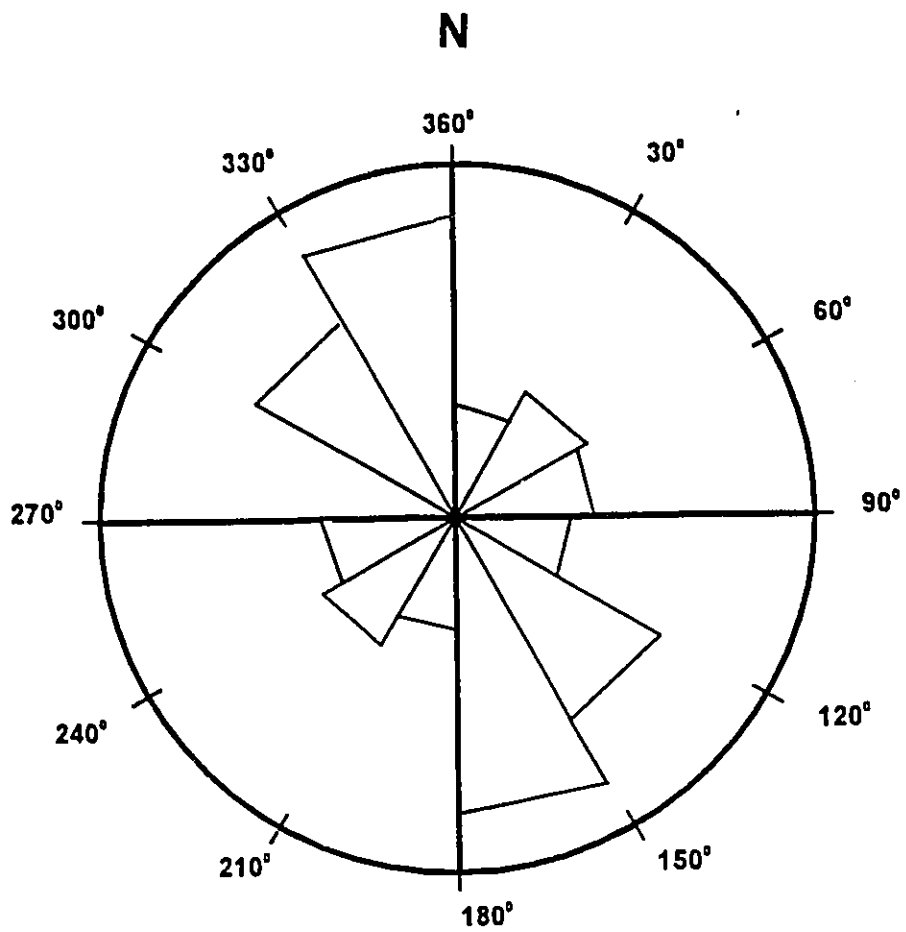


Figure 30- Rose diagram showing principal and secondary direction of the lineaments in Akole Taluka.

controlled by the lineaments.

The preliminary analysis of the major lineaments in the study area show eight lineaments. These are designated M1, M2, M3, M4, M5, M6, A7 and T8. Their orientations range from northwest - southeast, north- northeast - south- southwest to east-west. Several springs and seeps were found to intersect with these lineaments. Lineaments such as M1 and A7 evidence fracture zones in the stream bed in the form of fractures trending north-northwest - south- southeast. These are suggested as the possible sites of ground water occurrence in the study area. The lineaments that intersect the valley fills with unconsolidated material, also show promising features of potential ground water occurrence. However, no evidence of joint patterns or dykes was encountered for the lineaments through examination of satellite imagery.

A few ground features (BAIF, 1993), which may be significant from the point of influencing the groundwater movement, were also identified. Location of the ground features is shown in Figure 29. The ground features M1 and A2 observed in the study area show fracture zones running in a northwest - southeast direction. The ground feature A2 was found to cut across a stream bed. Two fractures trending north- northwest - south- southeast were also observed. All these features suggest that these are also the possible sites for the groundwater occurrence in the study area.

Conclusions

1) The Deccan Trap basalts in the Akole Taluka District of the Maharashtra State, India show fractional crystallization to be the dominant factor in the petrogenetic evolution of these basalts.

2) The study area comprises basaltic flows that show two petrographically distinct suites, but show an overlap in chemistry i.e. most of the samples from the study area belong to flows that are chemically similar rather than distinct. No physiographic breaks or marker horizons such as Giant Plagioclase Basalts were observed; hence no distinct boundary or intra-formational sub-divisions in the study area was interpreted.

3) Most of the samples from the study area are similar to the chemical type "THLONI" of the previous workers. The other chemical types PICRITE, MGT and THHICR are suggested to be missing from the present study area perhaps because these chemical types pinched out within a distance of few kilometres from the reference section of Khadri et al. (1988).

4) The lineaments and groundwater features occurring in the study area are the zones of structural weakness along which fractures developed. These are suggested as the possible sites of groundwater occurrence in the study area. The lineaments that intersect the valley fills with unconsolidated material and; the vesicular and weathered portion of basaltic flows are additional promising sites for groundwater occurrence in the study area.

References

- Agashe, L.V., Gupte, R.B., 1972. Mode of eruption of Deccan Trap basalts. *Bull. Volcanol.*, **35** : 591-601.
- Alexander, P.O., 1981. Age and duration of Deccan volcanism: K-Ar evidence. *Geol. Soc. of India, Mem. 3*, pp. 244-258.
- Alexander, P.O., 1980. Petrogenesis of low potassic quartz normative Deccan Tholeiites. *Jour. Geol. Soc. India*, **21** : 261-272.
- Auden, J.B., 1949. Dykes in western India. A discussion of their relationships with the Deccan Traps. *Trans. Nat. Inst. Sci. Incl.*, **3** : 123-157.
- Augustithis, S.S., 1978. Atlas of the Textural Patterns of Basalts and their Genetic Significance.
- Beane, J.E., Turner, Hooper, P.R., Subbarao, K.V., and Walsh, J.N., 1986. Stratigraphy, composition and form of the Deccan basalts, Western Ghats, India. *J. Volcano.*, **48** : 61-83.
- Beswick, A.E., Soucie, G., 1978. A correction procedure for metasomatism in an Archean greenstone belt; *Precambrian Research*, **6**: 235-248.
- Bose, M.K., 1972. Deccan Basalts. *Lithos*, **5** : 131-145.
- Cox, K.G., 1980. A model for flood basalt volcanism. *J. Petrol.*, **21** : 621-650.
- Deshmukh, S.S., Sehgal, M.N., 1988. Mafic dyke swarms in Deccan volcanic province of Madhya Pradesh and Maharashtra. *Geol. Soc. of India, Mem 10*, pp. 323-341.
- Deutch, E.R., Radhakrishnamurthy, C. and Sahasrabudhe, P.W. , 1959. Paleomagnetism of Deccan Traps. *Ann. Geophysics*, **15** : 39-59.
- Devey, C.W., Lightfoot, P.C. 1986. Volcanological and tectonic control of stratigraphy and structure in the western traps. *Bull. of Volc.*, **48**: 195-207.
- Duncan, R.A., Dyle, D.G. 1988. Rapid eruption of the Deccan Flood basalts, western India. *Geol. Soc. of India, Mem 10*, pp. 1-10.
- Dupy, C., and Dostal, 1984. Trace element geochemistry of some continental tholeiites. *Earth Plant. Sci. Lett.*, **67**: 61-69.

- Discussion on " A geological map of the southern Deccan Traps, India and its structural implications, 1991. *Journal of Volcanology*, **148**: 495-505.
- Fox, C.S., 1935. The age of Deccan Trap. *Current Science*, **3**: 428-430.
- Further comments on "A geological map of the southern Deccan Traps, India and its structural implications, 1991. *Journal of Volcanology*, **148**: 495-505.
- Geology of the Ahmednagar District, Maharashtra. *Geol. Surv. of India*, 1976, pp. 1-7
- Gilbert, N. H., Langmuir, C.H., 1978. Modelling of major elements in mantle-melt systems using trace element approaches. *Geochemica. et Cosmochimica Acta*, **42** : 725-741.
- Glendhill, J.A., 1985. Dinosaur extinction and volcanic activity. *EOS*, **66** : 153.
- Hooper, P.R., Subbarao and Beane, J.E. 1988. The Giant Plagioclase Basalt (GPBs) of the Western Ghats, Deccan Traps. *Geol. Soc. of India, Mem.* **10**, pp. 135-144.
- Hunt, C.D., Ewart, C.J., 1988. Hawaiian Islands. *In The Geology of the North America. Edited by W. Back, J.S. Rosenshein, and P.R. Seaber. Geological Society of America pp.* 255-262.
- Kaneoka, I., Haramura, H., 1973. K-Ar ages of successive lava flows from the Deccan Traps, India. *Ear. Planet. Sci. Lett.*, **18** : 229-236.
- Karmarkar, B.M., Kulkarni, S.R., Marathe, S.S, Sowani, P.V., Peshwa, V.V, 1972. Giant Plagioclase Basalt in the Deccan Trap. *Bull. Volcanol.*, **35** : 965-974.
- Khadri, S.F.R., Subbarao, K.V., Hooper, P.R., and Walsh, J. N., 1988. Stratigraphy of Thakurvadi Formation, western Deccan basalt province, India. *Geol. Soc. of India, Mem.* **10**, pp. 281-304.
- Krishnamurthy, P., Udas, G.R., 1981. Regional geochemical characters of the Deccan Trap lavas and their genetic implications. *Geol. Soc. Ind., Mem.* **3**, pp. 394-418.
- Lindholm, G.F., Vaccaro, J.J., 1988. Columbia lava plateau. *In The Geology of North America. Edited by W. Back, J.S. Rosenshein, and P.R. Seaber. Geological Society of America, pp.* 31-57.
- Mahoney, J.J., 1988. Deccan Traps. *In Continental Flood Basalts. Edited by J.J. Mahoney. Petrology and Structural Geology, pp.* 151-194.
- Mahoney, J.J., Macdougall, J.D., Lugmair, G.W., Gopalan, K., Krishnamurthy, P., 1985. Origin of contemporaneous tholeiitic and K-rich alkalic lavas: a case study from the northern Deccan Plateau, India. *Ear. Planet. Sci. Lett.*, **73** : 39-53.

- Marathe, S.S., Kulkarni, S.R., Karmarkar., B.M., and Gupte, B.E., 1981. Variations in the nature of the Deccan Trap volcanicity of western Maharashtra in time and space. Geol. Soc. Ind., Mem 3, pp. 143-152.
- Mitchelle. C, Widdowson, M, 1991. A geological map of the southern Deccan Traps, India and its structural implications. Journal of Volcanology, **148** : 495-505.
- Molano, S. 1987. Lineament identification and regional groundwater exploration in areas underlain by crystalline rocks. *In*: proceedings of the Harare, Zimbabwe, session 2, pp. 172-180.
- Norton, I.O., Sclater, J.G., 1979. A model for the evolution of Indian ocean and the break-up of Gondwanaland. J. Geophysics. Res., **84** : 6803-6830.
- Pal, P.C., 1975. Paleomagnetic reversals in the Deccan Traps. Geophysics. Res. Bull., **13** : 239-288.
- Paul, D.K., Kresten, P., Busman, T.R., McNutt, R.H.T., Brunfield, A.O., 1984. Geochemical and petrographic relations in some Deccan basalts, W. Maharashtra, India. J. volcanol., **35** : 709-718.
- Pearce, J.A., Norry, M.J., 1979. Petrogenetic implications of Ti, Zr, Y and Nb variations in volcanic rocks. Cont. to Min. and Petro., **69** : 33-47.
- Powar, K.B, 1981. Lineament fabric and dyke pattern in the western part of the Deccan volcanic province. Geol. Surv. of India, Mem. 3, pp. 48-55.
- Raja Rao, C.S., Sahasrabudhe, Y.S., Deshmukh, S.S., Raman, R., 1978. Distribution, structure and petrography of the Deccan Trap, India. Rep. Geol. Surv. Ind., **43** pp. 44- 67.
- Raju, A.T.R., Chawbe, A.N., Chowdhary, L.R., 1972. Deccan Trap and Geological framework of the Cambay Basin. Bull. volcanol. **35** : 521-538.
- Rao, B.R. J. and Yadagiri, P., 1963. Cretaceous intertrappean beds from Andhra Pradesh and their stratigraphic importance. *In*: Subbarao, K.V. and Sureshwala, R.N., Eds. Deccan Volcanism and related basalt provinces in other parts of the world. Extended Abstracts. Int. Group Discussion/Symposium, pp. 104-105.
- Sen, Gautam. 1988. Possible depth of origin of primary Deccan tholeiite magma. Geol. Soc. of India, Mem. 10, pp. 35-53.
- Sethna, S.F. and Sethna, B.S., 1988. Mineralogy and petrogenesis of Deccan Trap basalts from Mahabaleshwar, Igatpuri, Sagar and Nagpur areas, India. Geol. Surv. of India, Mem. 10, pp. 69-88.

- Shastri, V.V., 1963. A note on the foraminifera and ostracoda from the inter-trappean beds near Rajamundry, Andhra Pradesh. *Rec. Geol. Surv. India*, **92** : 299-331.
- Subbarao, K.V., Bodas, M.S., Hooper, P.R., Walsh, J. N., 1988. Petrogenesis of Jawar and Igatpuri Formations, western Deccan basalt province. *Geol. Soc. of India, Mem.* 10, pp. 253-280.
- Sukeshwala, R.N., Poldervaart, A. 1958. Deccan basalt of the Bombay area. *Bull. Geol. Soc. Amer.*, **69** : 1475-1497.
- Sukeshwala, R.N., 1981. Deccan basalt volcanism. *Geol. Soc. Of India, Mem.* 3, pp. 8-19.
- Thigle, S.S., 1983. The impact of physical determinants on the groundwater occurrence in the aggraded landforms associated with the Western Ghats of Maharashtra, India. *In: International Conference on Groundwater and Man*, **3** : 319-327.
- Walker, G.P.L., 1972. Compound and simple loava flows and flood basalts. *Bull. Volcano.*, Special Issue, Pt. I, pp., 579-589.
- Wood, D.A., Gibson, I.L., and Thompson, R.N., 1976. Elemental mobility during zeolite facies metamorphism of the Tertiary basalts of eastern Iceland. *Contr. Miner. Petrol.*, **55** : 241-254.
- Wood, W.W., Fernandez, L.A., 1988. Volcanic rocks. In *The Geology of North America. Edited by W. Back, J.S. Rosenshein, and P.R. Seaber.* Geological Society of America, pp. 352-367.

Appendix 1

General petrography **of samples from the study area**

Suite No 1

Sample /	% of Phenocrysts	Groundmass	Clays	% of Zeolites
TCN-2	Di = 2-3% ; Plg = 10-12% ; Cpx = 3-4%	Plg = 30% ; Cpx = 30% ; Fe oxides = 2% ; Glass = 10%	2-4	5-10
MM1-1	Di = 2% ; Plg = 10-12% ; Cpx = 3%	Plg = 30% ; Cpx = 30% ; Fe oxides = 2-3% ; Glass = 10-12%	1-2	8-10
MIK1-1	Di = 2-3% ; Plg = 10-12% ; Cpx = 2-3%	Plg = 30% ; Cpx = 35% ; Fe oxides = 2-3% ; Glass = 8-10%	1-2	5-8
WMM1-2	Di = 2-3% ; Plg = 10-11% ; Cpx = 3%	Plg = 30% ; Cpx = 25-30% ; Fe oxides = 1-2% ; Glass = 10-1	2-4	8-10
MSSB4-A	Di = 2% ; Plg = 8-10% ; Cpx = 2-4%	Plg = 35% ; Cpx = 30% ; Fe oxides = 2-3% ; Glass = 10%	1-3	4-5
MGG-1	Di = 2-3% ; Plg = 10% ; Cpx = 2-4%	Plg = 30-35% ; Cpx = 30% ; Fe oxides = 2-3% ; Glass = 10	1-2	5-8
ARKD1-1	Di = 1-2% ; Plg = 10% ; Cpx = 2-4%	Plg = 30-35% ; Cpx = 30% ; Fe oxides = 2-3% ; Glass = 8-10%	2-4	5-8
MGG-2	Di = 2-3% ; Plg = 10-15% ; Cpx = 2-3%	Plg = 30% ; Cpx = 25-30% ; Fe oxides = 1-2% ; Glass = 10-12	2-3	10
MMD2-1	Di = 2% ; Plg = 10% ; Cpx = 2-3%	Plg = 30% ; Cpx = 30% ; Fe oxides = 2-3% ; Glass = 10-15%	1-2	5-7
TCN-3	Di = 1-2% ; Plg = 10-12% ; Cpx = 3-4%	Plg = 30% ; Cpx = 35% ; Fe oxides = 2-3% ; Glass = 10-12%	2-3	7-8
ALDK1-1	Di = 2-3% ; Plg = 10-12% ; Cpx = 2-4%	Plg = 30% ; Cpx = 30% ; Fe oxides = 2-3% ; Glass = 10-12%	3-4	8
DPK1-1	Di = 2-3% ; Plg = 10% ; Cpx = 3-4%	Plg = 30% ; Cpx = 30% ; Fe oxides = 2% ; Glass = 12%	2-3	8-10
TP-1	Di = 1-2% ; Plg = 12% ; Cpx = 3-4%	Plg = 30% ; Cpx = 30% ; Fe oxides = 1-2% ; Glass = 12-15%	2-4	4-5
DP-1	Di = 2% ; Plg = 8-10% ; Cpx = 2-4%	Plg = 30% ; Cpx = 35% ; Fe oxides = 2-3% ; Glass = 10-12%	1-2	7-10
PCT1-1	Di = 1-2% ; Plg = 10% ; Cpx = 3-4%	Plg = 30% ; Cpx = 30-35% ; Fe oxides = 1-2% ; Glass = 12-1	2-3	6-8
WMM1-1B	Di = 2-3% ; Plg = 8-10% ; Cpx = 3-4%	Plg = 35% ; Cpx = 30% ; Fe oxides = 2-3% ; Glass = 10-15%	1-3	5-6
WA 1-1	Di = 2-4% ; Plg = 10% ; Cpx = 2-4%	Plg = 30% ; Cpx = 30% ; Fe oxides = 2-3% ; Glass = 10-15%	1-2	5-8
U1-1	Di = 2-3% ; Plg = 10-12% ; Cpx = 2-4%	Plg = 30-35% ; Cpx = 30% ; Fe oxides = 1-2% ; Glass = 10	1-2	7-10
UP1-1	Di = 2-3% ; Plg = 10-12% ; Cpx = 3%	Plg = 30% ; Cpx = 30% ; Fe oxides = 2-3% ; Glass = 12-15	1-2	8-10
TCSM-1	Di = 2-3% ; Plg = 10-12% ; Cpx = 2-4%	Plg = 30% ; Cpx = 35% ; Fe oxides = 2-3% ; Glass = 10-12%	2-4	5-8

Suite No 2

Sample /	% of Phenocrysts	Groundmass	clays	% of zeolites
PK1-1	Di = 2-3% ; Plg = 10-12% ; Cpx = 2-3% ; Mag = 2	Pig = 30% ; Cpx = 30% ; Fe oxides = 2-3% ; Glass = 12%	1-2	5-8
MM2-1	Di = 1-2% ; Plg = 8-10% ; Cpx = 3-4% ; Mag = 2	Pig = 35% ; Cpx = 35% ; Fe oxides = 2-3% ; Glass = 8-10%	2-4	5-7
PTV1-1	Di = 2-3% ; Plg = 10-12% ; Cpx = 3-4% ; Mag = 2	Pig = 30-35% ; Cpx = 30% ; Fe oxides = 2-3% ; Glass = 10%	1-2	7-8
MSSB-2	Di = 2-3% ; Plg = 8-10% ; Cpx = 3-4% ; Mag = 2	Pig = 30-35% ; Cpx = 30% ; Fe oxides = 2-3% ; Glass = 10-12	1-2	5-8
MSSB-3	Di = 1-2% ; Plg = 10% ; Cpx = 3% ; Mag = 1-	Pig = 30% ; Cpx = 30% ; Fe oxides = 1-2% ; Glass = 12%	2-3	8-10
ARRB1-1	Di = 2% ; Plg = 12% ; Cpx = 3-4% ; Mag = 2%	Pig = 30% ; Cpx = 25-30% ; Fe oxides = 2-3% ; Glass = 8-10	3-4	4-5
LRNB1-1	Di = 1-2% ; Plg = 10-15% ; Cpx = 3-4% ; Mag	Pig = 25-30% ; Cpx = 30% ; Fe oxides = 2-3% ; Glass = 10-15	2-3	7-10
ML1-1	Di = 2-3% ; Plg = 12-13% ; Cpx = 2-3% ; Mag	Pig = 30% ; Cpx = 30% ; Fe oxides = 2-3% ; Glass = 10%	2-4	6-8
PKS1-1	Di = 2-3% ; Plg = 12% ; Cpx = 2-4% ; Mag =	Pig = 30% ; Cpx = 25-30% ; Fe oxides = 2-3% ; Glass = 12%	1-2	8
LPRAD1-1	Di = 2-3% ; Plg = 10-12% ; Cpx = 2-3% ; Mag	Pig = 30% ; Cpx = 30% ; Fe oxides = 2-3% ; Glass = 8-10%	2-4	5-8%
AKB1-1	Di = 1-2% ; Plg = 10% ; Cpx = 3-4% ; Mag = 2	Pig = 30% ; Cpx = 25-30% ; Fe oxides = 2-3% ; Glass = 12-15	1-2	7-10
UC1-1	Di = 2-3% ; Plg = 8-10% ; Cpx = 3-4% ; Mag =	Pig = 30-35% ; Cpx = 30% ; Fe oxides = 2-3% ; Glass = 10%	2-3	8-10
MCD1-1	Di = 1-2% ; Plg = 12-15% ; Cpx = 3-4% ; Mag =	Pig = 30% ; Cpx = 30% ; Fe oxides = 2-3% ; Glass = 10%	1-3	5-7
DT1-1	Di = 2-3% ; Plg = 10-12% ; Cpx = 3% ; Mag = 2-	Pig = 30% ; Cpx = 30% ; Fe oxides = 2-3% ; Glass = 8-10%	3-4	7-8
MMD1-1	Di = 2-3% ; Plg = 8-10% ; Cpx = 3-4% ; Mag =	Pig = 30-35% ; Cpx = 30% ; Fe oxides = 2-3% ; Glass = 10-12	1-2	5-8
PS1-1	Di = 1-2% ; Plg = 8-10% ; Cpx = 3-4% ; Mag =	Pig = 30% ; Cpx = 30% ; Fe oxides = 2-3% ; Glass = 10-15%	2-3	8-10
MCM1-1	Di = 2% ; Plg = 8-10% ; Cpx = 3-4% ; Mag	Pig = 35% ; Cpx = 30% ; Fe oxides = 1-2% ; Glass = 10-12%	2-4	4-5
TGM1-2	Di = 1-2% ; Plg = 8-10% ; Cpx = 3-4% ; Mag	Pig = 30-35% ; Cpx = 30% ; Fe oxides = 1-2% ; Glass = 12-15	1-2	7-10
TGM1	Di = 2-3% ; Plg = 8-10% ; Cpx = 2-4% ; Mag = 1-	Pig = 30% ; Cpx = 30-35% ; Fe oxides = 1-2% ; Glass = 10-15	2-3	6-8
MSSB-1	Di = 1-2% ; Plg = 10% ; Cpx = 3% ; Mag = 1-	Pig = 30% ; Cpx = 30-35% ; Fe oxides = 1-2% ; Glass = 10%	3-4	5-6
UF-1	Di = 2% ; Plg = 10-15% ; Cpx = 2-3% ; Mag =	Pig = 25-30% ; Cpx = 30% ; Fe oxides = 1-2% ; Glass = 10%	2-5	2-5
PC1-1	Di = 1-2% ; Plg = 8-10% ; Cpx = 3-4% ; Mag = 1	Pig = 30-35% ; Cpx = 30% ; Fe oxides = 2-3% ; Glass = 10%	2-4	7-10
LPB-1	Di = 1-2% ; Plg = 10% ; Cpx = 3-4% ; Mag =	Pig = 30% ; Cpx = 30% ; Fe oxides = 2-3% ; Glass = 10%	2-4	8-10
TPZ-1	Di = 2-3% ; Plg = 10% ; Cpx = 3% ; Mag = 2	Pig = 25-30% ; Cpx = 30% ; Fe oxides = 2-3% ; Glass = 12-	1-2	5-7
MM3-1	Di = 1-2% ; Plg = 8-10% ; Cpx = 3-4% ; Mag = 2	Pig = 30-35% ; Cpx = 30% ; Fe oxides = 2-3% ; Glass = 10	1-2	8-10
MM3-2	Di = 2-3% ; Plg = 8-10% ; Cpx = 3% ; Mag =	Pig = 30% ; Cpx = 30% ; Fe oxides = 2-3% ; Glass = 10-12	2-3	5-7

Apendix 2

**Petrographic description of a few samples from
Suite No. 1 and 2.**

**Thin Section Description
of Deccan Basalts**

Observer: Shashank Agarwal

Rock Name: MGG-2	Texture: Intergranular, intersertal, ophitic-subhohitic, glomeroporphyritic
Sample Location:	Grain Size: Fine grained

Phenocrysts	Present (%)	Original (%)	Size Range (mm)	Morphology	Comments
<i>Olivine</i>	2-3	2-3	1-2.5	Euhedral	Altered and oxidised
<i>Plagioclase</i>	10-15	10-15	2-4	Subhedral	Twinned, zoned, engulfing groundmass material
<i>Clinopyroxene</i>	2-3	2-5	1-2	Subhedral	Aggregates
<i>Magnetite</i>	x	x	x	x	x
Groundmass					
<i>Clinopyroxene</i>	30	30	<1	Subhedral	
<i>Plagioclase</i>	30	35	<1	Euhedral-subhedral	
<i>Olivine</i>					
<i>Glass</i>	10-12	10-15			
<i>Iron oxides</i>	2-3	1-2	<1	Euhedral	Magnetite or Hemnite
<i>Clays</i>					

Secondary Mineralogy	%	Replacing/Filling	Comments
<i>Clays</i>	2-3	Olivine & Groundmass	
<i>Chlorite</i>			
<i>Zeolites</i>	10	vesicles	
<i>Others</i>			
Total	100 Appx.	☞ Must equal 100%	

Vesicles	%	Size (mm)	Filling	Shape	Comments
Present	10	2-10	zeolites	irregular	some are pipe shaped, circular

Comments: Olivine phenocrysts are completely altered. Margins are oxidized. Clays are distributed throughout the groundmass. Glass is partially devitrified. Vesicular boundaries are altered. Hand sample shows surface weathering is prominent. Iron oxides in the groundmass were not identified because of devitrification.

**Thin Section Description
of Deccan Basalts**

Observer: Shashank Agarwal

Rock Name: UP 1-1	Texture: Glomeroporphyritic, intergranular, intersertal, subohitic.
Sample Location:	Grain Size: Fine to medium

Phenocrysts	Present (%)	Original (%)	Size Range (mm)	Morphology	Comments
<i>Olivine</i>	2-3	2-3	2-2.5	Euhedral-subhedral	Completely altered
<i>Plagioclase</i>	10-12	10	2-4	Subhedral	Twinned, zoned
<i>Clinopyroxene</i>	3	5	1-2	Subhedral	Aggregates
<i>Magnetite</i>	x	x	x	x	x

Groundmass					
<i>Clinopyroxene</i>	30	30-35	<1	Eu-subhedral	
<i>Plagioclase</i>	30	30-35	<1	Subhedral	
<i>Olivine</i>	x	x	x	x	
<i>Glass</i>	12-15	10			Devitrified
<i>Iron oxides</i>	2-3	2-5	<1		
<i>Clays</i>					

Secondary Mineralogy	%	Replacing/Filling	Comments
<i>Clays</i>	2-3	Groundmass minerals	
<i>Chlorite</i>	1	Olivine	
<i>Zeolites</i>	8-10	Vesicles	
<i>Others</i>			
Total	100 Appx.	☞ Must equal 100%	

Vesicles	%	Size (mm)	Filling	Shape	Comments
Present	2	2-4	Zeolites	circular	Irregular

Comments: Olivine is altered to iddingsite. Some of them have chlorite as an altered material. Glass is devitrified. Iron oxides in the groundmass are not identified because of the devitrification of glass. Clinopyroxene phenocrysts show irregular margins and occur in aggregates. Clays are present throughout in the groundmass.

**Thin Section Description
of Deccan Basalts**

Observer: Shashank Agarwal

Rock Name: WA 1-1	Texture: Glomeroporphyritic, Intergranular, intersertal, subohitic.
Sample Location:	Grain Size: Fine to medium

Phenocrysts	Present (%)	Original (%)	Size Range (mm)	Morphology	Comments
<i>Olivine</i>	2-4	4-5	1-2	Euhedral-subhedral	Completely altered, margins oxidized
<i>Plagioclase</i>	10	5-10	2-4	Subhedral	Twinned, zoned
<i>Clinopyroxene</i>	2-4	5	1.5-2	Subhedral	Aggregates
<i>Magnetite</i>	x	x	x	x	x

Groundmass					
<i>Clinopyroxene</i>	30	30-35	<1	Eu-subhedral	
<i>Plagioclase</i>	30	30-35	<1	Subhedral	
<i>Olivine</i>	x	x	x	x	x
<i>Glass</i>	15	15			Devitrified
<i>Iron oxides</i>	2-3	2-5	<1		Scattered throughout
<i>Clays</i>	x	x	x	x	x

Secondary Mineralogy	%	Replacing/Filling	Comments
<i>Clays</i>	1-2	Groundmass minerals	
<i>Chlorite</i>			
<i>Zeolites</i>	5-8	Vesicles	
<i>Others</i>			
Total	100 Appx.	☞ Must equal 100%	

Vesicles	%	Size (mm)	Filling	Shape	Comments
<i>Present</i>	5-7	2-5	Zeolites	circular	Irregular

Comments: Olivine is altered and margins are highly oxidized. Groundmass is oxidized. Glass is devitrified. Iron oxides in the groundmass are not identified because of oxidation. Plagioclase phenocrysts enclose groundmass material.

**Thin Section Description
of Deccan Basalts**

Observer: Shashank Agarwal

<i>Rock Name:</i> MMC 1-1	<i>Texture:</i> C lomeroporphyritic, intergranular, intersertal, subohitic.
<i>Sample Location:</i>	<i>Grain Size:</i> Medium

Phenocrysts	Present (%)	Original (%)	Size Range (mm)	Morphology	Comments
<i>Olivine</i>	2	2-3	1.5-2	Euhedral-subhedral	Completely altered
<i>Plagioclase</i>	10-12	10	2-4	Subhedral	Twinned, zoned
<i>Clinopyroxene</i>	3-4	5	1.5-2	Subhedral	Aggregates
<i>Magnetite</i>	2-3	2-4	1-2	Eu-subhedral	Scattered

Groundmass					
<i>Clinopyroxene</i>	30	30-35	<1	Eu-subhedral	
<i>Plagioclase</i>	30	30-35	<1	Subhedral	
<i>Olivine</i>					
<i>Glass</i>	10-12	10			Devitrified
<i>Iron oxides</i>	2-3	2-5	<1		
<i>Clays</i>					

Secondary Mineralogy	%	Replacing/Filling	Comments
<i>Clays</i>	1-2	Groundmass minerals	
<i>Chlorite</i>	1	Olivine	
<i>Zeolites</i>	8-10	Vesicles	
<i>Others</i>			
<i>Total</i>	100 Appx.	☞ Must equal 100%	

Vesicles	%	Size (mm)	Filling	Shape	Comments
<i>Present</i>	2	2-4	Zeolites	circular	Irregular

Comments: Olivine is altered to iddingsite. Some of them have chlorite as an altered material. Glass is devitrified. Iron oxides in the groundmass are not identified because of the devitrification of glass. Clinopyroxene phenocrysts show irregular margins and occur in aggregates.

**Thin Section Description
of Deccan Basalts**

Observer: Shashank Agarwal

Rock Name: UF 1-1	Texture: Intergranular, intersertal, sub-ophitic, glomeroporphyritic
Sample Location:	Grain Size: Medium to fine grained

Phenocrysts	Present (%)	Original (%)	Size Range (mm)	Morphology	Comments
<i>Olivine</i>	2	5	2-4	Eu- subhedral	Altered to Iddingsite, oxidised
<i>Plagioclase</i>	10-15	10-15	2-4	Subhedral	Normal zoning and Twinning (Polysynthetic.)
<i>Clinopyroxene</i>	2-3	2-3	1-2	Subhedral	Aggregates
<i>Magnetite</i>	2-3	2-5	1-2	Eu-Subhedral	Scattered
Groundmass					
<i>Clinopyroxene</i>	35	30-35	<1	Subhedral	
<i>Plagioclase</i>	30	30-35	<1	Subhedral	
<i>Olivine</i>	x	x	x	x	
<i>Glass</i>	12	10		Devitrified	
<i>Iron oxides</i>	1-2	1-2	Subhedral		
<i>Clays</i>					

Secondary Mineralogy	%	Replacing/Filling	Comments
<i>Clays</i>	2-5	Olivine & Groundmass	
<i>Chlorite</i>			
<i>Zeolites</i>	4-5		
<i>Others</i>			
Total	About 100	☞ Must equal 100%	

Vesicles	%	Size (mm)	Filling	Shape	Comments
<i>Present</i>	4-5	1-2	Zeolites	circular	

Comments: Olivine is completely altered to iddingsite. Clays are distributed throughout the groundmass. Glass is devitrified.

**Thin Section Description
of Deccan Basalts**

Observer: Shashank Agarwal

Rock Name: TPZ -1	Texture: Glomeroporphyritic, intergranular, intersertal, subohitic.
Sample Location:	Grain Size: Fine to medium

Phenocrysts	Present (%)	Original (%)	Size Range (mm)	Morphology	Comments
<i>Olivine</i>	2-3	4-5	1-2	Euhedral-subhedral	Completely altered, margins oxidized
<i>Plagioclase</i>	10	10	2-4	Subhedral	Twinned, zoned
<i>Clinopyroxene</i>	3	5	1.5-2	Subhedral	Aggregates
<i>Magnetite</i>	2-4	2-4	1	Eu-subhedral	Scattered

Groundmass					
<i>Clinopyroxene</i>	30	30-35	<1	Eu-subhedral	
<i>Plagioclase</i>	25-30	30-35	<1	Subhedral	
<i>Olivine</i>					
<i>Glass</i>	10	15-20			Devitrified
<i>Iron oxides</i>	2-3	2-5	<1		
<i>Clays</i>					

Secondary Mineralogy	%	Replacing/Filling	Comments
<i>Clays</i>	1-2	Groundmass minerals	
<i>Chlorite</i>			
<i>Zeolites</i>	5	Vesicles	
<i>Others</i>			
Total	100 Appx.	☞ Must equal 100%	

<i>Vesicles</i>	%	Size (mm)	Filling	Shape	Comments
Present	2	2-4	Zeolites	circular	Irregular

Comments: Olivine is altered and margins are highly oxidized. Groundmass is oxidized. Glass is devitrified. Iron oxides in the groundmass are not identified because of oxidation.

Appendix 3

Statistical analysis of length and frequency for the lineaments

The following results are for:

Angle $\delta = a$

Total observations = 11

	Angle	Length
No of Cases	11	11
Minimum	3	0.664
Maximum	28	6.247
Range	25	5.583
Mean	14.545	1.8999
Varlance	66.673	2.999
Standard Deviation	8.165	1.732
Std. Error	2.462	0.522
Skewness (G1)	0.033	1.569
Kurtosis (G2)	-0.919	1.548
Sum	160	20.893
C.V.	0.561	0.912
Medlan	15	0.996

The following results are for :

Angle $\delta = b$

Total observations = 15

	Angle	Length
No of Cases	15	15
Minimum	30	0.415
Maximum	59	6.3
Range	29	5.885
Mean	39.6	1.548
Varlance	70.4	2.539
Standard Deviation	8.39	1.593
Std. Error	2.166	0.411
Skewness (G1)	0.752	2.011
Kurtosis (G2)	-0.168	3.342
Sum	594	23.221
C.V.	0.212	1.029
Medlan	37	0.999

The following results are for:

Angle S = c

Total observations = 14

	Angle	Length
No of Cases	14	14
Minimum	60	0.166
Maximum	89	3.915
Range	29	3.749
Mean	70.786	1.285
Variance	105.104	0.988
Standard Deviation	10.252	0.994
Std. Error	2.74	0.266
Skewness (G1)	0.733	1.279
Kurtosis (G2)	-0.779	1.501
Sum	991	17.983
C.V.	0.145	0.774
Median	70	1.206

The following results are for:

Angle S = d

Total observations = 12

	Angle	Length
No of Cases	12	12
Minimum	97	0.498
Maximum	112	3.74
Range	15	3.242
Mean	104.25	1.365
Variance	28.75	0.936
Standard Deviation	5.362	0.967
Std. Error	1.548	0.279
Skewness (G1)	0.07	1.414
Kurtosis (G2)	-1.559	1.016
Sum	1251	16.379
C.V.	0.051	0.709
Median	103	0.955

The following results are for:

Angle S = e

Total observations = 24

	Angle	Length
No of Cases	24	24
Minimum	120	0.415
Maximum	149	3.98
Range	29	3.565
Mean	135.33	1.084
Variance	51.623	0.644
Standard Deviation	7.185	0.803
Std. Error	1.467	0.164
Skewness (G1)	0.066	2.48
Kurtosis (G2)	-0.592	5.845
Sum	3248	26.017
C.V.	0.053	0.74
Median	134	0.898

The following results are for:

Angle S = f

Total observations = 31

	Angle	Length
No of Cases	31	31
Minimum	150	0.456
Maximum	180	3.9
Range	30	3.444
Mean	162.484	1.24
Variance	80.391	0.919
Standard Deviation	8.966	0.959
Std. Error	1.61	0.172
Skewness (G1)	0.439	1.784
Kurtosis (G2)	-0.763	2.13
Sum	5037	38.455
C.V.	0.055	0.773
Median	160	0.916

Summary Statistics for Angle

Bartlett Test for Homogeneity of Group Variances

CHI-Square = 5.649 DF= 5 Probability= 0.342

Analysis of the variance

Source	Sum of Square	DF	Mean Square	F	Probabilit
Between Group	295054.215	5	59010.843	859.545	0
Within Groups	6934.01	101	68.654		

Summary Statistics for Length

Bartlett Test for Homogeneity of Group Variances

CHI-Square = 5.649 DF= 5 Probability= 0.342

Analysis of the variance

Source	Sum of Square	DF	Mean Square	F	Probabilit
Between Group	6.091	5	1.024	0.928	0.466
Within Groups	131.053	101	1.298		

Shashank Agarwal

Date of Birth September 29, 1969

Education

- 1992-1994 **M.Sc. in Geology**- University of Windsor, Windsor Ontario, Canada N9B 3P4
G.P.A. 3.5/4
- 1990-1992 **M.Sc. in Geology**- University of Lucknow, Lucknow, India
Grade Average: A (First class)
- 1987-1990 **Bachelor of Science in Geology**- University of Lucknow, India
Grade Average: A (First class)

Awards

- * Graduate Research Assistantship, Department of Geology, University of Windsor for the year 1993-94
- * University of Windsor Visa Differential Fee Waiver bursaries awarded for the year 1993-94
- * Graduate Teaching Assistantship, Department of Geology, University of Windsor for the year 1993-94

Work Experience

- * Graduate Teaching Assistant at the Department of Geology, University of Windsor, Ontario, Canada (Sept. 1992-94)
- * Research Assistant, University of Windsor, Ontario (Summer 1993 - 94):

Laboratory Experience:

- * Geochemical analysis of major and trace elements on Inductive Couple Plasma- Mass Spectrometer
- * Thin sections preparation and microscopy

Activities:

- * Active member within "Indian Students Association" and "Graduate Student Society", University of Windsor
- * Associate member, Society for the Advancement of Environmental Sciences (sponsored by the Govt. of India, Lucknow; 1987-1991)
- * Voluntarily acted as one of the judges at **Windsor Regional Science Fair** organized by the Govt. of Ontario to evaluate the creativity of high school students in Essex County

Personal Profile:

- * Success oriented, with outgoing attitude, creative, flexible and efficient, having good written and oral skills
- * Strengths in administration and organization functions. Experience in exercising judgement and making decisions
- * Having strong public relations and interpersonal skills

Reference(s): Available upon request